Spring 4-2-2018

REGIONAL STRESS REGIME STUDY OF EAST TEXAS BASED ON ORIENTATION OF FRACTURES IN THE WECHES FORMATION

Cory D. Ellison
Stephen F Austin State University, coryellison@hotmail.com

REGIONAL STRESS REGIME STUDY OF EAST TEXAS BASED ON ORIENTATION OF FRACTURES IN THE WECHES FORMATION

By

CORY DEAN ELLISON, Bachelor of Science

Presented to the Faculty of the Graduate School of

Stephen F. Austin State University

In Partial Fulfillment

Of the Requirements

For the degree of

Master of Science

STEPHEN F. AUSTIN STATE UNIVERSITY
May 2018

REGIONAL STRESS REGIME STUDY OF EAST TEXAS BASED ON ORIENTATION OF FRACTURES IN THE WECHES FORMATION

By

CORY DEAN ELLISON, Bachelor of Science

APPROVED:

Dr. Chris Barker, Thesis Director

Dr. Wesley Brown, Committee Member

Dr. LaRell Nielson, Committee Member

Dr. Chris Aul, Committee Member

Pauline Sampson, Ph.D.
Dean of Research and Graduate Studies

ABSTRACT

Fractures in the Weches Formation in a roughly 50 mile radius around Nacogdoches, Texas were observed and measured at many outcrops. This data was used to infer the direction of maximum/minimum horizontal stresses that created the fractures. These joints are typically steeply dipping (70^0 – 90^0) and iron filled. Crack-seal formation, steep dip and a lack of shear movement suggests these fractures were predominantly opening mode joints. Slickenlines are visible on some fracture planes; however, their bearings show random orientation indicating unloading movement during erosion. Limonite veins and iron ledges are a late stage diagenetic event which indicates a late origin for fractures during exhumation. Orientation data of 540 fractures from 14 different outcrops show three main joint sets: N75-85W, N75-85E, and N40E. These sets persist over distances of up to 90 miles (145 km). The orientations are believed to be the result of Neogene to very recent tectonic stress states related to large scale deformational events including gulfward extension, salt movement in the East Texas Basin and possibly the Sabine Arch or basement faulting.

TABLE OF CONTENTS

LIST OF FIGURES

LIST OF TABLES

LIST OF APPENDICES

CHAPTER 1: INTRODUCTION

Overview: Joints in East Texas

Fractures in a rock are a form of brittle deformation induced by stress (Collins and Luneau 1986). They differ from faults (also a type of fracture) which can be described as planar features with displacement of rock material on either side. Joints refer to a certain type of fracture which have been defined by Narr and Suppe (1991) as “planar tensile opening-mode fractures with little or no displacement parallel to the fracture plane”. These form when the tensile strength of a rock is exceeded. Joints are ubiquitous features with influence in many fields of geology: in structural geology because they give insight into the mechanical properties of rocks and their tectonic and/or localized history, in resource exploration and hydrogeology because they act as conduits facilitating liquid flow and can become sites of mineral precipitation and to civil engineering when roads, bridges, buildings or other structures are built upon fractured rock units. Joints may be related to local perturbations in the stress field caused by nearby geologic structures, or to the trajectories of far field stress regimes or ancient paleostress regimes which are caused by forces at some distance. Many stress fields are driven by large scale tectonic events and sustained over long periods of time (Fossen, 2016).

East Texas is an area of steady urban grown. Development will increase when an Interstate highway is completed in this area, yet there is a lack of information about the structural properties of near surface geologic formations. The Eocene age Weches, Sparta and Queen City Formations are the main geologic units exposed in East Texas. These are the rock units upon which will be built roads, homes, buildings and bridges. In some areas these rocks are drilled through by wells or quarried and utilized as resources. Many pelitic (clay-rich) rocks similar to the Weches Formation are also significant potential hydrocarbon targets. Knowledge of the fracture pattern, types of jointing, susceptibility to jointing and general structural properties of such rock units are particularly useful information for engineering and drilling applications. For the above reasons, this study can have a beneficial impact for engineering, construction and resource exploration.

When differential stress on a rock surpasses its tensional strength, a set of joints with a common strike and a regular spacing – a joint set – often forms. These joints allow minor geometrical changes within the rock unit to occur (Pollard and Aydin, 1988). Each joint set in a single rock unit is considered to form instantaneously in geologic time, often with consistent orientation or gradual change over large distances (Engelder and Geiser, 1980). Additionally, the orientation of these joints is strongly related to the stress in a rock and only weakly to the rock fabric (Olson and Pollard 1989).

When joints form they propagate normal to the direction of least stress (also referred to as extension, or minimum horizontal compressive stress or S_{Hmin}), following the trajectory of the stress field. This means that the joint opens in the direction of least horizontal compressive stress and propagates in the direction of maximum horizontal compressive stress (S_{Hmax}). This allows the rock to expand beyond what its elastic strength allows. It then follows that measuring the strike of a joint is equivalent to measuring the direction of S_{Hmax}. This is a useful property because structural geologists describe the stress regime as a function of these two stresses. While local interferences (faults, folds, erosion, etc.) can create a level of complexity that make it appear as if joints form randomly, this is not generally the case. Instead, joints are often systematic deformation features that provide valuable insight into the stress that created them. For these reasons, joint sets have been studied as regional stress and paleostress markers (Nickelson and Hough 1967, Hancock 1985, Lorenz et al. 1991, Gough and Bell 1982).

This thesis study is an analysis of patterns of fractures in the Weches Formation in East Texas which should allow insight into current and past stress regime in the area. In order to ascertain the type of stresses the Weches Formation has undergone, fracture patterns were observed, and joint and fault surfaces were measured. This data was used to determine the nature and origin of the causative stresses that affected the Weches Formation, furthering our understanding of those stresses, as well as the susceptibility of the Weches Formation to deformation and the tectonic influences on East Texas.

A Brunton Compass was used to measure the orientation of approximately 540 fractures in the Weches Formation where the unit is exposed in quarries, road cuts, stream beds and man-made cliffs in the East Texas region. The large number of measurements should mitigate the effects of localized stresses caused by surficial factors including erosion, weathering, and topography. Since the Weches is a non-resistant sandy claystone unit, it weathers to low slopes and flat areas with little topographic relief. Therefore, most measurements of joints were found in streambeds, quarries, road cuts and man-made cliffs. The data was compiled and analyzed with rose diagram software and mean orientations were compared with known stress orientations in the East Texas area. Observations were made about the interaction between different fracture sets, as well as close inspection of the nature of these fractures and veins. These investigations into the origin and nature of the joints in the Weches Formation are essential for determining the timing and type of stress. As will be discussed later, three main orientations of joints were found in East Texas.

Study Area

The study area is focused on outcrops of the Weches Formation within a radius of approximately 50 miles (80 km) around Nacogdoches, Texas (figure 1). In East Texas, The Weches Formation crops out in a large arc-shaped pattern on the west side of the Sabine uplift. (The Sabine Uplift is along the Texas-Louisiana border and will be described under “Structural Setting”.) Further to the south, the Weches is exposed in a long thin zone that trends parallel to the Texas coastline; however, this southern extension of the Weches was not considered in this study. While most of the Weches is an easily eroded sandy clay unit, it also contains resistant ferruginous beds that allow the unit to maintain some structural integrity in steep exposures. Where the Weches is the surface formation, these resistant ironstone beds commonly cap hills accounting for some of the topography in the East Texas region.

The Weches Formation occurs commonly in East Texas and is almost always jointed. However, good exposures are rare because the unit weathers readily to soil and is typically covered by lush vegetation. Specialized borehole electrical logs can provide some joint information, but the Weches Formation is often too poorly indurated to obtain borehole data. Because of this, the amount of locations with measurable joint orientations is somewhat limited. Despite these challenges, field work was conducted in three different quarries, one riverbed and eleven road cuts along TX Highway 21 from Alto to the Louisiana border and along US Highway 69 from Alto to Jacksonville. Figure 1 shows all the locations in a regional map view while figures 2 – 9 show the exact location of each outcrop. The study area can be broken up into four regions on the basis of location and joint trends: eastern region, central region, western region and northern region.

Eastern Region

This region consists of sites 4, 6 and 13. The locations for these sites are shown in figures 2, 3 and 4.

Site 4 is located in a road cut on the north side of Texas State Highway 21 West near Chireno, Texas at 31.506436, -94.344648. The road cut trends N65^{0}E and exposes about 20 feet (6 meters) of the unit. The Weches here is a highly fossiliferous greenish-grey to black clay with multiple ironstone beds. The fossils are typically relatively well preserved bivalves and burrows. The elevation at this location is 248 feet (76 meters).

Site 6 is in a quarry located just outside the city of Milam on Texas State Highway West, at 31.429348, -93.863285, at an elevation of 265 feet (81 meters). The quarry is owned by Big 4 Inc.

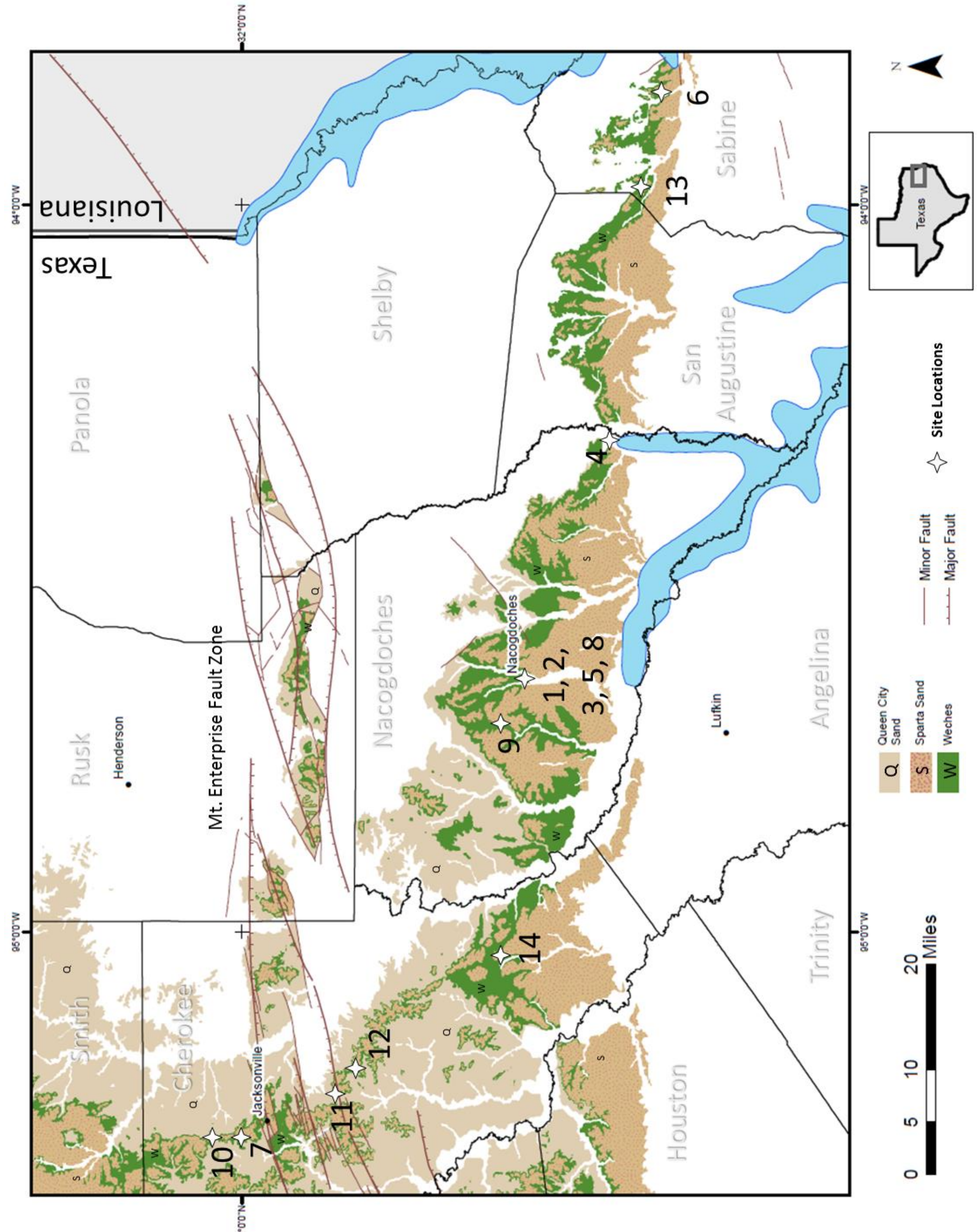

Figure 1. Geologic map of study area. The Weches Formation (dark green) and bounding formations are shown. The stars represent outcrops where data was taken. Note the normal faults which have an approximate trend of N780E. Geologic units shapefile from USGS geologic database of Texas.

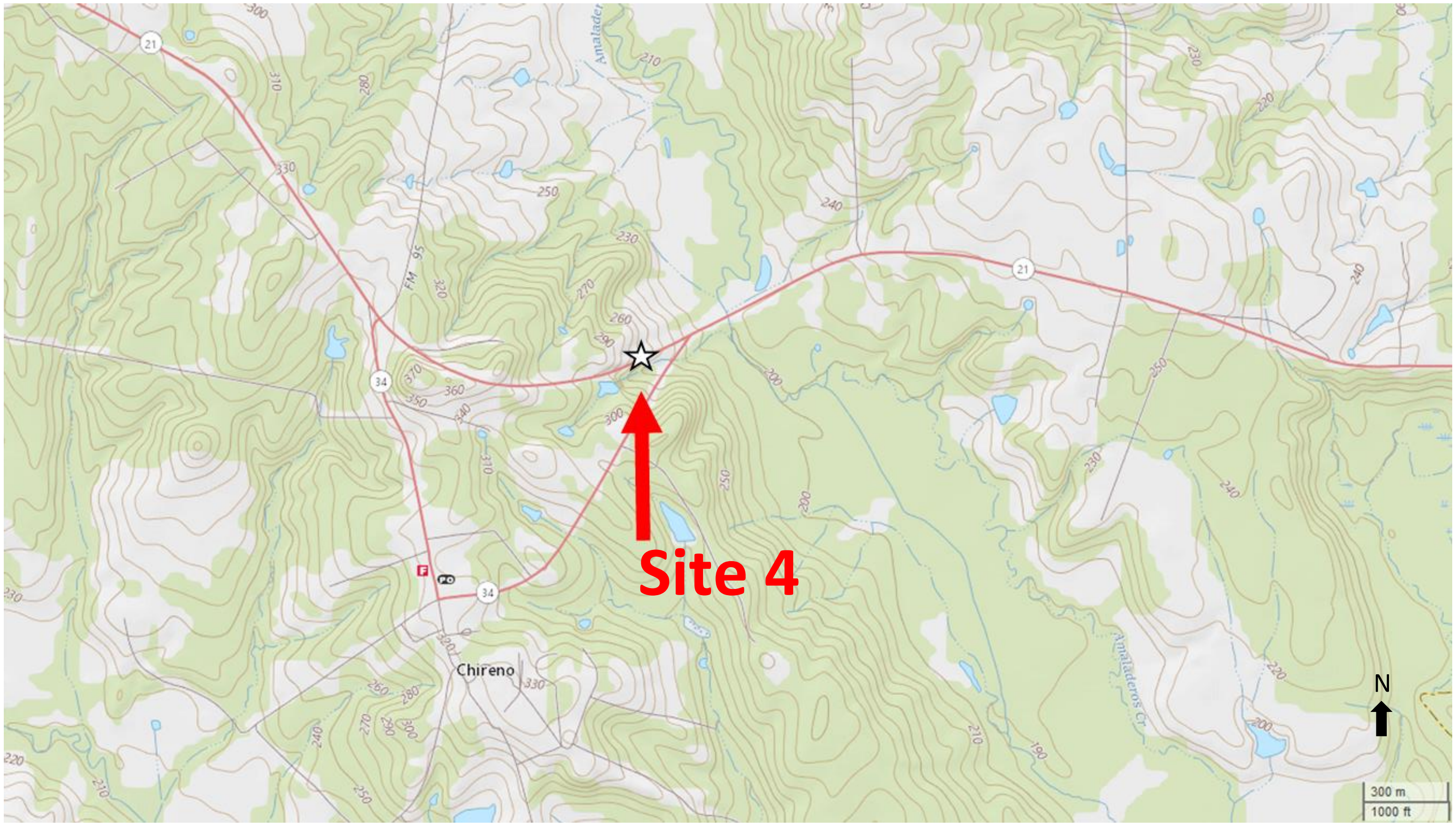

Figure 2. USGS topographical map of site 4. Shown by star. Located to the east of Nacogdoches near Chireno (bottom left).

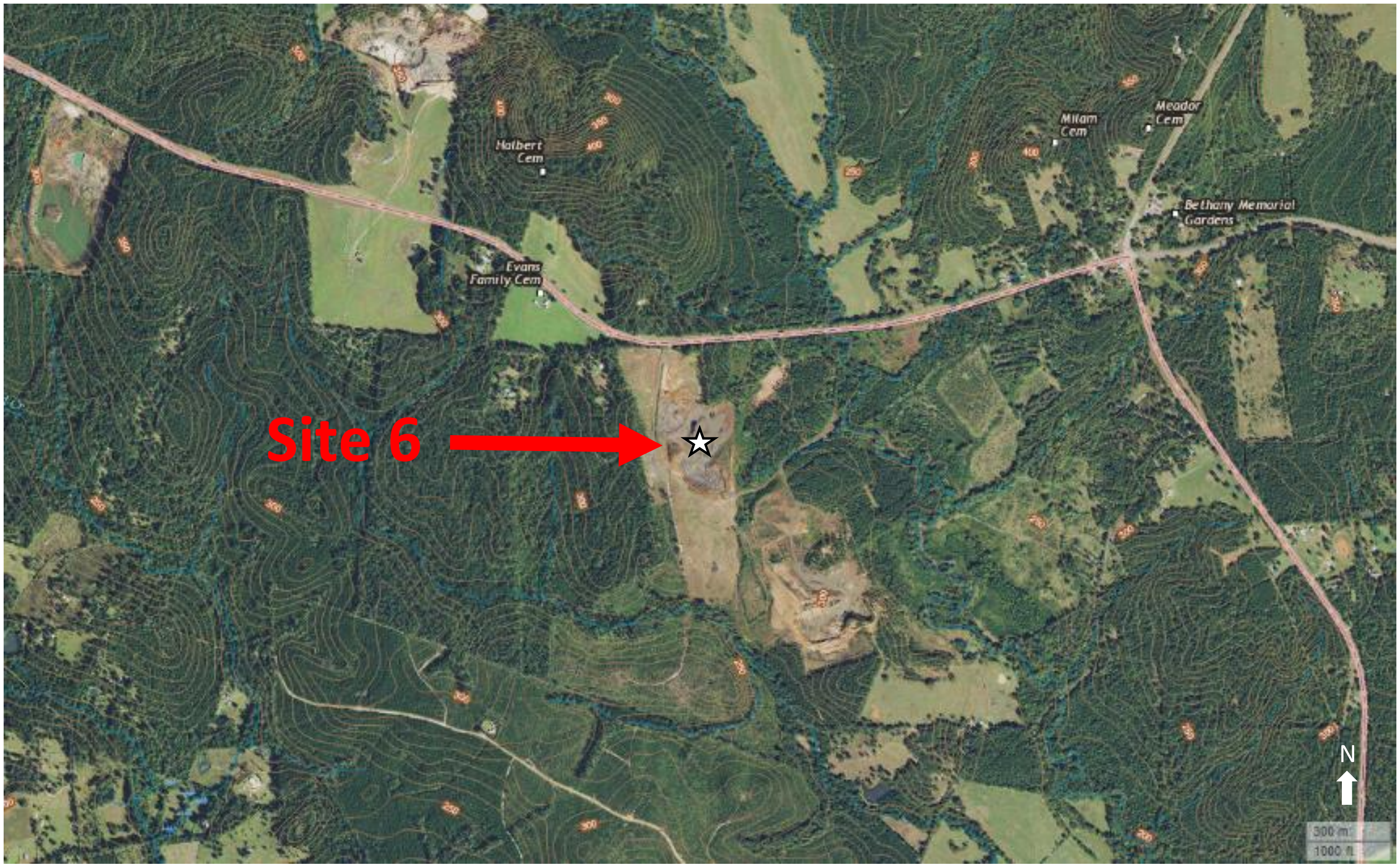

Figure 3. USGS topographical map of site 6. Shown by star. Located in a quarry in Milam, Texas.

The Weches Formation here is exposed near the contact between the overlying Sparta Formation as indicated by a thick (~6 feet) ferruginous section with overlying clayey sandstone above.It is better indurated at this location than outcrops to the west and is dark green and is made up almost entirely of sand-sized, glauconite pellets. There are small pockets of silicified skeletal fragments and nodular concentric iron concretions. Cross-bedding and herringbone structure are present in some areas and fossils are not well preserved. The only iron ledge present is at the Sparta contact. Most of the joints terminate at this contact and have iron infilling. An adjacent quarry at a lower elevation was active and not available for study, however samples of the rock from this area were much more fossiliferous and brighter green claystone that was less indurated than the section near the Sparta contact.

Site 13 is a quarry owned by Attoyac Construction LLC which exposes Weches up to 60 feet (18 meters) thick. It is located off of Eddings Lane, northeast of the city of San Augustine, at 31.449025, -93.978194, at an elevation of 280 feet (85 meters). Iron ledges are infrequent at this location. The lithology at this outcrop is similar to Site 6. It is predominately well indurated, dark gray to green, sand-sized, glauconitic pellets with sparse fossils. Joints are not as common as in the previous quarry but are typically N80W with no iron infilling and surfaces that are not well defined. A total of four very small faults and three large faults were observed in this area. All of these faults appear to be normal faults dipping to the north except one large fault that dips to the south.

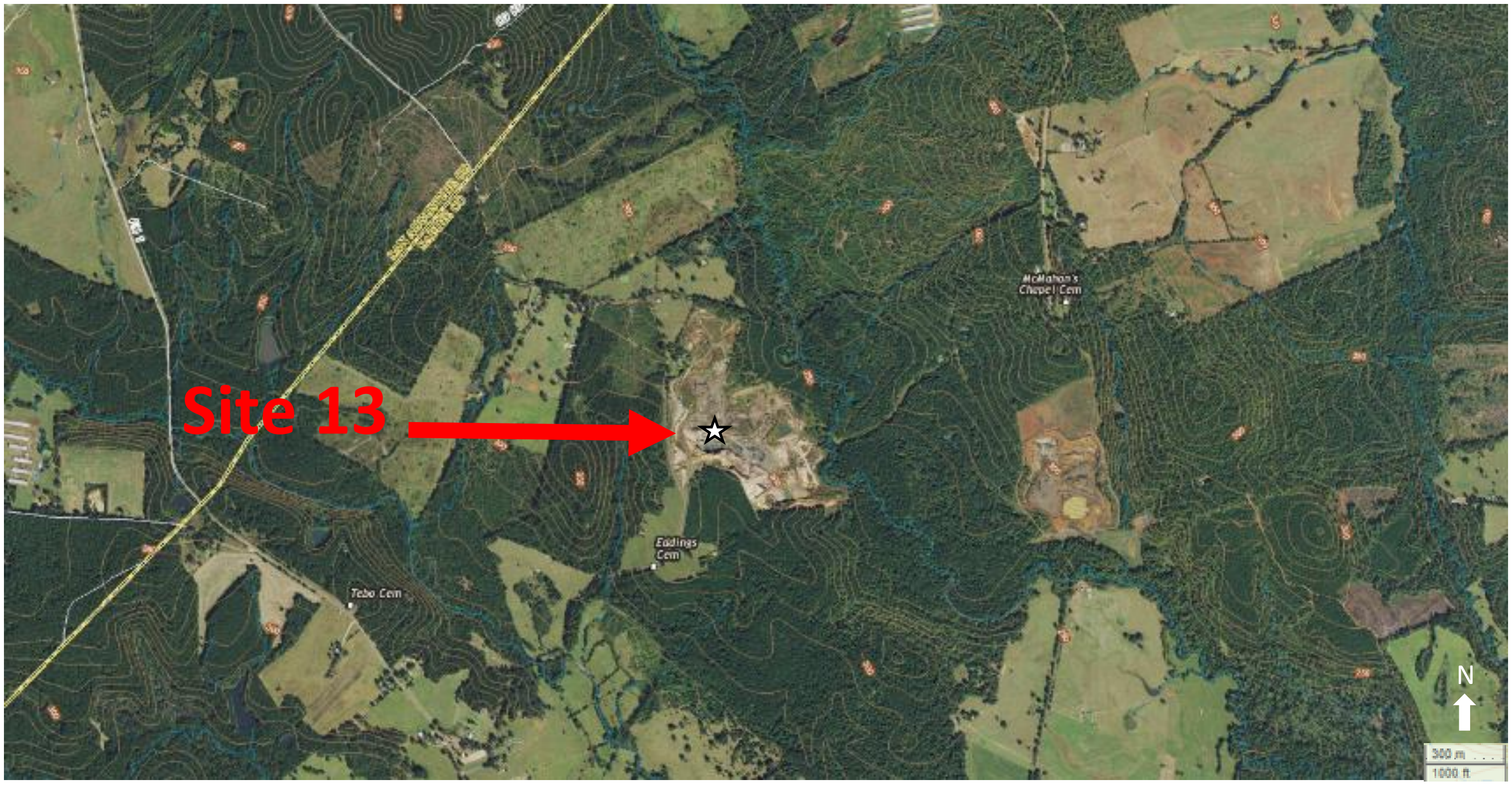

Figure 4. USGS topographical map of site 13. Shown by star. Located in a quarry northeast of San Augustine, Texas.

Central Region

The central region is made up of outcrops in Nacogdoches and includes sites 1-3, 5 and 8 (figure 5).

Site 1 is a cliff located between the El Indigo Tire Shop and Metro PCS on 1019 South Street, at 31.596404, -94.661457, at an elevation of 303 feet (92 meters). This outcrop exposes about 15 feet (4.5 meters) of Weches Formation with three continuous iron ledges present. Contact with the overlying Sparta Formation is visible and is marked by thick iron deposit at the top of the outcrop. The Weches here is a poorly indurated, greenish brown, fossiliferous clay with abundant jointing. The outcrop itself trends ~N45E, with N80^{0}E striking joints present at a spacing of about 8 - 10 feet (2.5 - 3 meters).

Site 2 is a stream bed located near 101 West Main Street, 37.133, -95.786, at an elevation of 262 feet (80 meters). Where the Bonita Creek river bed is accessible and partially dry it often exposes the Weches. This site is accessible, when dry, near the Pillar St Bridge. The Weches here forms the river bed and also makes up the river bank on one side. Jointing is more common on the river bed than the banks. The lithology here is similar to site 1, but better indurated and more weathered from river flow. The joints orientations are scattered but there is a concentration of joints trending northeast and a smaller concentration of joints trending east-northeast.

Site 3 is located in a road cut on the north side of 715 W. Main Street, at 37.1328, -95.7855, at an elevation of 340 feet (104 meters). Here the Weches is a greenish-grey to yellowish color and is highly weathered and covered in vegetation. About 6 feet (1.8 meters) of the unit is exposed.

Site 5 is located at 628 North University Drive, at 31.606270, -94.641599, at an elevation of 316 feet (96 meters). Here the Weches is exposed in a manmade cliff on the east side of the road behind the Kline's and Wrap It Up stores. About 50 feet (15 meters) of formation is visible; however, only the bottom 10 feet (3 meters) is accessible because of the steepness of the cliff and the amount of foliage cover near the top. The outcrop itself trends N19^{0}E. The Weches here is made up of greenish-grey, clayey, fossiliferous beds alternating with hard reddish to yellowish brown, fossiliferous and ferruginous beds. East-northeast trending joints are present at a spacing of about 8 - 10 feet (2.5 - 3 meters). These joints often terminate in segmented sections of slightly different strike. The strike of the lower segmented section of the joint differs by about 10^0 to 15^0 trending closer to an east-west direction. The upper section of the outcrop contains a much denser assemblage of ironstone beds and jointing. The orientation of the joints near the top of the outcrop are out of reach but appear to strike in a similar direction to those at the base.

Figure 5. USGS topographical map of sites in Nacogdoches, Texas. Shown by stars

Site 8 is located in a road cut on the north side of 1200 East Main Street and Timberlake St, at 31.599637, -94.644926, at an elevation of 309 feet (94 meters). About 6 feet (2 meters) of the formation is exposed here and is heavily weathered with extensive foliage cover. It is tannish to brown-grey fossiliferous sandy claystone that is poorly indurated except where it has hardened due to iron accumulation. Joint orientations at this location are sporadic. There is a grouping of joints trending roughly north; however, they are dipping at a low angle down the slope of the outcrop which suggests either erosional influence.

Western Region

The western region is made up of two sites west of Nacogdoches, site 9 and site 14 shown in figure 6 and 7.

Site 9 is located in a road cut off of Texas State Highway 21 East, at 31.622073, -94.721249, at an elevation of 390 feet (119 meters). About 15 feet (4.5 meters) of Weches is exposed at this location. The formation here is mostly well indurated, highly fossiliferous, grey to green clay interbedded with frequent iron ledges. Fossils are predominately well preserved bivalves and burrows. At the base of the outcrop the clay becomes a dark black-green and poorly indurated, likely due to water flow off the road. Joints in this section trend east-northeast spaced about 8-10 feet (2.5 - 10 meters) apart.

Site 14 is located in a privately owned quarry two miles east of Alto, Texas, off of the south side of Texas State Highway 21 West, at 31.645767, -95.057657, at an elevation of 648 feet (198 meters). This quarry, which has been inactive for some time, exposes up to 30 feet (9 meters) of Weches Formation. The contact with the overlying Sparta Formation is visible and is indicated by a thick ferruginous layer and overlying tan sand common at this interface. The surfaces are fairly weathered and often covered by foliage but iron infilling is common, preserving the fracture faces. Where not weathered, the Weches is a bright green fossiliferous claystone with sparse iron beds and joints. Fossils are prevalent and well preserved and are made up almost entirely of bivalves and shark teeth. Joints at this location are most common along the Sparta contact and typically dip gently, seemingly without a preference north or south. The strike of joints resembles that of joints in the central region; however, the dip is generally gentler than previously observed joints of this orientation.

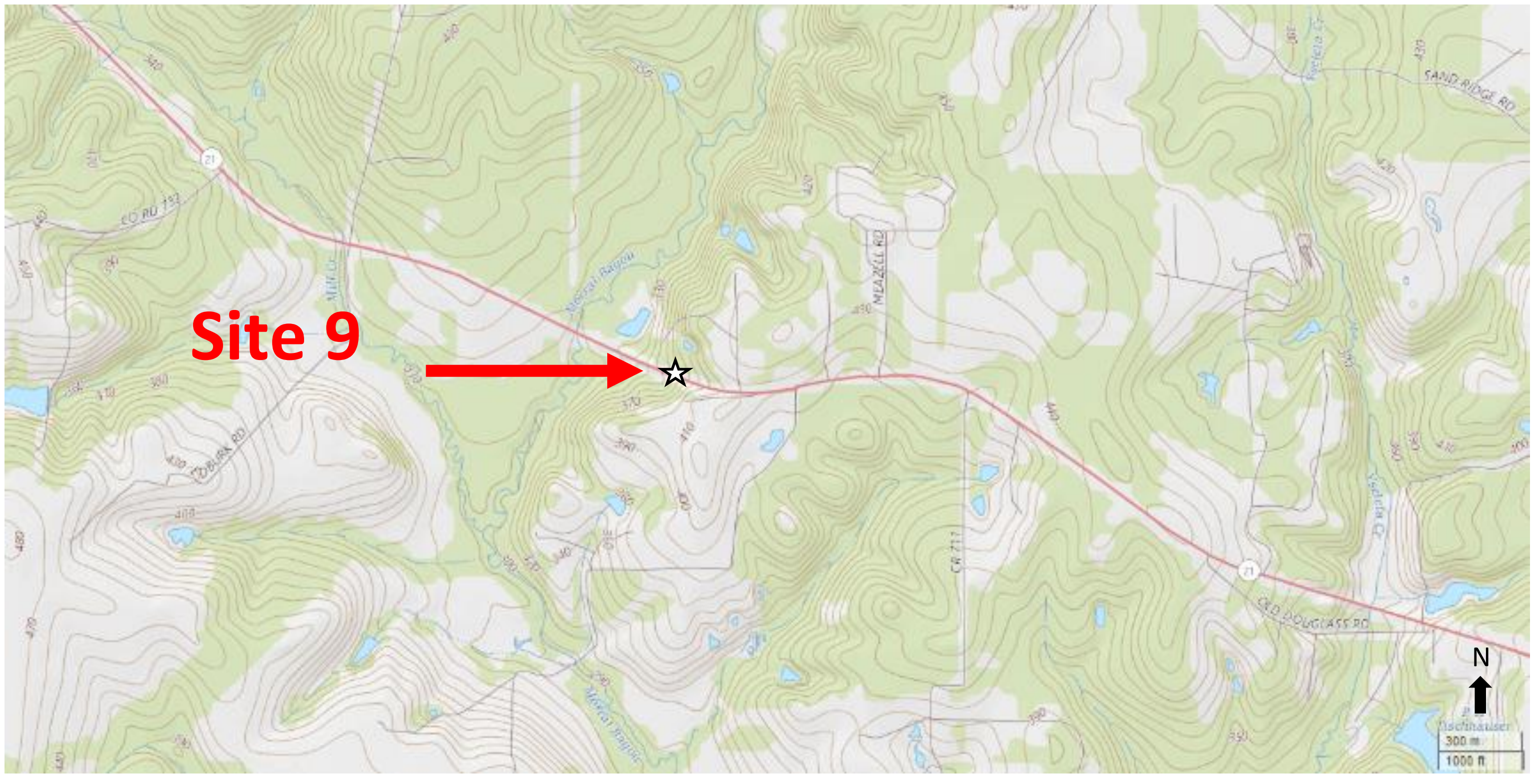

Figure 6. USGS topographical map of site 9. Shown by star. Located roughly 10 miles west of Nacogdoches.

Figure 7. USGS topographical map of site 14. Shown by star. Located in a quarry just east of Alto, Texas.

Northern Region

This region is made up of sites 7, 10, 11 and 12 located along US-69, between the cities of Rusk and Tyler, Texas (figures 8 and 9).

Site 10 is located in a road cut on either side of US-69, north of Jacksonville, 1 mile north of Burns Rd, at 32.058132, -95.283182, at an elevation of 636 feet (194 meters). About 50 feet (15 meters) of Weches is exposed in a road cut on either side of the road. The formation here is a tannish-green claystone with abundant sand-sized pellets, frequent iron concretions and sparse fossils (mostly iron replaced bivalves and burrows). Jointing is abundant and typically trends northeast with a spacing of 4-5 feet (1-1.5 meters).

Site 7 is located in a road cut off of US-69 near Loves Lookout Park, Jacksonville, at 32.030583, -95.281111, at an elevation of 650 feet (198 meters). Around 40 feet (12 meters) of Weches is exposed just north of the turn in for Loves Lookout Park, on the east side of the road, trending N15E. Here the Weches is a beige – grey claystone interbedded with numerous iron beds throughout. No fossils were found. Much of the section is inaccessible due to foliage and steep cliffs. Joints in this section are bound by the ironstone ledges. The dominant joint trend is roughly west-northwest to east-west which resembles that of joints measured in the eastern regions however with a much closer spacing of 1 - 2 feet (0.3-0.6 meters) apart.

<u>Site 11</u> is located on US-69, south of Jacksonville and just east of Cherokee County Airport, at 31.874265, -95.215188, at an elevation of 620 feet (189 meters). About 20 feet (6 meters) of the Weches is exposed on the east side of the curved highway. The formation here is unfossiliferous and heavily altered to a reddish and yellowish ferruginous material and veins are abundant. Botryoidal iron concretions are present at this area as well as a large fissure filled with ironstone. There did not appear to be significant slip along this surface. Some unaltered green clay is present but is sparse. The joints in this section trend northeast and are spaced about 8 feet (2.5 meters) apart.

<u>Site 12</u> is located in a road cut south of Jacksonville on US 69 just south of County Road 1506, at 31.868769, -95.208721, at an elevation of 648 feet (198 meters). About 10 feet (3 meters) of the Weches is exposed here. Like site 11 the formation here unfossiliferous and is almost completely altered to ironstone. Unaltered clay has been stained red from weathering. The joints here predominately trend northeast, which is common for sites in the northern region.

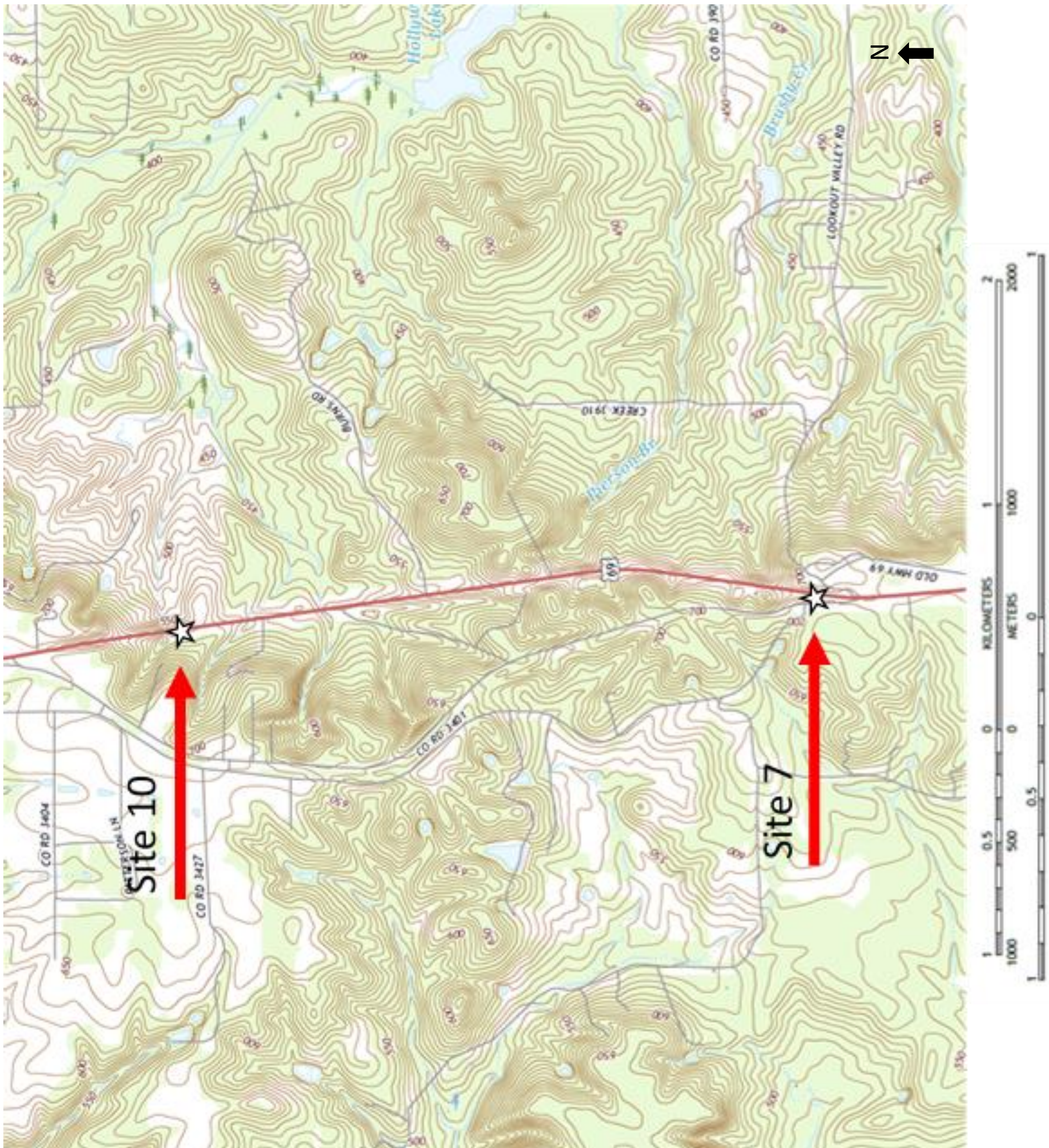

Figure 8. USGS topographical map of sites 7 and 10. Shown by stars. Located north of Jacksonville, Texas, on Highway US-69.

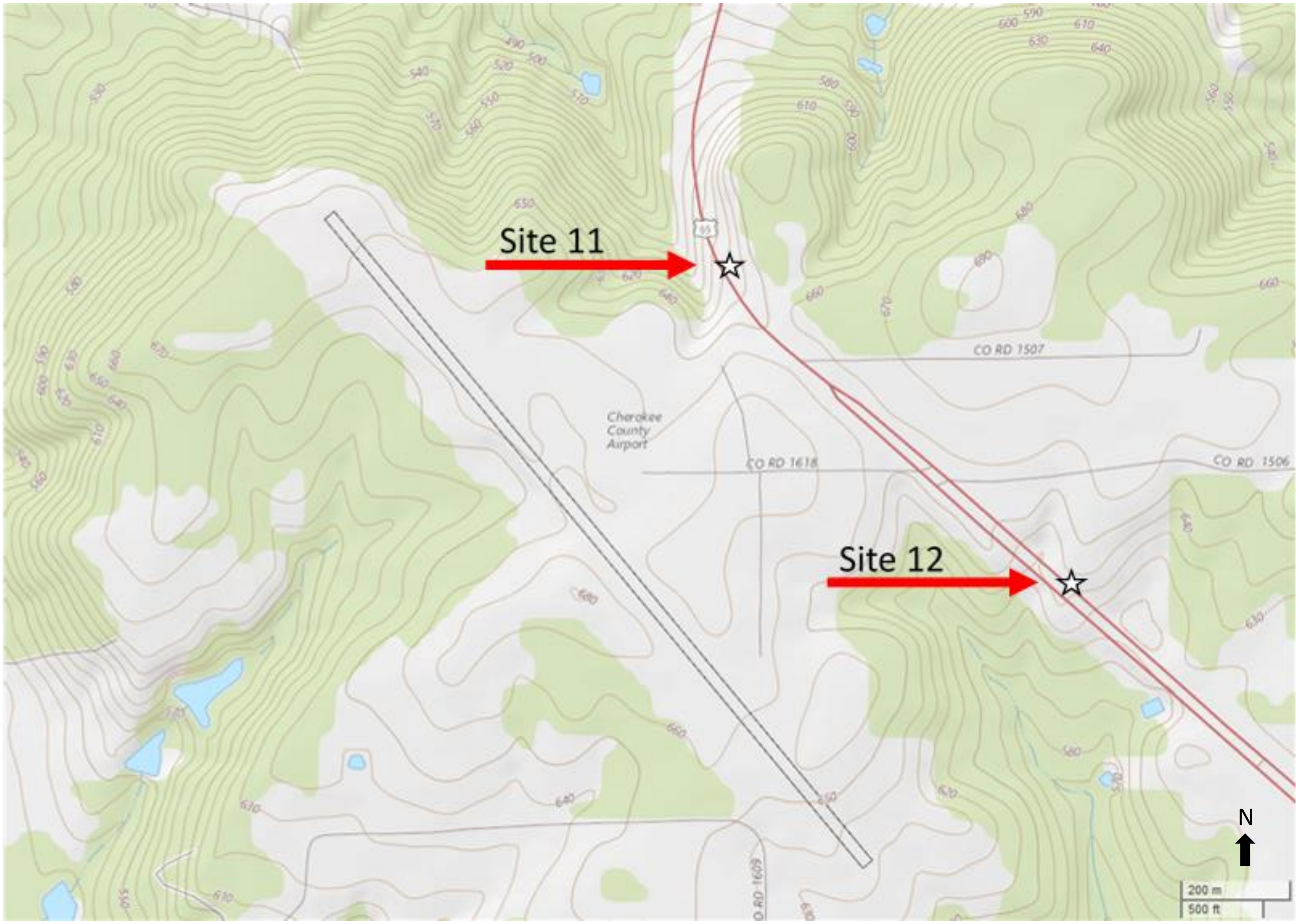

Figure 9. USGS topographical map of sites 11 and 12. Shown by stars. Located south of Jacksonville, Texas, on Highway US-69, next to the Cherokee County Airport.

CHAPTER 2: STRATIGRAPHY

The Weches Formation is part of the Claiborne Group which crops out across a large portion of east and south Texas, stretching from Texarkana to Laredo. The Claiborne group consists of the Cook Mountain, Sparta, Weches, Queen City, Reklaw and Carrizo Formations (figure 10) and has been described as a textbook example of cyclic sedimentation (Eargle 1968). Its units were created by a series of transgressions and regressions caused by fluctuations of the shoreline that occurred in the middle Eocene. This resulted in a vertical succession of alternating marine to non-marine facies beginning with a transgression in that resulted in deposition of the Wilcox Formation. These overall fluctuations in water level are displayed in figure 11. These facies successions are delineated by contrasting materials and textures. The non-marine facies contain primarily, nonmarine and/or near-shore blanket quartzose sands, while the marine facies are characterized by glauconitic fossiliferous marine mudstones (Dumble, 1920; Berg, 1979; Collins, 1980; Galloway, et al., 2000). Rather than large-scale, eustatic seal-level changes, these cycles are likely the result of lateral migration of large fluvial and deltaic complexes in a gently subsiding basin which has led to great lateral and vertical variability (Davies and Ethridge, 1971). The Claiborne units are middle Eocene in age, about 48 to 37 Ma. The changing facies of the Claiborne Group resulted in vertical sequences of alternating marine and nonmarine or near-shore marine units with the marine layers containing high amounts of glauconitic, fossiliferous clay. The non-marine to shallow-water marine formations include sandstones that formed in beach, dune and lagoonal environments; occasionally they are interlayered with fluvial sandstones (Eargle 1968; Berg, 1979).

The Weches Formation, which lies conformably on the Queen City Sand, is a relatively thin unit with a diverse fauna deposited in normal shallow water marine conditions (Stenzel, 1938). Figure 12 shows the relative thickness compared to the underlying and overlying units. It outcrops in an arcuate pattern around east Texas and into central Texas. Its outcrop is shown in figures 13 and 14. The Weches Formation is comprised of glauconitic shales and sandstones containing fossiliferous, glauconitic, dark greenish-gray clay with some interbedded ironstone, marl and limestone concretions. The composition of the Weches varies somewhat between locations. Near VanZandt, Henderson and Smith Counties the formation is coarser and more siliceous. Eastward, towards the Sabine uplift, it thins rapidly and becomes more sandy, while in Nacogdoches and surrounding counties it is a glauconitic, fossiliferous mudstone (Sellards et al., 1932; Stella, 1986). In East Texas the Weches is about 50 feet (15 meters) thick (Wendlandt and Knebel, 1929).

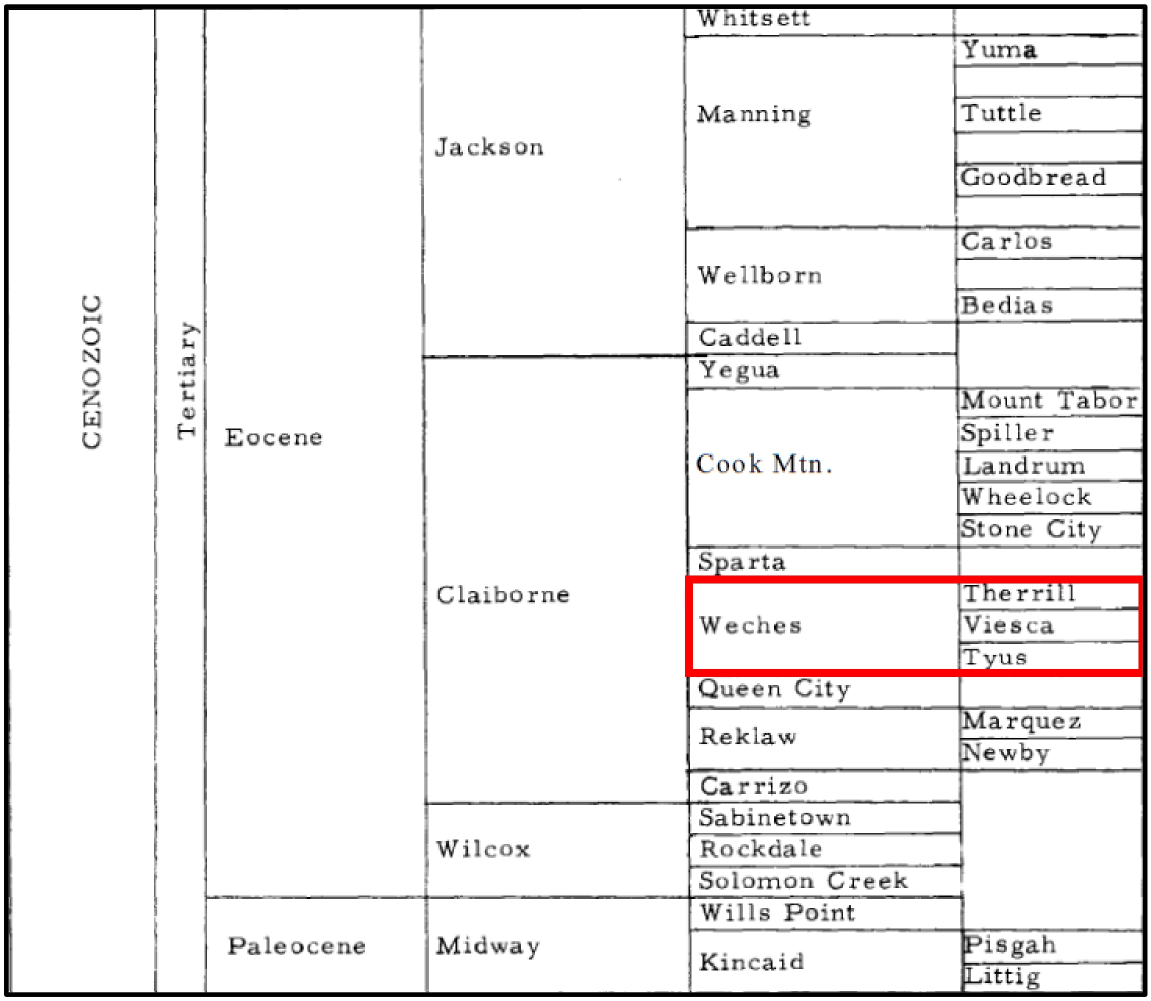

Figure 10. Stratigraphic column for East Texas Basin. The Weches is located near the middle of the Eocene aged Claiborne group and is split into three different members (from Smith, 1962).

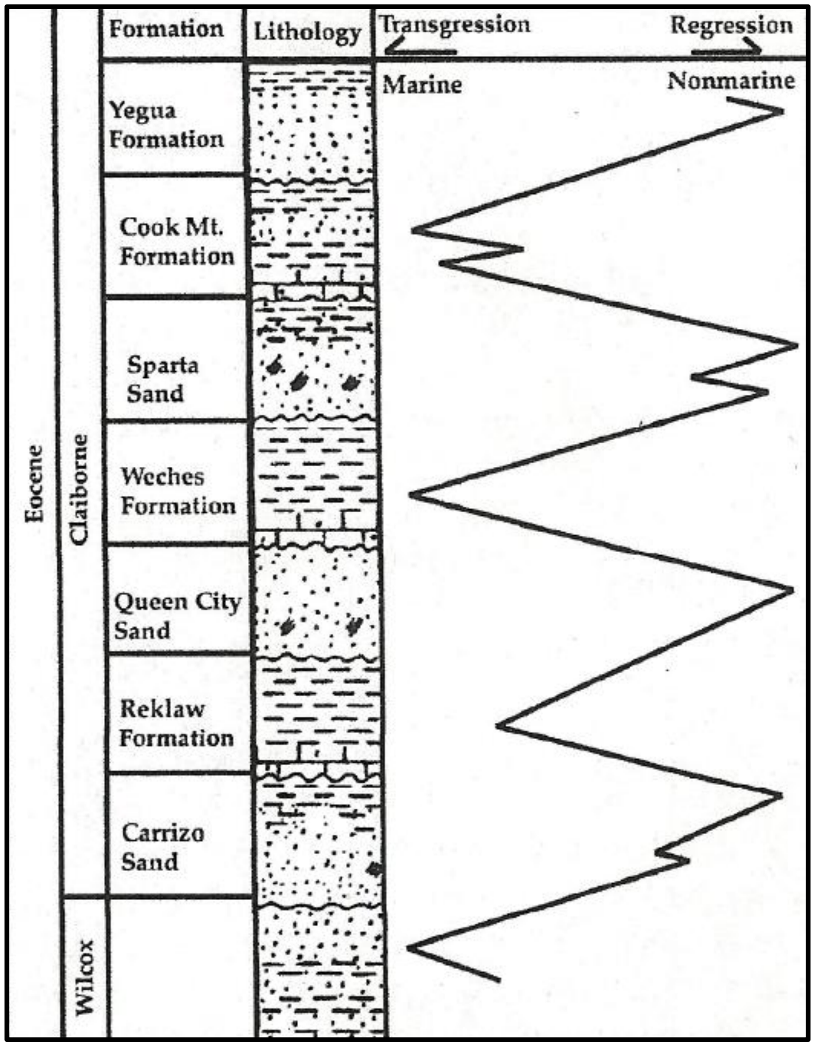

Figure 11. Stratigraphic section of the Eocene Claiborne Group showing transgressive/regressive cyclic sedimentation. The curving line in the right column represents the sea level changes based on sediment assemblage. These cycles took place roughly every 1 to 2 million years. Note that the Weches Formation is part of a transgression and therefore consists of marine sediment (from Ledger 2006).

The upper surface of the Weches Formation is defined by the presence of either unfossiliferous massive sandstone or a thick layer of reddish-brown to yellow (weathered) or dark brown to black (unweathered) porous iron ore in contact with the gray and buff sand of the Sparta Formation (Eckel, 1938). This represents a transition into the continental environment of the overlying Sparta Formation. At the base of the Weches, a highly fossiliferous glauconitic layer is in contact with gray unfossiliferous sand known as the Queen City Formation. Both the upper and lower contacts of the Weches Formation in East Texas are more or less conformable (Sellards et al.,1932). The Weches has been dated by Ghosh (1972) as being around 45 Ma, which is in the Upper Eocene Epoch of the Paleogene Period. The Weches can be subdivided into multiple units based on major sequence boundaries and flooding surfaces identified through seismic and well log data. It was originally divided by Stenzel (1938) into three formal members in Texas which are (from youngest to oldest): Therrill Member, Viesca Member and Tyus Member. However, for this study, the Weches is considered as a single unit.

The basal part of the Weches Formation is a highly fossiliferous, glauconitic mudstone with bioturbations. Going upward in the unit, sediments were deposited during a transgression in progressively deeper water. Therefore, fossils become sparser but better preserved, bioturbation decreases, and sand lenses may be present. Finally, at the top of the Weches, fossils are absent, and a thinly laminated siltstone is present representing an offshore facies that formed in water depths estimated to have been around 1200 to 3600 feet (365 - 1090 meters) deep (Sellards et al., 1932). While the contact in certain areas is disconformable, in East Texas the Weches conformably transitions into the non-marine massive sandstone Sparta Formation (Choung, 1975). This rapid change in environment is not representative of a typical regression from a deep water environment to shoreface. Instead, Payne 1968 postulated that the base of the Sparta represents a forward prograding river delta indicated by evidence of delta plain, delta front sandstone, and prodelta mudstone facies present in outcrop. Ricoy and Brown (1977) supported this theory with seismic data and borehole analysis. Their model for the Sparta depositional system is illustrated in figure 15. Stella (1986) summarized much of the literature and presented new theories for analyzing the depositional environment of the Weches with an emphasis on relating faunal successions and sedimentary structures present. This includes work from authors such as Andrews (1975), Stenzel (1938), Feray (1948), Curtis (1955), etc. Additionally, while little has been done on the structural controls on the Weches there is a wealth of work done on the general structure of East Texas.

Claiborne Group

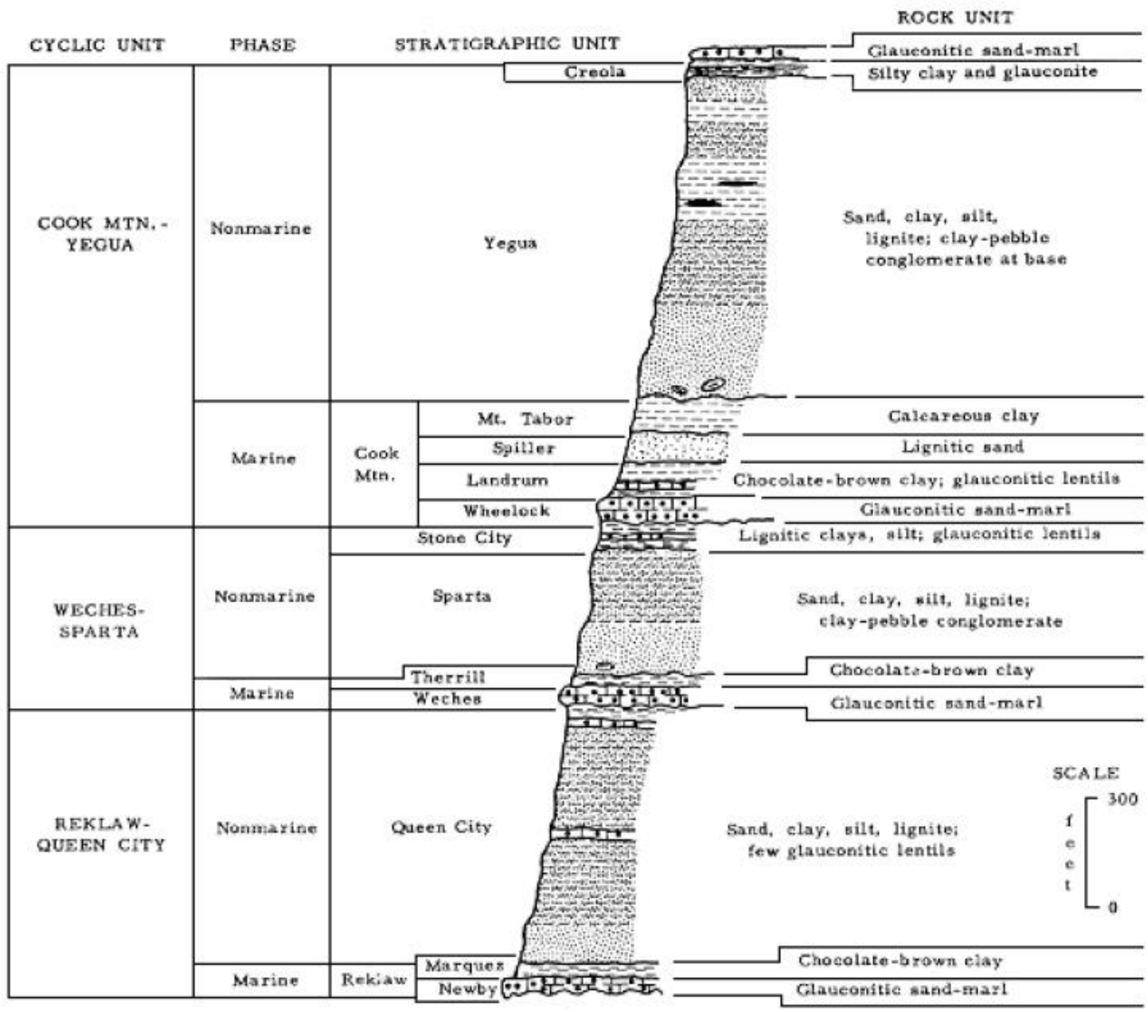

Figure 12 Stratigraphic Column for the study area. The Claiborne Group includes all, but is not limited to, the units shown. Note the Weches Formation, which is the principal unit for this study (from Fisher 1964).

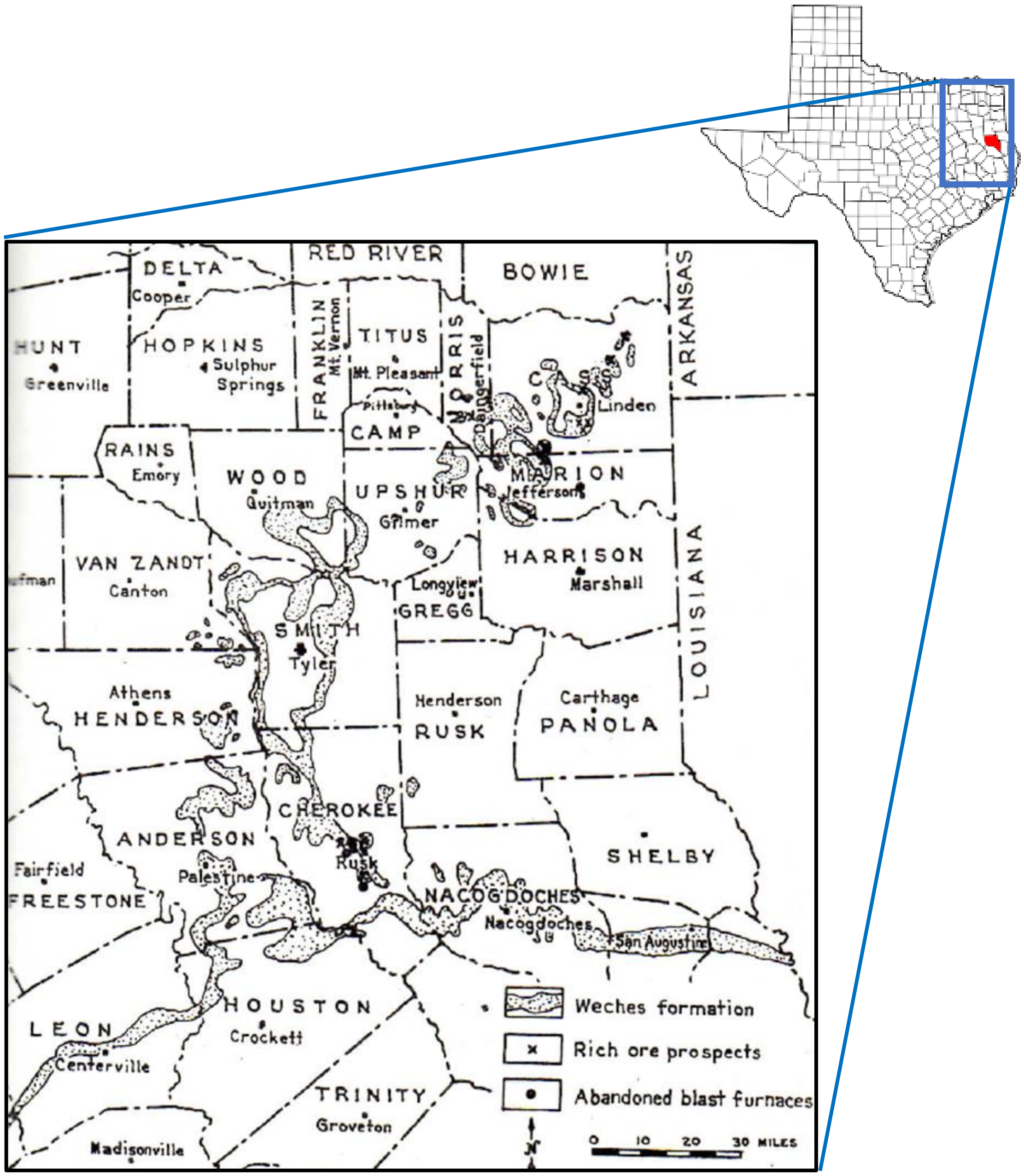

Figure 13. Weches Formation exposures in East Texas. Weches outcrops are shown in stippled pattern and form an arc as they bend around the Sabine Uplift (see figure 14) which straddles the Texas/Louisiana border. Nacogdoches County is outlined in red (modified from Sellards et al., 1932).

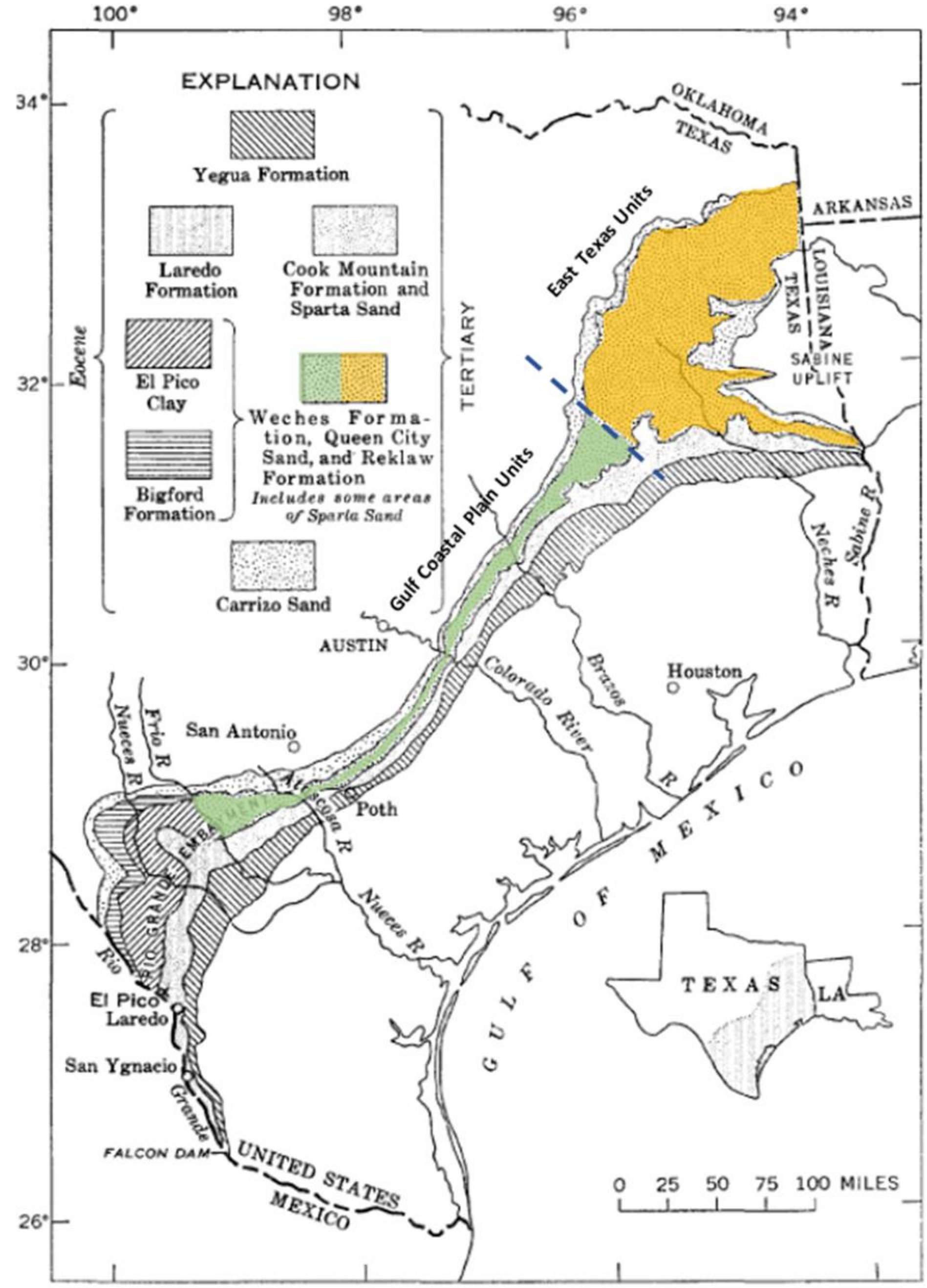

Figure 14. Regional view of Eocene Formations. The lower Claiborne units are highlighted with the eastern extent in yellow and Gulf Coastal Plain area in green (from Eargle 1968).

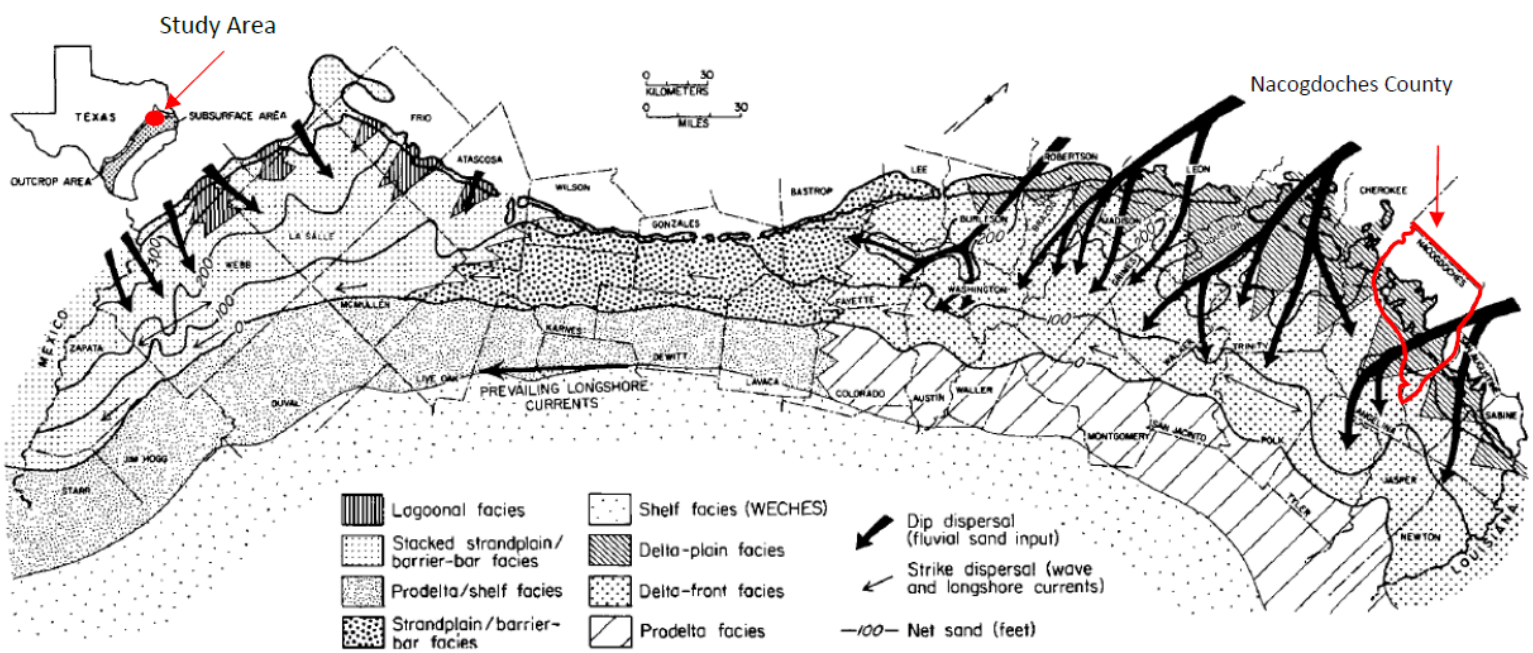

Figure 15. Distribution of facies and inferred dispersal systems of Sparta depositional systems, Texas Gulf Coast Basin. Illustrates how the Sparta Formation originated as a prograding Delta in East Texas. This delta would have migrated over the Weches Formation explaining how the environment rapidly changed from marine to non-marine (From Ricoy and Brown 1977).

The Weches Formation Depositional Setting

The deposition that occurred in the East Texas basin can be summarized as: (1) Jurassic deposition of a thick layer of salt unconformably on Paleozoic basement rocks, (2) platform carbonates and evaporates (Smackover, Buckner, and Gilmer Formations), (3) Travis Peak siliciclastics progradation as deltas, and (4) Late Cretaceous and younger units alternating between marine carbonates and siliciclastics (Seni and Jackson, 1984).

The Weches Formation is in the middle of the Eocene aged Claiborne group as shown in figures 10, 11 and 12. As demonstrated by faunal assemblages (Andrews, 1975), marine sediments and stratigraphic relationships, the Weches Formation represents a marine transgression. At its base (Tyus Member; figure 10) the Weches represents a moderately shallow, clear marine water, littoral facies (Crocker, 1995). Shells at the base of the Formation are rolled and waveworn and fragmented indicating high energy wave action (Sellards et al., 1932). Stenzel (1938) came to the same conclusion on the basis of shallow water gastropods. Feray (1948) suggested that the environment of the Tyus Member was warm, clear, agitated water less than 36 feet (11 meters depth), based on relationships between foraminifera and sedimentary characteristics. Stella (1986) noted that communities of organisms deposited in the Weches are dominated by suspension feeding organisms which indicates clear waters with low turbidity and low rates of sedimentation in order for those organisms to flourish.

The overlying Viesca Member is thought to represent slightly deeper waters. Feray (1948) noted an abundance of glauconite and bioturbation and postulated that the Viesca Member may have been around 36 to 89 feet (11 to 27 meters) deep in a subtidal zone. Curtis (1954) interpreted the Viesca as having a slow rate of deposition in chemically stable water and that it had minimal influence from tectonic activity based on the glauconite. He also concluded that water depths ranged from approximately 3 to 300 feet (1 - 100 meters) in the Smithville area based on variations in frequency percentage of foraminifera, and temperatures of around 14º C, pH of around 8 and a low turbidity of water based on the presence of oyster banks (Curtis 1954). However, since those early studies, no significant amounts of glauconite have been found using XRD analysis (Ledger, 2006). While the term glauconite is often employed to describe the green clay in the Weches, this should be considered a field term probably does not actually represent the mineral glauconite. Instead, the green clay has been described by Brown et al. (1969) as a mixed-layer montmorillonite, which can mean a clay with a very disorganized structure. Hugget et al., (2006) identified the multiple layers and determined that the assemblage closely resembles a berthierine-like serpentine clay (Foos, 1985; Godley, 1998; Hsieh and Yapp, 1999). Berthierine is a clay from the chlorite group of phyllosilicate minerals. More specifically, berthierine is a hydrous aluminum clay silicate with iron thought to form on the inner shelf (Ledger, 2006), but it has also been found presently forming on the outer shelf of New South Wales (Marshall, 1983). Hugget et al., (2006) believed this assemblage of clay minerals to be representative of having formed in approximately 68^0 F (20^0 C) waters. For simplicity, in this paper, the term glauconite should be considered a field term denoting a green to dark greenish clay.

In East Texas, the Weches Formation has been interpreted as a marine unit deposited on or near the middle shelf (Stella, 1986). This is consistent with observations of the outcrops throughout this study, with samples typically being greenish glauconitic claystone with fossils that are well preserved when present. The rock is typically weakly indurated with no fissility and is made up primarily of sand-sized pellets with a green to grey clay matrix which weathers to yellow or red. Andrews (1975) determined that the upper and lower Members of the Weches Formation, the Therrill and Tyus, represent prodelta shallow water and low energy regimes while the middle Member, the Viesca represents a deeper water, normal marine shelf environment. Stella (1986), with a thorough paleocommunity study, concluded that there was a depth increase from the base of the Weches to the top and that the shoreface migrated northward later in the Eocene.

Many of the studies concerning individual members of the Weches are focused on a single locale. The variation in findings may indicate that the Weches is not as laterally uniform as has been thought. According to Crocker (1995) the initial Weches deposition occurred in near constant estuarine circulation. The reason behind this theory is that iron in the Weches is in the ferrous state. Formation of ferrous state iron requires anoxic/acidic conditions. In order for these conditions to exist in a shallow marine environment Crocker proposed that the freshwater influx brought in enough nutrients to support high rates of plant life, enough to create a barrier of decaying plant detritus conducive to an anoxic environment at the sea floor. This idea does not conflict with the idea that the Weches was deposited with low sedimentation rates because the estuarine fresh water influx did not necessarily have to be carrying sediment with it. While a lagoon could also provide favorable conditions, there is no evidence for a structural barrier restricting the ocean (Crocker, 1995).

CHAPTER 3: STRUCTURAL SETTING

Overview

The tectonic history of East Texas is more complex than its gently rolling hills and flat-lying surface strata might suggest. Hidden in the subsurface on the west side of the East Texas basin is the Ouachita/Marathon fold belt which originated during the Late Paleozoic collision of the North American plate with smaller continental fragments such as the Yucatan plate and eventually with South America (Pindell, 1985; Viele and Thomas, 1989; Wickham et al., 1976). The Ouachita system is a belt of deformed Paleozoic and older rocks bordering the southern edge of the cratonic interior of North America, and, like the Appalachian system on the eastern edge, originated during assembly of Pangea. The Ouachita fold belt is comprised of complex folds, imbricates, thrust faults, duplexes and refolded structures (Abbott, 1973; Muehlberger and Tauvers, 1989). The base of the Ouachita belt is a major décollement juxtaposing allochthonous Ouachita rocks over North American basement while the upper surface is a low-relief erosional surface which originated prior to deposition of the Jurassic strata of the Gulf Coastal Plain (Viele, 1989). The Pennsylvanian Ouachita fold and thrust belt crops out in Arkansas and Oklahoma but is buried across most of north and central Texas. It extends in the subsurface to southwest Texas beneath Mesozoic sediment and reemerges in west Texas in the Marathon fold Belt (Thomas, 1976) (figure 16). The supercontinent Pangea was fully assembled by approximately 335 Ma then later broke apart – which led to the opening of the Atlantic – starting around 180 Ma and continuing to the early Cretaceous (Klitgord et al., 1984).

The Gulf of Mexico began to form when proto-North America and the Yucatan microplate started to rift apart in the Triassic (Pindell and Dewey, 1982; Salvador, 1991). Its evolution took place largely in the Jurassic and can be split into to four phases: (1) large scale extension between the Yucatan microplate and North American plate from 210 – 163 Ma (Late Triassic to Late Mid-Jurassic) with the Louann Salt deposited on the resultant depressed and extended lithosphere; (2) salt deposition from 163 – 161 Ma (Late Jurassic); (3) post-salt crustal stretching and spreading of the basin from the middle, separating it into two halves from 161 to 154-149 Ma (Late Jurassic); (4) and sea floor spreading from 154-149 to 137 Ma (Late Jurassic – Early Cretaceous) (Hudec et al., 2013). Major regional subsidence of the Gulf of Mexico basin occurred during the Late Jurassic and Cretaceous and continued through the Tertiary along with uplift of its northwestern margin (Murray 1961; Abbott 1973). Crustal extension caused by subsidence of the Gulf of Mexico geosyncline and the accompanying uplift of the Edwards plateau led to the formation of the Balcones Fault zone as tensional stresses created a system of down-to-the-coast, en-echelon, high angle normal faults that presently extend as a 10 to 12-mile-wide zone paralleling the Ouachita trend (Abbott, 1973; Foley 1926; Collins, 1995). This feature can be seen in figure 17. While the Balcones Fault Zone appears to be influenced by the buried Ouachita structure (the Balcones fault zone parallels the Ouachita trend changing from a nearly east-west to nearly north-south between Dallas and Austin) the faults in the system have relatively consistent strike (between 55^0 to 65^0) that accommodated Paleogene to Neogene regional extension, most of which occurred during the late Oligocene to early Miocene (Weeks, 1945; Young, 1962; Ferril and Morris 2008). This pattern of faulting in the Balcones fault system is indicative of a direction of greatest horizontal compressive stress in the direction of approximately N60^0E (Ferrill et al., 2004b).

To the east, in the central gulf coastal plain of Mississippi, lies the Mississippi Reelfoot Rift beneath The Mississippi River valley (figure 16). This structure has been interpreted as a Cambrian aulacogen buried under up to 5 miles (8 km) of Phanerozoic sediments, and reactivated during Pangaean assembly (Ervin and McGinnis, 1975; Thomas, 1991). Quaternary reactivation of Reelfoot Rift basement faults has resulted in an area of high seismic activity known as the New Madrid seismic zone (Csontos, 2007). Csontos et al., 2008 has interpreted this area as being influenced by a Quaternary N60^0E maximum horizontal compressive stress field of eastern North America; this resulted in relative uplift and subsidence of the eastern and western halves of the Reelfoot rift as well as the formation of compressional stepovers.

Closer to Nacogdoches, the structural setting of East Texas is defined by five main features: (1) The East Texas Salt Basin, (2) the Sabine Uplift, (3) the Angelina-Caldwell Flexure, (4) the Mexia-Talco Fault Zone and (5) the Elkhart-Mt. Enterprise Fault Zone (locations shown on figures 16 and 17). Most of these structures are characteristic of a passive margin basin (Jackson and Laubach, 1988). Because the Weches Formation was deposited in the Eocene, special attention is given to Cenozoic tectonism. Fault geometries in and around the East Texas Basin are typically normal or listric normal faults oriented between NE/SW and E/W which accommodated moderate, mostly southeast-directed, Cretaceous to Tertiary extension, with mobilization likely due to subsurface salt movement (Jackson and Laubach, 1988; Jackson, 1982) and possibly also basinward creep. The nature and relationship of the features listed above are briefly summarized in the remainder of this section and then each feature is discussed in more detail in the following sections.

The East Texas Salt Basin is a structural low in the northeastern corner of Texas that was initiated during the breakup of Pangea and continued to subside from sediment load (McGookey, 1975). The Mexia-Talco Fault Zone is a graben system that stretches from Bowie to Robertson County following the shape of the buried Ouachita Mountains and which defines the updip limit of the Louann salt

(Jackson, 1982). The Sabine Arch is a broad structural dome located on the eastern flank of the East Texas Basin, while the Angelina Flexure is an anticlinal hinge defining the southern margin of the basin. The Elkhart-Mt. Enterprise Fault Zone is located just north of Nacogdoches and extends from the center of the Sabine Arch to the Angelina Flexure (figure 17). The Angelina-Caldwell Flexure is a structural high separating the East Texas basin from the Gulf basin that formed as a hingeline between flexural subsidence in the south from Cenozoic loading and flexural uplift and erosion in the north (Ewing, 2009).

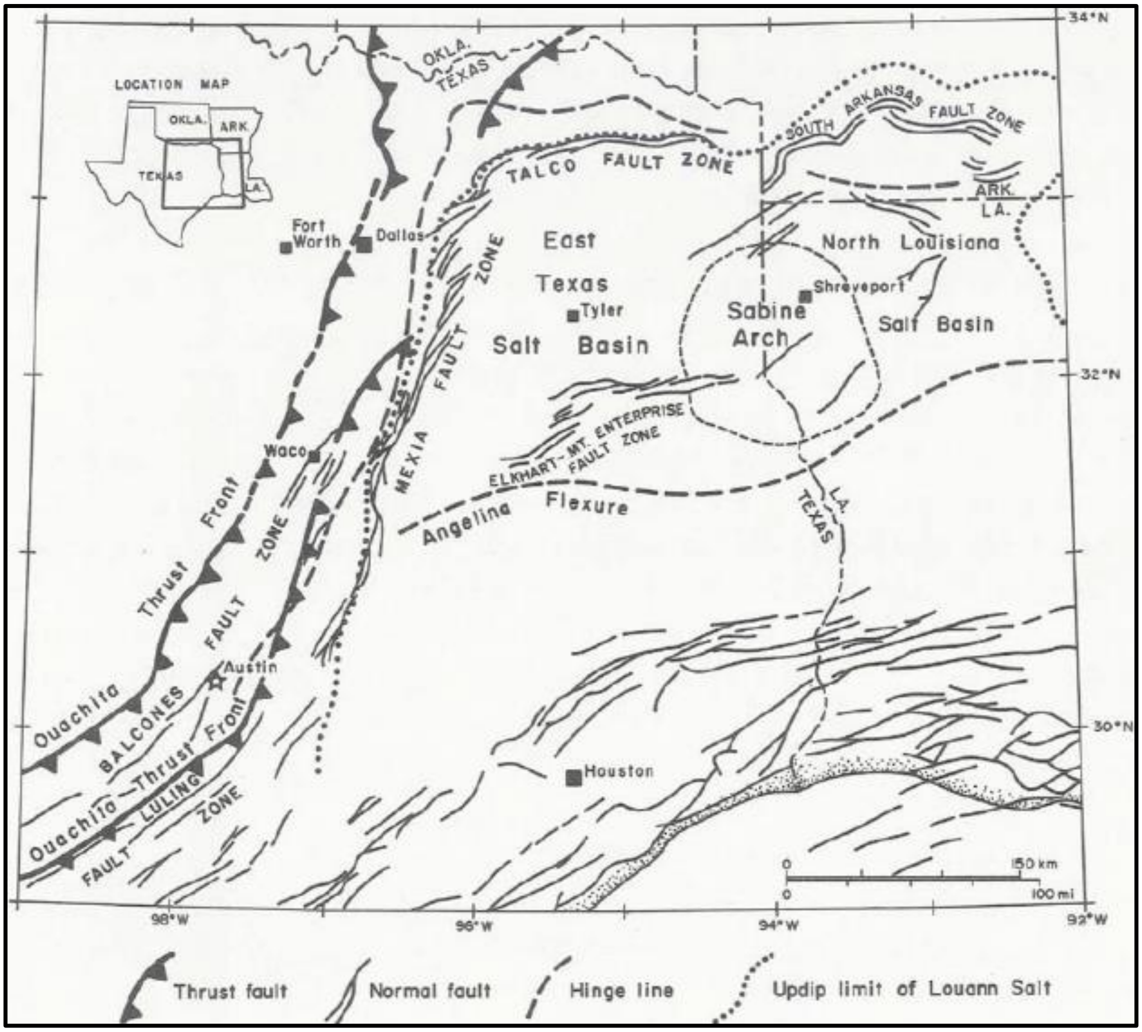

Figure 16. Regional setting of Ouachita-Marathon Fold Belt. In the southwestern corner of the map the Balcones Fault Zone can be seen trending from west to northeast paralleling the Mexia-Talco Fault Zone. The Ouachita Thrust Front follows the same trend and curves back east-west to the north off of the map. The trace of this feature through Central and East Texas sets the trend for the Mexia-Talco Fault Zone (modified from Gleason et al., 2007).

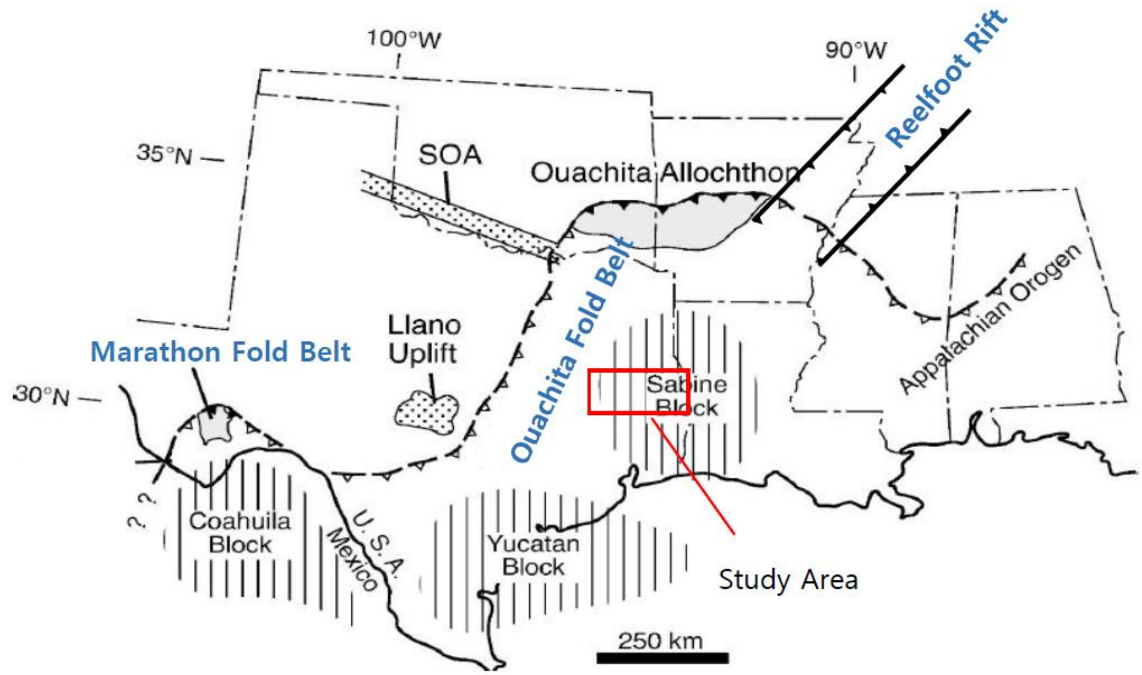

Figure 17. Regional tectonic setting of East Texas. Note the position of the East Texas basin with the Angelina Flexure forming the structural southern border, and the Sabine Arch, Mexia and Talco Fault Zones bounding the other borders (from Jackson 1982).

East Texas Basin

The East Texas Basin is a structural low located in the northern margin of the Gulf Coastal Plain. Like many other Mesozoic basins originating in the Triassic period from Texas to Florida, it formed as a rift basin during the Late Triassic-Early Jurassic break up of Pangaea (Wood and Walper, 1974; McGookey, 1975). Initial subsidence and crustal attenuation was conducive to deposition and the weight of accumulating sediments caused further subsidence of the central part of the basin to a depth of around 7,000 m (Foote, 1988). The East Texas Basin is about 100 miles (160 km) across and is located in the northeastern corner of Texas near the Louisiana border. It is bounded to the east by the Sabine uplift, to the south by The Mt. Enterprise Fault Zone and Angelina Flexure and to the west and north by the Mexia-Talco Fault Zone. A detailed map of the basin border was made by Baumgardner (1987) and can be seen in figure 18. The basin is made up of sedimentary formations ranging in age from Upper Triassic to Neogene (cross section in figure 19). Strata in the east, west and north dip towards the depocenter of the basin where salt has been evacuated vertically (Jackson and Seni, 1984). Subsurface faults in the central part of the basin are salt-related structures. Seismic interpretation has confirmed the spatial correlation of salt structures with faulting and with development of clusters of lineaments (surficial linear features often produced by faulting) around salt body locations (Seni and Jackson 1984; Dix and Jackson 1981; Wood and Giles, 1982). Igneous and metamorphic basement rocks beneath the basin are made up of Paleozoic units and Triassic rift fill. An erosional event created a planar surface on this basement where large amounts of Jurassic Louann salt (up to 1,500 to 2,100 m) would be deposited. The immense amount of salt deposition was the result of the widespread formation of evaporates in the incipient Gulf of Mexico during rifting between the North American and South American Plates as the developing basin was periodically inundated with sea water (Salvador, 1991). This salt layer has been the source for all salt bodies in the basin and, because it was weak, provided a surface for overlying sediment to glide over leading to movement both vertically and laterally (Rowan et al., 1999). Compared to the post-Louann salt units, the basement itself has remained fairly undeformed with some gentle downwarping caused by sediment loading and some uplift in the Sabine area (Granata, 1962; Kreitler et al., 1981). However, Fowler (1964) postulated that normal faults and grabens in the younger strata may be genetically linked to deep vertical faults in the Paleozoic basement rock. He found that surface and gravity data from a survey in Cass County, Texas indicated a basement fault merging with normal faults of the Talco Fault Zone (Fowler 1964). A generalized illustration of the theory is shown in figure 20.

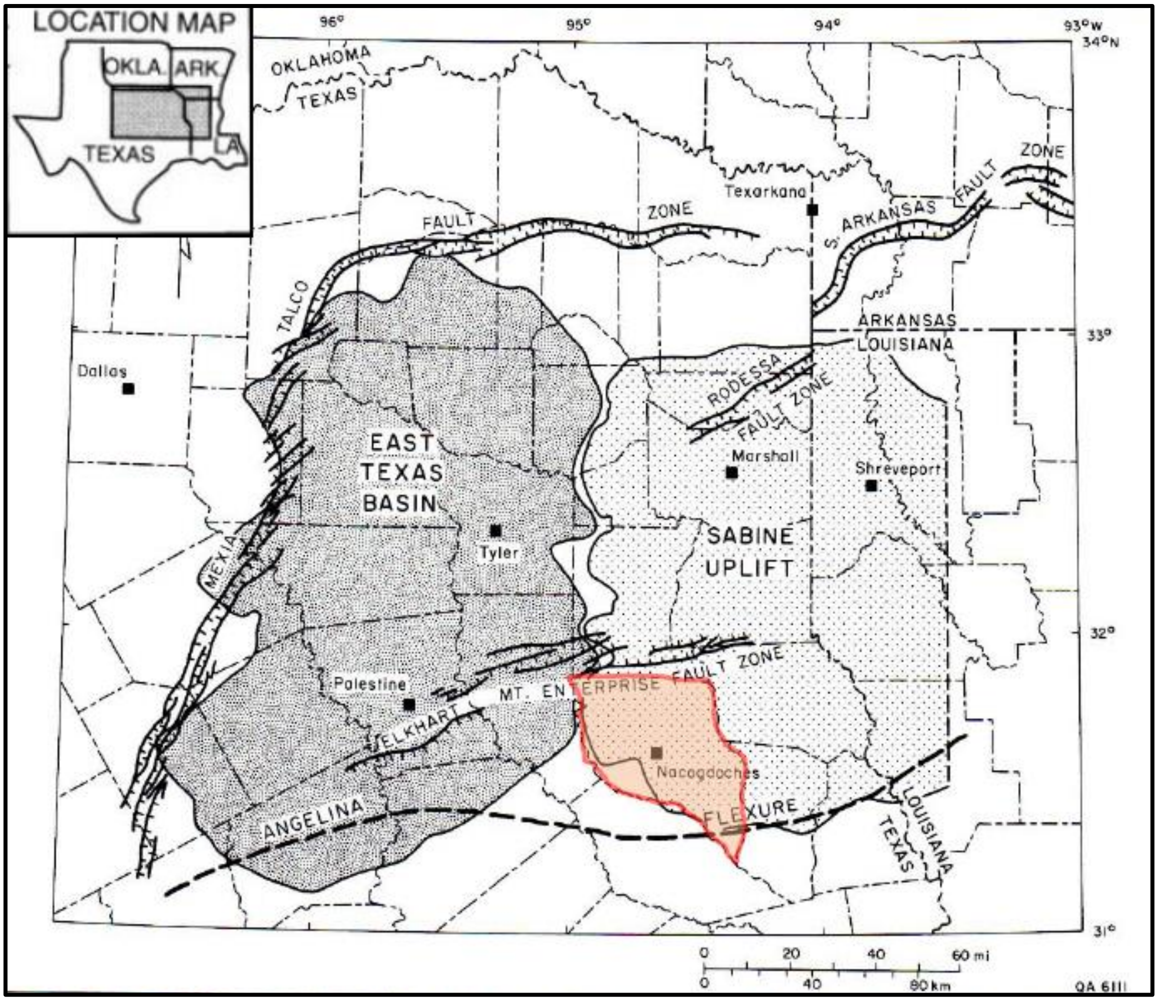

Figure 18. Structural setting of major East Texas features with detailed delineation of East Texas Basin and Sabine Uplift border (modified from Baumgardner 1987).

The salt diapir province in the East Texas Basin contains parallel normal faults in the deep subsurface related to movement of underlying salt. Salt diapirs in the East Texas basin vary in size but none are located in the direct vicinity of Nacogdoches. While many of the structural elements in East Texas are tied to the movement of Louann Salt, the Sabine Arch and the Angelina-Caldwell Flexure, however, are not related to salt movement (as will be discussed below). Studies of the growth rates of salt-domes in East Texas has shown that by the Early Paleogene they had reached a mature stage of growth characterized by slow, steadily declining rates of rise, estimated to be less than 0.004 inches (.1mm) per year (Seni and Jackson, 1983). The outer section of the basin contains planar salt surrounding an irregular area of salt pillows with salt diapirs in the center of the basin (Jackson 1982). The pattern of salt structures can be seen in map view in figure 21.

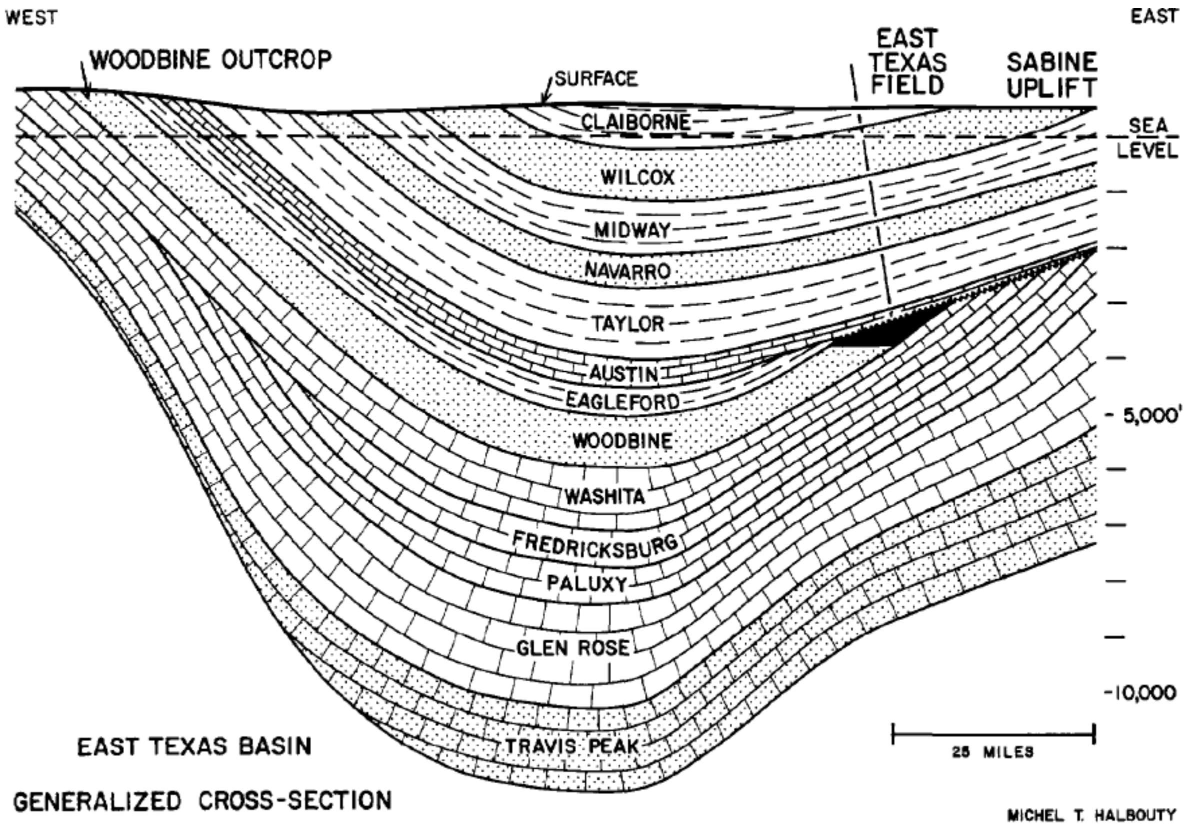

Figure 19. Generalized cross section of the East Texas Basin. It is based on seismic and borehole data. The trace is oriented E/W going approximately through the center of the basin. Note the East Texas field, a structural and stratigraphic trapped accumulation of oil. This cross-section does not show the older formations in the basin, such as the Jurassic Louan Salt (From Halbouty, 1991).

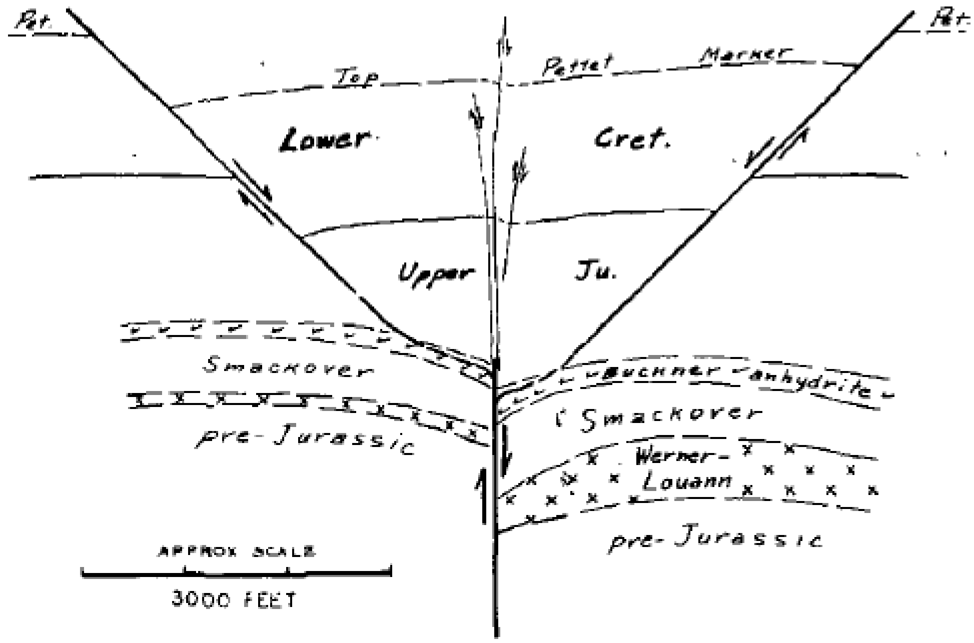

Figure 20. Diagram illustrating the link between deep vertical faults in the East Texas basement rock to normal faults and grabens in the overlying younger strata (from Fowler, 1965).

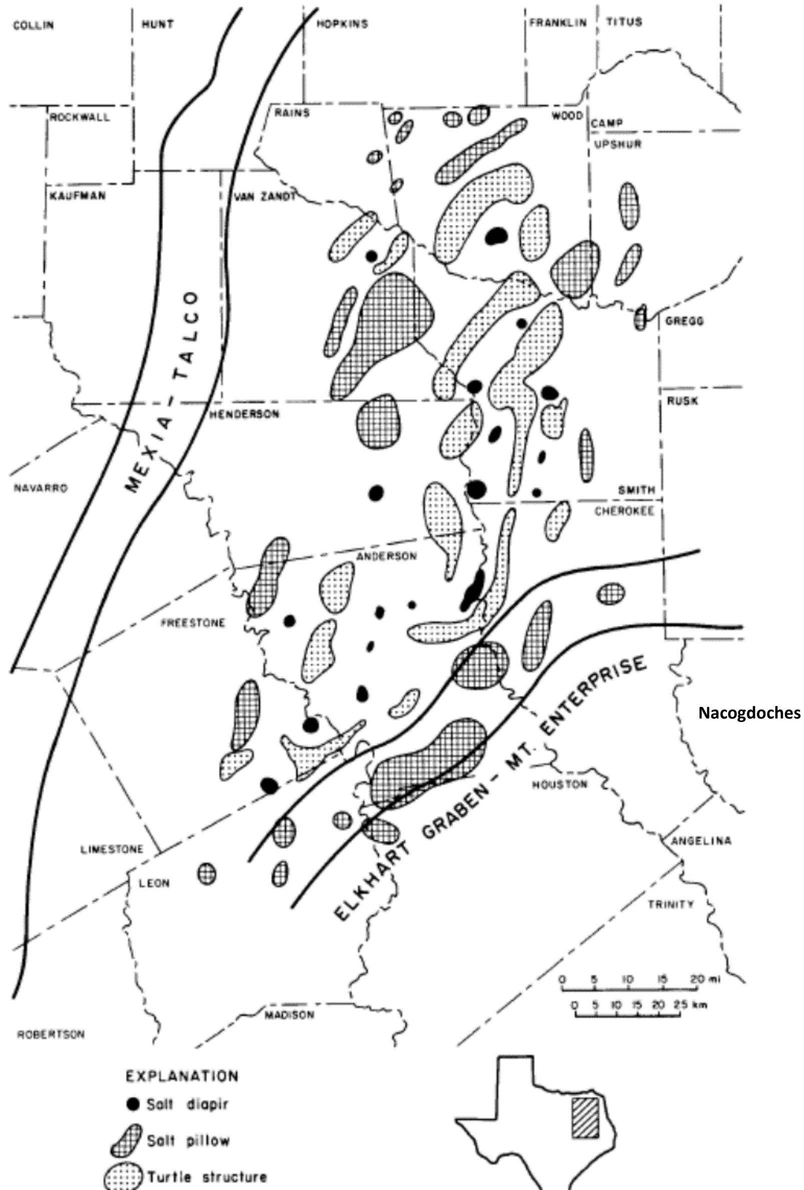

Figure 21. Map of salt structures in the central East Texas Basin. Three main salt related structures prevail in the East Texas Basin: (1) Salt diapirs which are cylindrical columns of salt that form passively between minibasins or actively as an upward migration, (2) Salt Pillows which are a rounded upwellings of salt that form during the earliest stages of salt doming and (3) turtle structures which are minibasins that expand outward as the base of the salt structures that form the flanks of the basin migrate outward. Note the pattern of salt diapirs in the center of the basin and pillows on the outer areas with turtle structures in between (from Seni and Jackson 1983).

Mexia-Talco Fault Zone

The Mexia and Talco Fault Zones are strike-parallel normal fault systems connected by a zone of en echelon normal faults at the “Great Bend” in Kaufman and Hunt Counties (where the trend changes from NE-SW to almost E-W) and are about 5 to 10 miles (8 to 16 km) wide (Walthall and Walper, 1967; Jackson, 1982). These fault zones coincide with the updip limit of the Louann Salt (as shown in a cross section of the Mexia-Talco Fault Zone in figure 22) (Wood et al., 1981). Each graben in the Mexia Fault Zone averages about 1 to 1.4 (1.6 to 2.3 km) miles in width and 5 to 15 (8 to 24 km) miles in length with an average strike of about N45^{o}E while the fault system itself trends approximately N20^{o}E along the western border of the East Texas Basin (Rodgers, 1984). Figures 16 and 18 illustrate the trend of the Mexia-Talco Fault Zone in map view. The Mexia Fault Zone intersects the Talco Fault Zone to the north and the Balcones and Luling Fault Zones to the southwest. Together, the Mexia-Talco Fault Zone forms the northern and western boundary of the East Texas basin. The Mexia Fault Zone connects with the Talco Fault Zone in Hunt County and trends east towards Arkansas. Grabens in the Talco Fault Zone are 1 to 2 (1.5 to 3 km) miles wide and 8 to 15 (13 to 24 km) miles long with strike deviating from the general trend (east) of the system by about 5^{0} to 10^{0} north (Rodgers, 1984). Movement of these fault zones was contemporaneous, with both being active from the Jurassic to at least the Eocene where late stage faulting accommodated Paleogene regional extension (Jackson, 1982; Rodgers, 1984; Ferrill and Morris 2008). The faults extensively displace Mesozoic and lower Paleogene strata. The fault system has been interpreted as having initially originated during the opening of the Gulf of Mexico as part of a series of step faults bounding the northern margin of the gulf which lasted until about the Middle Jurassic when the spreading center had migrated farther into the center of the Gulf (Buffler et al., 1980; Rodgers 1984). The mobilization of subsequent Louann salt deposits in the Late Jurassic to Eocene utilized these pre-existing faults to form a pull-apart structure between autochthonous salt-free strata (strata native to its original location) and downdip motion of parautochthonous strata (sediment being moved a small distance from its original location) above the salt layer (Wood et al., 1981; Jackson 1982; Rodger, 1984).

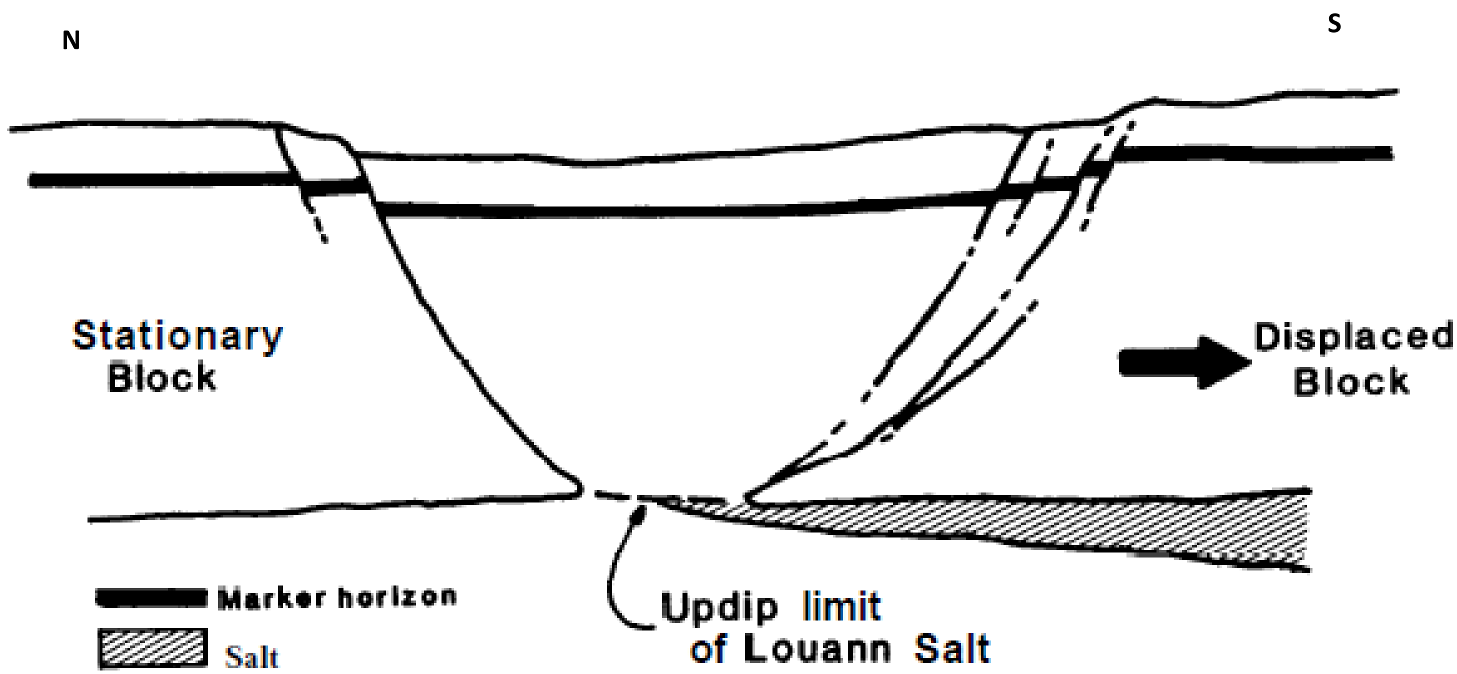

Figure 22. Sketch of a Mexia-Talco graben acting as the updip limit of Louann Salt movement. This type of graben system is common for the Mexia-Talco Fault Zone and is facilitated by the southward extension caused by salt gliding (From Jackson, 1982).

Elkhart Graben – Mt. Enterprise Fault Zone

The Elkhart Graben makes up the western edge of the Elkhart-Mt. Enterprise Fault Zone and overlies salt pillows which likely initiated the fault movement (Jackson, 1982). It consists of parallel, normal faults with multiple offsets that define a graben approximately 25 miles (40 km) long trending east-west from Leon to Cherokee County. The location of the fault system in the study area is shown in figure 23. Most of the displacement occurred in the Early Cretaceous and shares a similar timing and mechanism to the salt movement-induced normal faults in the central basin (based on fault geometry) (Jackson 1982). The youngest unit transected by the Elkhart-Mt. Enterprise Fault Zone is the Cook Mountain Formation (Claiborne Group) which formed during the Eocene, approximately 40 Ma (see stratigraphic section figure 10) (Rodgers, 1984; Jackson, 1982). The Elkhart faults are downthrown to the north towards the East Texas basin resembling the listric growth faults of the Gulf Coast, but with an opposite orientation. A cross section through the central part of the fault system is shown in figure 24.

The Mt. Enterprise Fault Zone makes up the eastern half of the system and trends almost E-W with dips of 35 to 60^{o} northward or southward. An approximate trend of the major faults in this system is shown in figure 25 and bears a striking resemblance to the joints measured in the Western and Central Region of the study area. This relationship is discussed in Chapter 7.

It is made up of approximately parallel and en-echelon normal faults. The Mt. Enterprise Fault Zone does not overlie any major salt structures, coincide with the Angelina flexure or show any geometric relation to the growth of the Sabine Arch (Jackson 1982). The Mt. Enterprise Faults are similar in appearance to Gulf Coast growth faults but with an opposite sense of throw. It is likely that the fault zone is still active with earthquake activity recorded northeast of the town of Mt. Enterprise in 1957 (Collins et al., 1980).

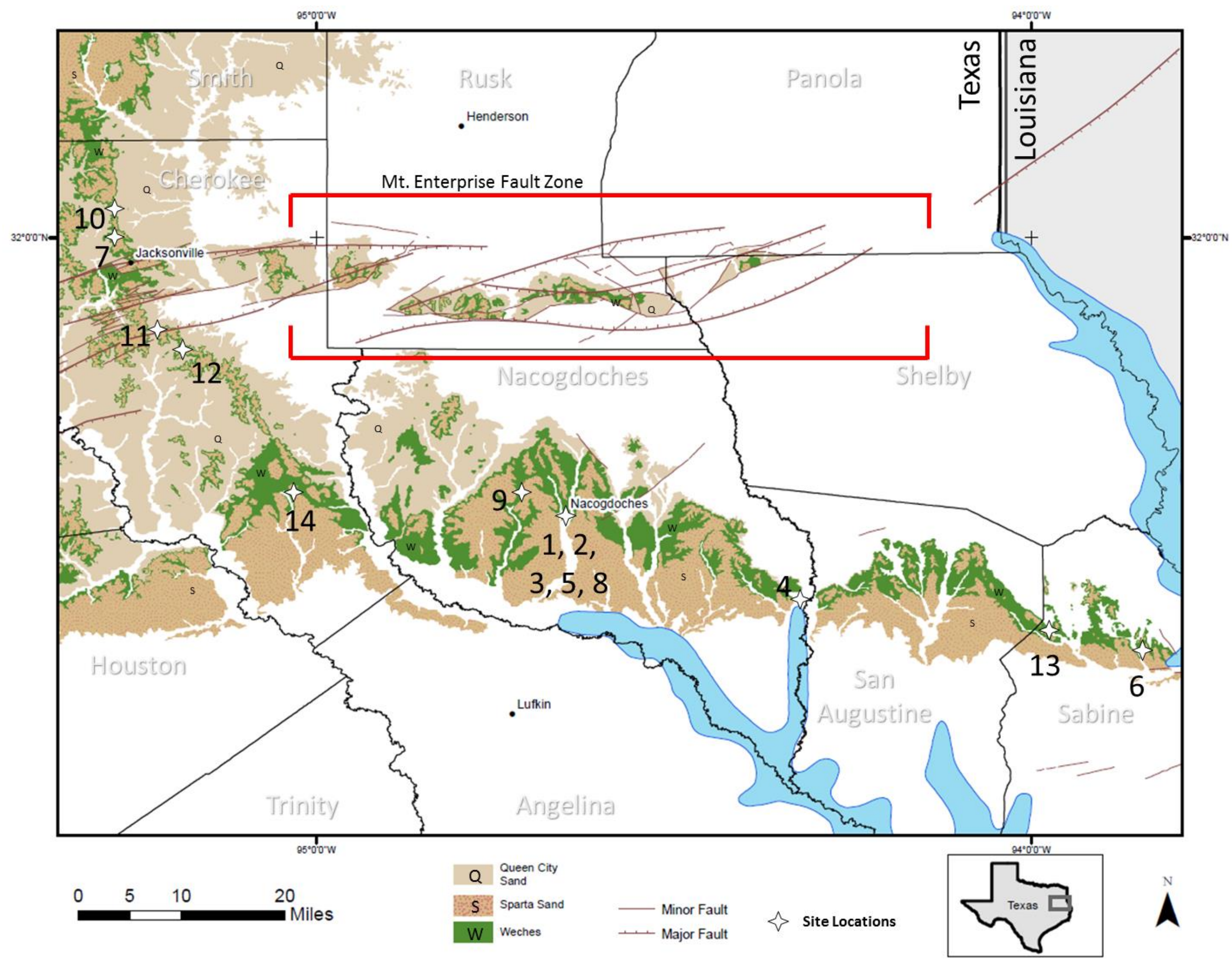

Figure 23 Figure: Geologic map of study area with Mt. Enterprise Fault Zone highlighted. Note the proximity to the site locations and interaction with the Weches Formation. Because of this It is important to consider the possible influence the fault zone could have on stress in the Weches Formation and thus joint formation.

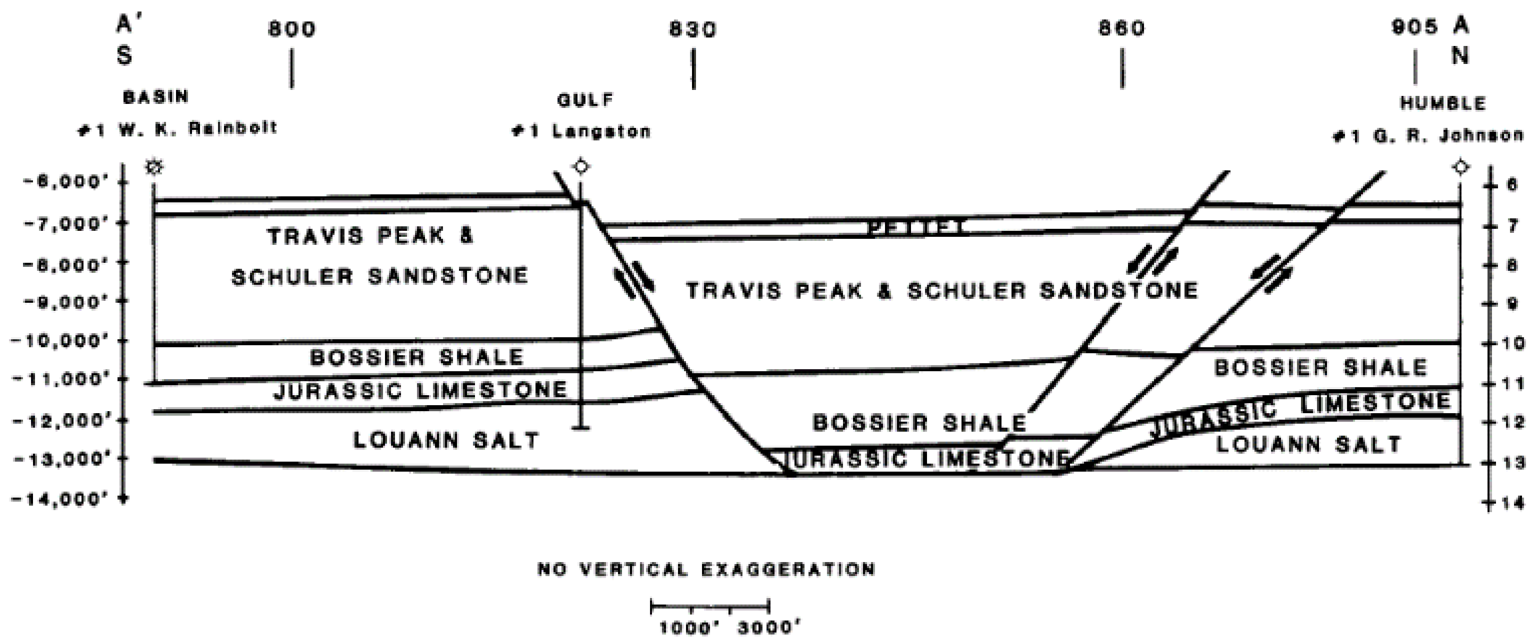

Figure 24. Cross section across the central part of the Mt. Enterprise Fault Zone. Displayed here is an east-west oriented graben running through southern Rusk County. Note the greater thickness of Louann Salt in the southern portion of the graben. This has been interpreted by Wood et al., (1981) and Ferguson (1984) as an upwelling of salt caused by sediment load which may explain the development of the Mt. Enterprise Fault system (from Ferguson 1984).

N=15

Mean Orientation: N78^{0}E

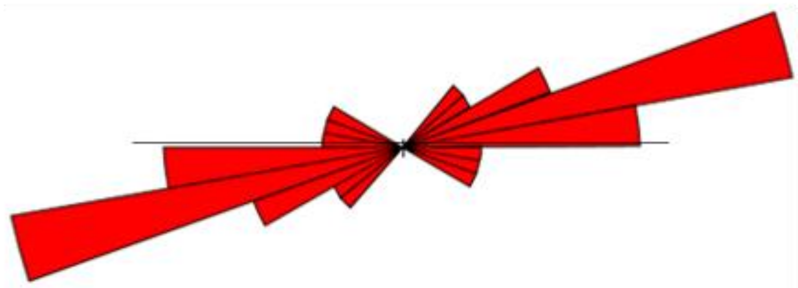

Trend of major faults in the **<u>Mount Enterprise Fault System.</u>**

N = 150

Mean Orientation = N80^{0}E ± 6^0

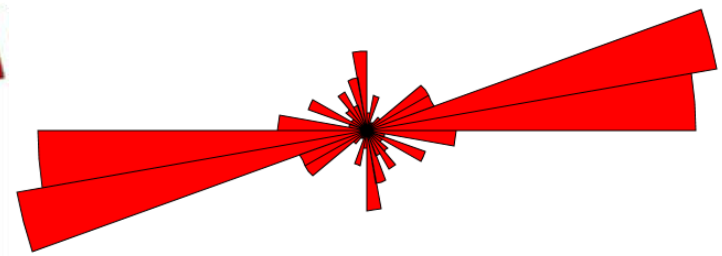

<u>Joints from the Central and Western Region</u> of the study area.

Figure 25 Rose diagram of the trend of faults in the Mt. Enterprise Fault system compared to joints in the central and western region. An approximation of the trends of 15 major faults in the fault system is shown here. This was done by measuring the trace of faults taken from the Geologic Atlas of Texas. Note that the average strike is N78^{0}E, which is roughly the same as one of the main sets of joints in the Weches Formation.

There are two prevailing tectonic models explaining fault development of the Mt. Enterprise Fault Zone. (1) Fowler (1964) supported a model indicating these faults were extensions of faults in the basement pre-Jurassic rocks (the same mechanism displayed in figure 20). (2) Collins (1980) supported a model that tied the Mt. Enterprise Fault Zone to uplift created by post-Louann sediment deposition squeezing salt upwards. This theory was supported by Wood et al., (1981) and Ferguson (1984) who used seismic, borehole, and gravity data to show that the top of the Louann salt is structurally high to the south of the fault zone. A time sequence diagram for this theory is shown in figure 26. Prolonged extension and differences in rates of subsidence between the Louann and post-Louann strata may have had additional influence on fault movement (Jackson 1982).

Sabine Arch

The origin of the Sabine Arch (location shown in figure 18) has been vigorously debated for years (Granata, 1963; Halbouty and Halbouty, 1982; Adams, 2009; Jackson and Laubach 1988). It has bounded the eastern margin of the East Texas Basin since around the Early Jurassic Period (Granata, 1962; Halbouty and Halbouty, 1982). Because there are basins to the west and east, the uplift is a structural high between Cenozoic extension-related salt basins (Adams, 2009; Ewing, 2009). A cross-section of the boundary between the East

Texas Basin and the west flank of the Sabine Arch is shown in figure 27. The Sabine Uplift formed during the Triassic as a structurally high area during the same time that rifting formed the Gulf of Mexico. Current depths to the basement over the structure are much shallower than in the basins to the east and west (Adams, 2009). The Sabine Arch experienced uplift in the mid-Cretaceous and early Eocene (Jackson and Laubach, 1988). Possible mechanisms for arching were summarized by Jackson and Laubach (1988) as being: (1) uplift from deep-seated plutons, (2) lateral tectonic compression causing low-amplitude folding, or (3) buoyancy of the crustal element. The lateral tectonic compression model is typically the most accepted one, however, the two compressional tectonic events that took place when the arch was forming were the Laramide and Sevier orogenies whose main fold belts manifested much farther west. Jackson and Laubach (1991) noticed that faulting and folding in the uplift was contemporaneous with the Laramide Orogeny on the west side of North America. Adams (2009) has proposed that these compressional forces indeed had influence on the Sabine Uplift and were transmitted by a Laramide continental-scale wrench fault which originated near Saltillo, Mexico.

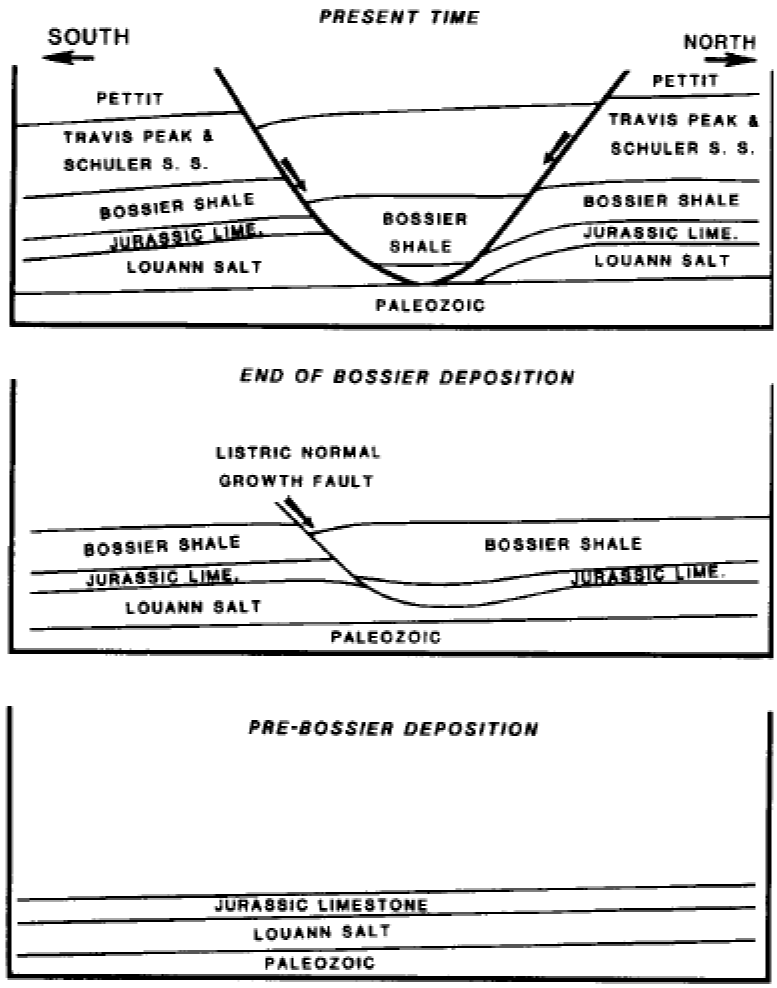

Figure 26. Time sequence diagram showing the evolution of the Mt. Enterprise Fault Zone caused by upwelling of salt to the south. This upwelling would have been caused by sediment load on the Louann salt layer to the north (from Ferguson, 1984).

Figure 28 illustrates in map view that this fault, correlated by surface and buried faults along with historical sites of seismicity, trends NE from Saltillo, Mexico until it is offset by the Mt. Enterprise Fault Zone where it then crosses over the Sabine Uplift and then continues NE/SW through the Reelfoot Rift system. In this theory the Sabine Uplift is a fault-fold or a pop-up block at the point of impingement (cross section of this model shown in figure 29). Periods of major uplift of the Sabine block were contemporaneous with Laramide tectonic activity, which support this theory (Jackson and Labauch, 1988). Figure 30 shows the results of a lab experiment designed to illustrate how restraining stepovers in strike-slip faults produce uplift (McClay and Bonora, 2001). A stepover is an area of localized compression or extension between to strike slip faults. The latter, known as a releasing stepover, can lead to normal faults and grabens while the former is known as a restraining stepover can lead to uplifts or “pop-up” structures which is a term describing domal uplift (Stone, 1995).

Synthesizing and understanding the principle tectonic activity over time as well as the structural setting in East Texas is essential for determining the stresses in the Weches Formation that generated jointing. This study focuses on Nacogdoches County and the surrounding area and joints in the Weches that may be tied to tectonic activity that occurred from the Cenozoic onward. The possible tectonic influences are discussed in Chapter 8 and include Cenozoic Gulfward tilting and subsidence, Paleogene extension and salt movement in the East Texas

Basin, theorized basement fault movement and/or lateral relief caused by Sabine Uplift.

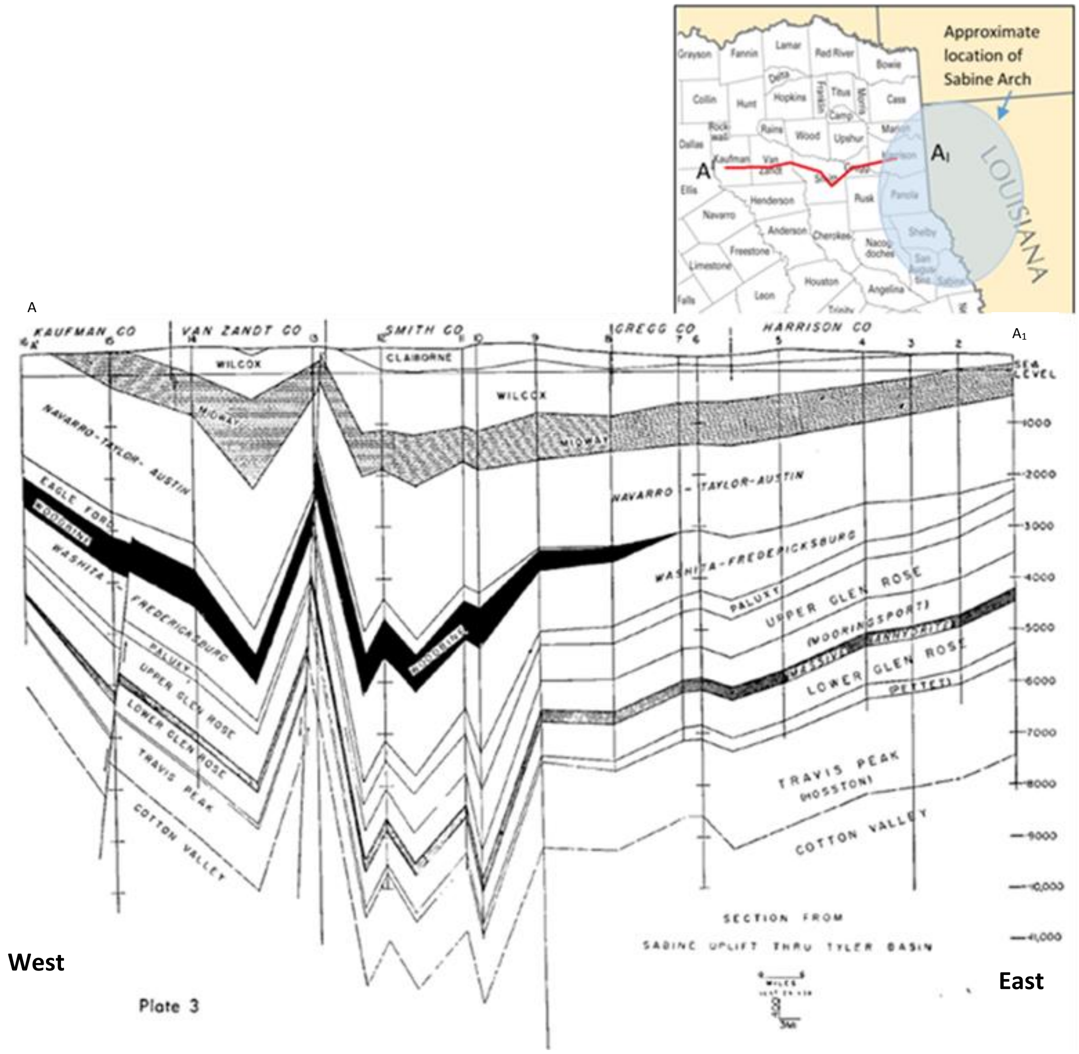

Figure 27. Cross section through the East Texas Basin and east flank of the Sabine Arch. Notice the likely presence of salt structures at Van Zandt and Smith Co and the gentle westward dipping of units moving closer to the Sabine Arch (from Coon 1956).

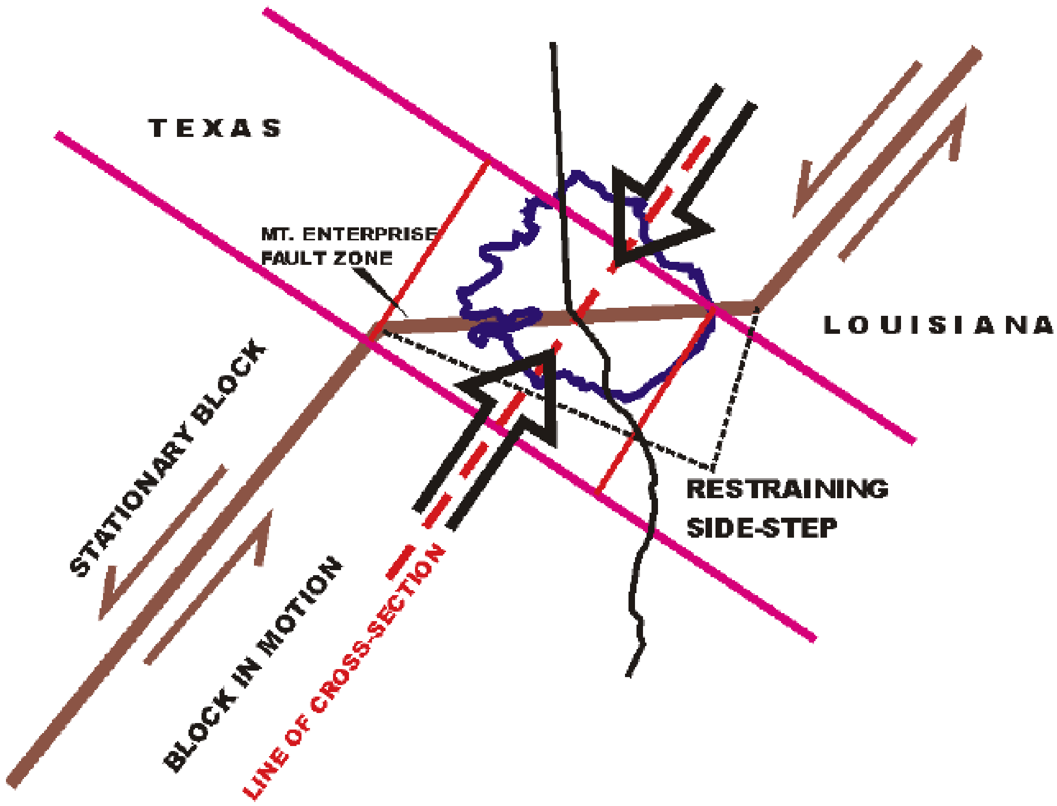

Figure 28. Regional view of a continental scale wrench fault oriented NE/SW. The fault becomes offset at the Mt. Enterprise Fault Zone where it crosses over the Sabine Uplift (dark, circular shape) (From Adams 2009).

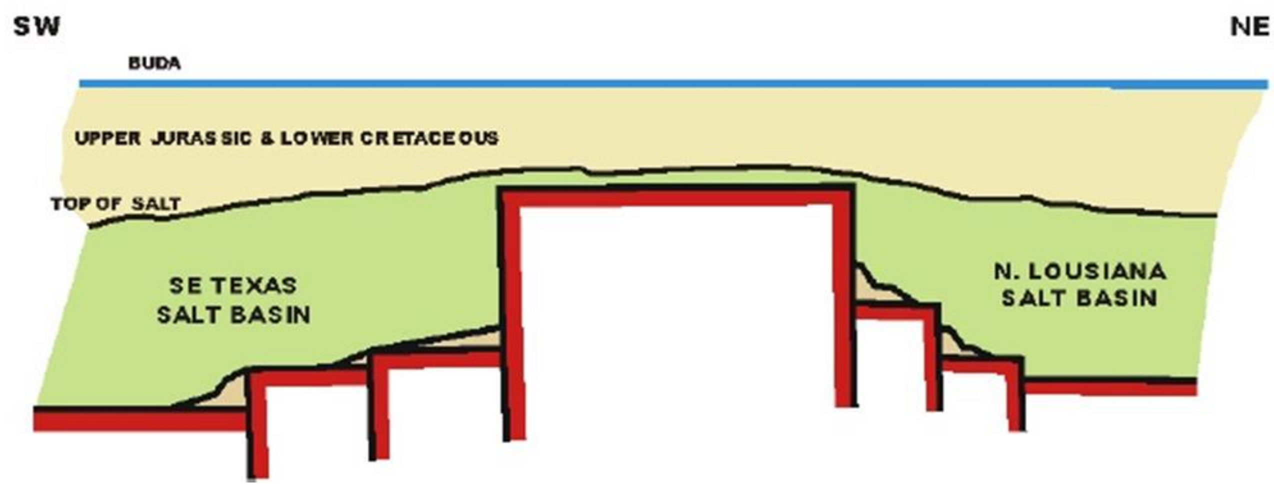

Figure 29. Crossection through the fault restraining side step. This illustrates structural elements in in the "Saltillo-St. Lawrence Shear System" illustrating how the Sabine Arch might have been a pop-up block (From Adam, 2009).

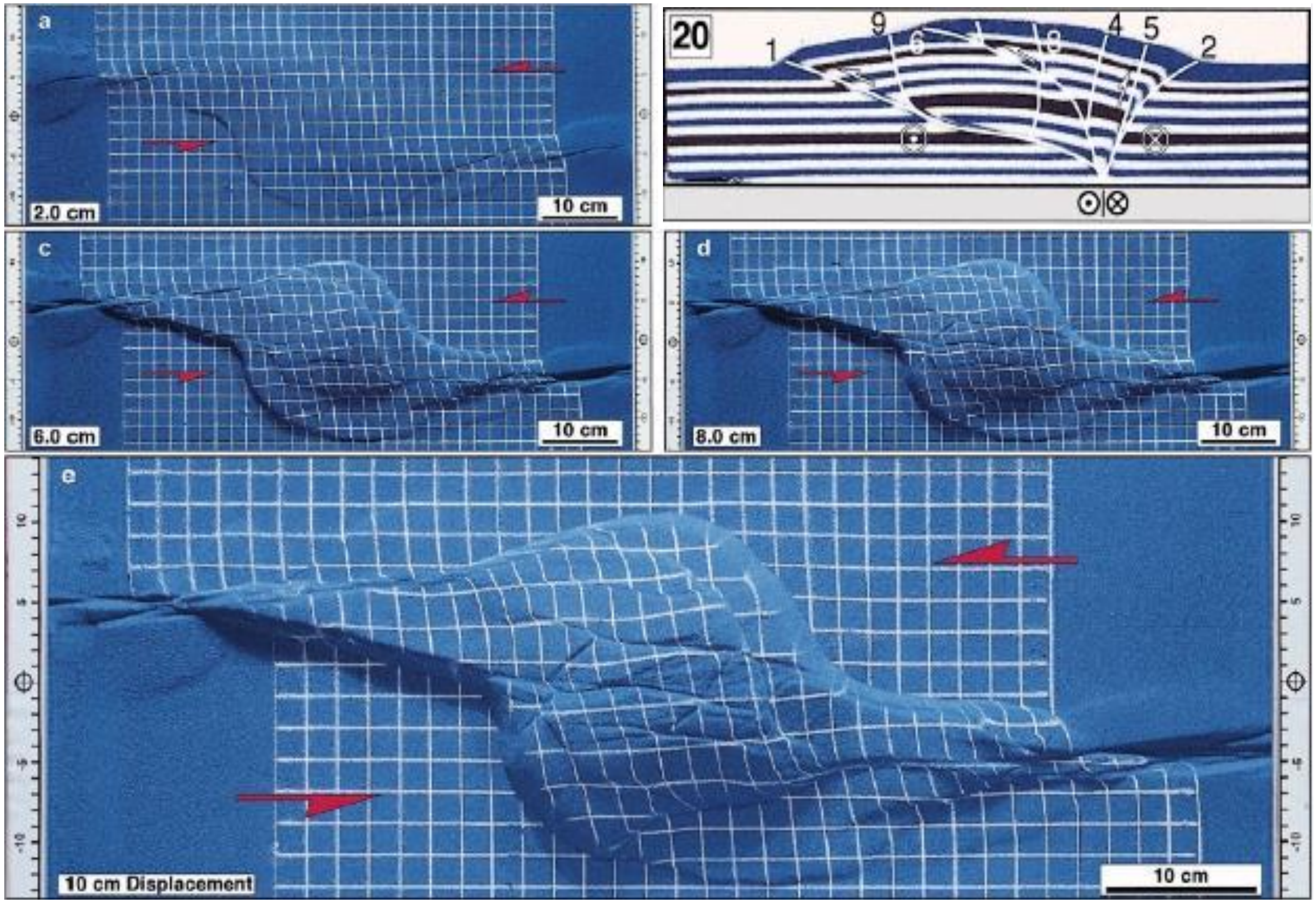

Figure 30. Lab study showing the mechanics of restraining step-overs in strike slip faults modified from (McClay and Bonora, 2001).

CHAPTER 4: STRESS REGIME AND FRACTURE ANALYSIS

Our understanding of joints

Fractures are one of the most ubiquitous features geology and can be found in almost any sedimentary rock at the surface. Despite this, the mechanics behind their formation remained mysterious for the better part of modern geology. By the 1980s our understanding of jointing had greatly increased. Kulander et al. (1979) provided a wealth of knowledge on the mechanics of fracturing as well as a basis of criteria for how to describe natural and core-induced fractures in an outcrop study. Pollard and Aydin (1988) summarized old and new concepts involving studies of jointing over the previous 100 years in published papers from the Geological Society of America Bulletin in their paper, “Progress in understanding jointing over the past century”.

Inferring stresses from natural fracture patterns

One of the most important properties of joint formation is that their strike is directly related to the direction stresses they formed in. Specifically, they propagate normal to the minimum principal stress and follow the trajectories of the stress field present at the time of formation (Engelder and Geiser, 1980). This makes them fairly reliable indicators of stress regime. Examples of published studies using natural and core-induced fractures as stress-indicators are presented in the following paragraphs.

Engelder and Geiser (1980) published one of the first studies relating jointing to the stress regime. They used joint orientations in the Appalachian Plateau to infer paleostress fields and to produce a kinematic model for the evolution of the New York Plateau. More recent studies have focused on the possibility of “neotectonic joints” or recently formed joints less than ~ 500 m from the surface (Engelder, 1985). Khadikikar (2002), examined systematic joints forming in late quaternary aeolianites in the Surashtra Peninsula, India. Their strike was found to closely resemble the trend of nearby stress trajectories determined through well-bore and seismic analysis.

Many papers have been published on stress regime and fracture analyses of rock units throughout Texas and elsewhere which were used in this study as a reference, or guidelines. Gough and Bell (1982) described the stress regime in East Texas using the orientation of borehole breakouts in the Schuler Formation which they concluded were parallel to the least principle stress. They described the stress regime in East Texas as being a tensional province, and postulated it was caused by Paleogene extensional listric normal faults in the East Texas area. They concluded that in such faults the maximum principal stress vector should be approximately vertical and the minimum principal stress horizontal and oriented at right angles to the extensional faults. It should be noted that the minimum horizontal compressive stress is, in effect, the same as the maximum extensional stress. The results from their study are shown in figure 31. Strubhar et al. (1975) presented similar results showing vertical fractures essentially oriented east-west in an inclined well drilled in northwestern Louisiana. Zemanek et al., (1969) and Brown et al. (1980) showed similarly oriented fractures in their studies of East Texas / Northwest Louisiana. Laubach 1989 studied the Travis Peak formation in the Western Flank of the Sabine Arch. From analysis of 565 natural and coring-induced fractures, Laubach determined that fractures in the Travis Peak formation of East Texas had an east-north east strike and provided a potential for acting as a conduit for oil and gas. Laubach was able to determine propagation depth as well as fracture diagenesis by studying the nature of the vein minerals and using SEM to observe microcracks. He postulated that the role of tectonism was necessary to create a systematic set of east-northeast striking joints. The conclusion was that this came in the form of south-south east directed extension which may have resulted from Gulfward tilting and subsidence in the Cretaceous or Paleogene northeast-directed compression during the growth of the Sabine Arch. Collins and Luneau (1986) studied fractures in the Palo Duro basin area, and Mainster and Coppinger (1986) studied fractures in the Austin Chalk in the Olmos basin. Brown et al. (1980) identified subsurface fracture orientations in the Cotton Valley Group of East Texas in an effort to optimize the locations of wells for effective drainage.

Gough and Bell believed that the Gulf Coast tensional provenance lies as far north in East Texas as the Mexia-Talco Fault Zone. Recent fault movement in the Elkhart-Mt. Enterprise Fault Zone (Collins et al., 1980), along with hydraulic-fracture stress tests in the Travis Peak Formation (Holditch et al., 1987), suggest that the modern least horizontal stress trends north-northwest. Since 2009 an ongoing collaborative effort has been made to compile global present-day stress field information in what is called the World Stress Map Project. Figure 32 shows the East Texas portion of this map.

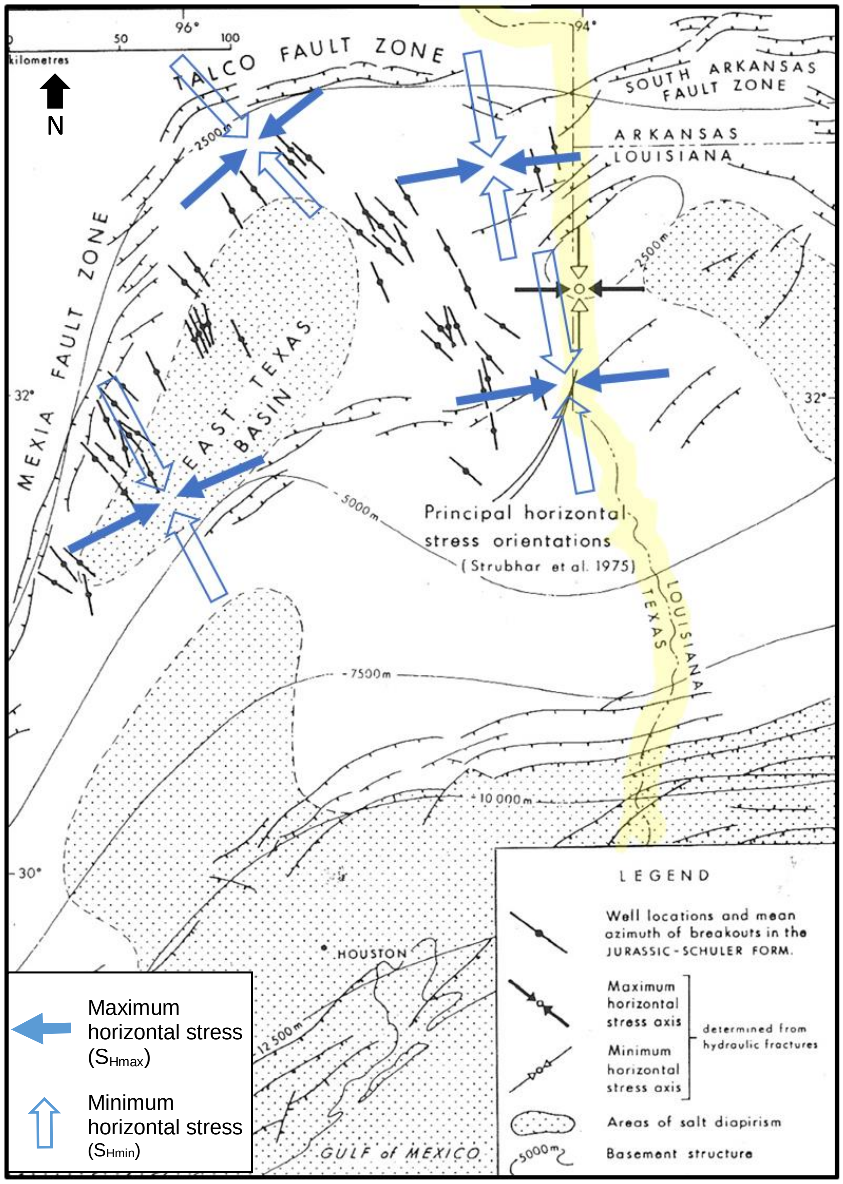

Figure 31. Structural setting of borehole breakouts measured in sandstones of the Schuler Formation of east Texas, illustrating their relationship to extensional faulting. Borehole breakouts form in the walls around a wellbore. As rock is removed, stress around the wellbore builds up surpassing the compressive strength of the rock which causes pieces of the borehole wall to fall off. Note that the indicators in this map show the direction of borehole breakouts, not the direction of maximum horizontal compressive stress (S_{Hmax}). Unlike joints, borehole breakouts form perpendicular to the direction of S_H and in the direction of minimum compressive stress (S_{Hmin}). Colored arrows display the approximated S_{Hmax} / S_{Hmin} directions. Modified from Gough and Bell, (1982).

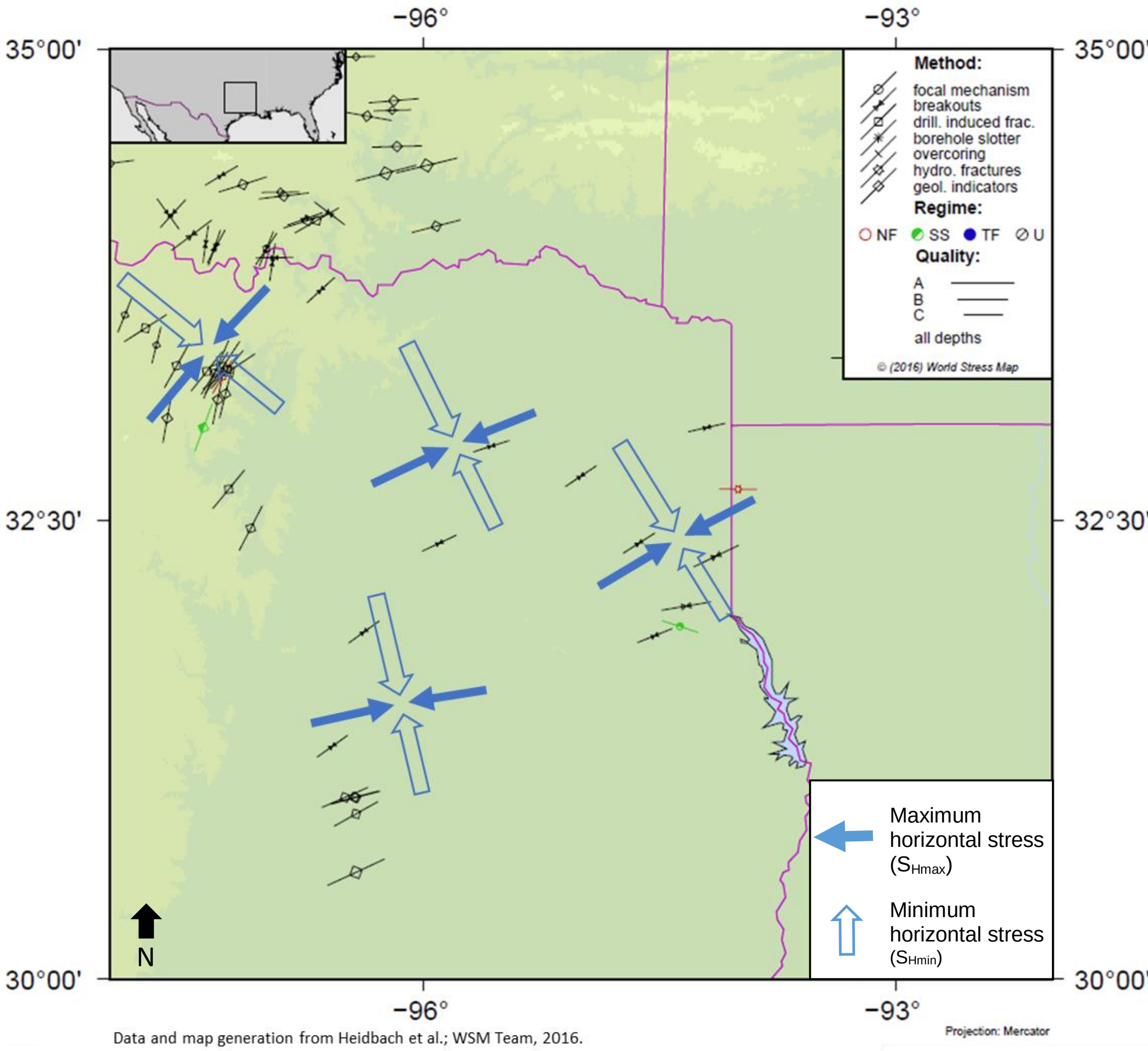

Figure 32. Stress map of east Texas generated from the World Stress Map database. The WSM is an open-access global compilation of information on the present-day crustal stress field. The indicators (short line segments) trend in the direction of maximum horizontal stress; thus, maximum extension is normal to the indicators. The indicators were determined by various methods shown in the key. The abbreviations NF, SS, TF and U the different types of focal mechanisms: normal, strike slip, transform and unknown, respectively. The "method" section in the key denotes the different means of acquiring the stress data. Most of the indicators in East Texas were acquired through borehole breakouts and drilling induced fractures which are both features measured in boreholes at depth. Colored arrows display the approximated S_{Hmax} / S_{Hmin} directions. Data and map generation from Heidbach et al.; WSM Team, (2016).

Lineaments as Stress Indicators

A lineament is “a straight pattern of tones, textures, contours, and other such features that is linear and continuous, has definable endpoints and lateral boundaries, and hence has discernable azimuth” (Woodruff and Caran, 1984). Essentially, they are regional, linear, geologic or vegetative features viewed in an aerial extent. Lineaments are relevant to this study because they may represent surficial faults or fractures.

Many studies of lineaments have been conducted in the region. In 1987 Robert W. Baumgardner, Jr conducted a lineament analysis and related it to the stress regime in East Texas. The aerial extent of this analysis is shown in figure 33. Using Landsat Imagery, Baumgardner overlaid lineaments in east Texas on major structural features and found that the orientations were nearly identical to . He concluded that this correlation meant that the regional stress regime likely had strong influence on the lineaments. Figure 34 shows the lineaments mapped in their study area. Owen Dix and M. P. A. Jackson (1981) conducted a lineament analysis of the East Texas Basin in an effort to determine the suitability of salt domes as nuclear repository sites. They found that areas above shallow salt domes are associated with higher lineament densities and lower preferred orientation, meaning the salt domes have caused deformation at the surface, but do not tend to be as systematic as other areas near the East Texas Basin, for example, faults in the Mt. Enterprise Fault Zone. Finley and Gustavson (1981) found evidence in a lineament analysis of the Texas Panhandle that “strongly supports the hypothesis that joints can provide a path of lower resistance along which linear surface drainage preferentially develops”. Lineaments near Nacogdoches County in theory can be correlated to jointing in the Weches Formation used as additional data in conjunction with joint orientations.

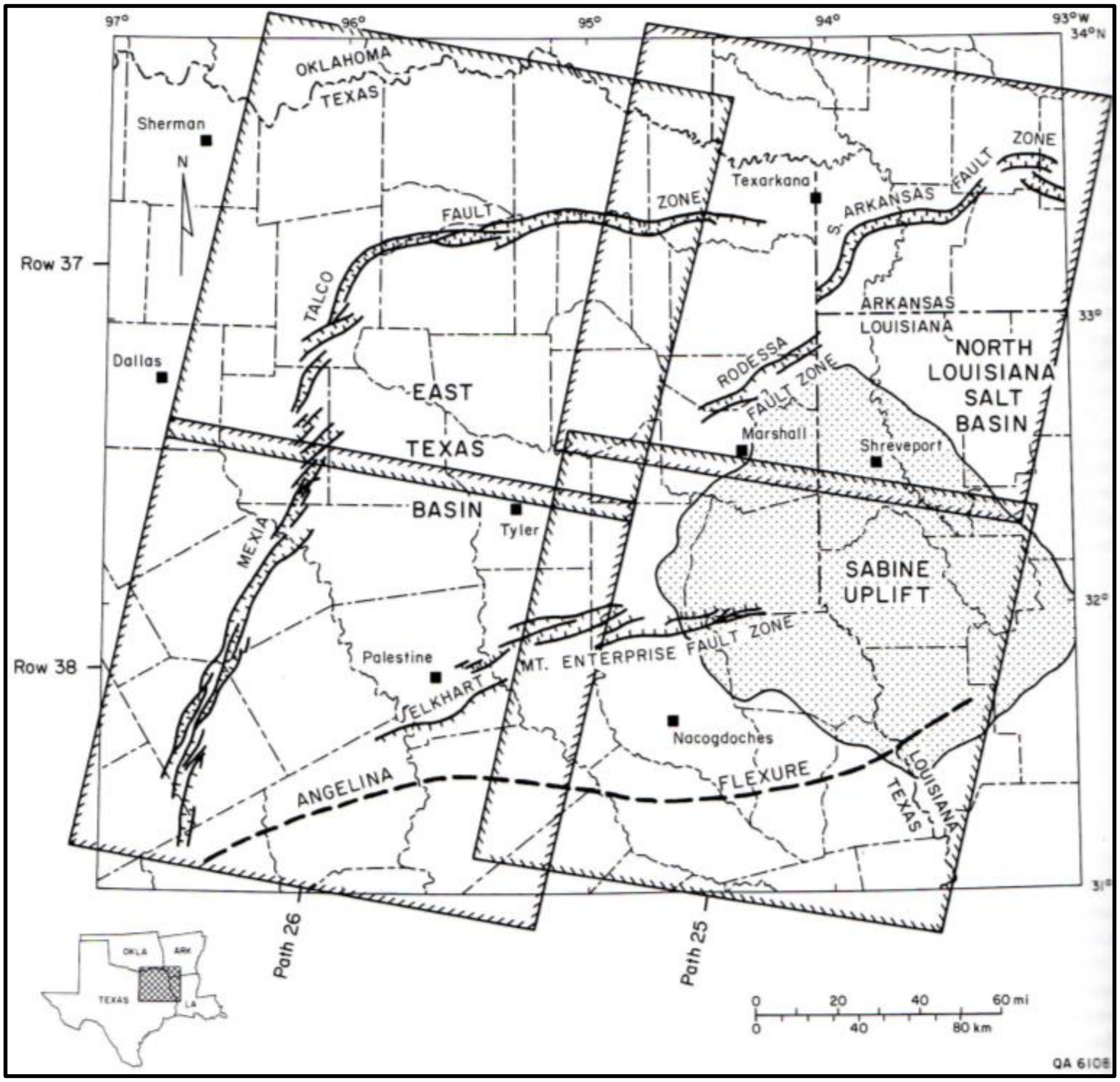

Figure 33. Map illustrating the area extent of lineament acquisition (from Baumgardner 1987).

Figure 34. Map of Landsat lineaments mapped from a lineament analyses study in East Texas (from Baumgardner 1987).

CHAPTER 5: ORIGIN AND NATURE OF JOINTS

Introduction

Understanding the relationship between fractures and their causative stresses is key to inferring the state of modern or paleostress regime and structural properties of a rock unit. The main factors that cause fracture generation in rocks have only recently been agreed upon. For many years geologists postulated that there must be some driving force that causes extensive, consistently oriented and spaced fractures in exhumed rock bodies. Phillips (1855) wrote, "Now, surely nothing can be more certain than the inference that some general and long continued agency, pervading at once the whole mass of these dissimilar and successively deposited strata, was concerned in producing this remarkable constancy of direction in the fissures which divide them all." Through the years many different “agencies” have been proposed: torsion, earthquakes, cleavage, magnetic force, contraction of sediments, etc (Hodgson, 1961). Today it is understood that fractures are formed in response to stresses acting on rocks, usually either tension, shear or compression or some combination. These stresses can arise from tectonic processes, removal of overburden or even temperature changes. “Fracture” is a general term that is employed when the causative stress is unknown. The term “joint” refers to fractures that originate through tension and thus are dilatational, meaning displacement is solely perpendicular to the joint face.

Origin of joints

The generation of tensional force required for joint formation can occur as a result of at least three phases or settings: (1) syntectonic deformation (meaning that it occurred at the same time as some deformational tectonic event), (2) deep in the crust during maximum vertical load (where the greatest direction of stress is oriented vertically) and (3) much shallower during exhumation (Fossen, 2016). Because the stress regime in buried rock is almost always compressive, the formation of tensional brittle deformation perplexed geologists for some time. We now know that some joints form during burial through natural hydrofracturing caused by pore fluid overpressure (Poyard and Aydin 1988). Secor (1969) showed that even though the stress regime at these depths is compressional, not tensional, the force of liquids trapped in the pores of the rock exert an outward stress from within the rock that can surpass the compressional forces so that joints can form at the site of tiny imperfections. This requires the rock unit to be saturated with liquid trapped by lithologic boundaries. At this depth joints form vertically – due to highest amount of stress caused by vertical loading, or in the case of hydrofractures, because that is the shortest path to the surface – with their strike controlled by the direction of highest horizontal stress. Joints formed later during uplift are the result of surface-related processes including relaxation of confining pressures, unloading and contraction due to temperature decrease. Both joints formed during burial and during exhumation have been shown to strike toward the direction of maximum horizontal compressive stress (S_{Hmax}) at the time of initiation and perpendicular to the direction of minimum horizontal compressive stress (S_{Hmin}). Figure 35 displays the relation between fracturing and the principle stresses on a rock unit. Joints form perpendicular to the minimum principle compressive stress axis (σ3) and in the plane of the maximum principle compressive stress (σ1) and the intermediate compressive stress (σ2). The intersection of the σ1 and σ2 planes with the horizontal plane forms the strike of the joint marking the direction of maximum horizontal compressive stress (S_{Hmax}) in the rock at the instant of joint formation (Rawnsley et al., 1992).

As mentioned earlier, joints from due to extension. The direction of extension, in mathematical terms, can be thought of as the direction of minimum compressive stress, σ_3, in figure 35. When considering tectonic stresses, structural geologists are concerned with the direction of these stresses in the horizontal plane, which include the minimum horizontal compressive stress S_{Hmin}, and maximum horizontal compressive stress, $S_{Hmax.}$ Other than exfoliation joints (which form sub-horizontal to the topography) exhumation joints are typically near vertical and have an orientation that can be controlled by either the tectonic stress at the time of jointing or remnant, pre-exhumation stress that was preserved in the rock pre-exhumation (Fossen, 2016).

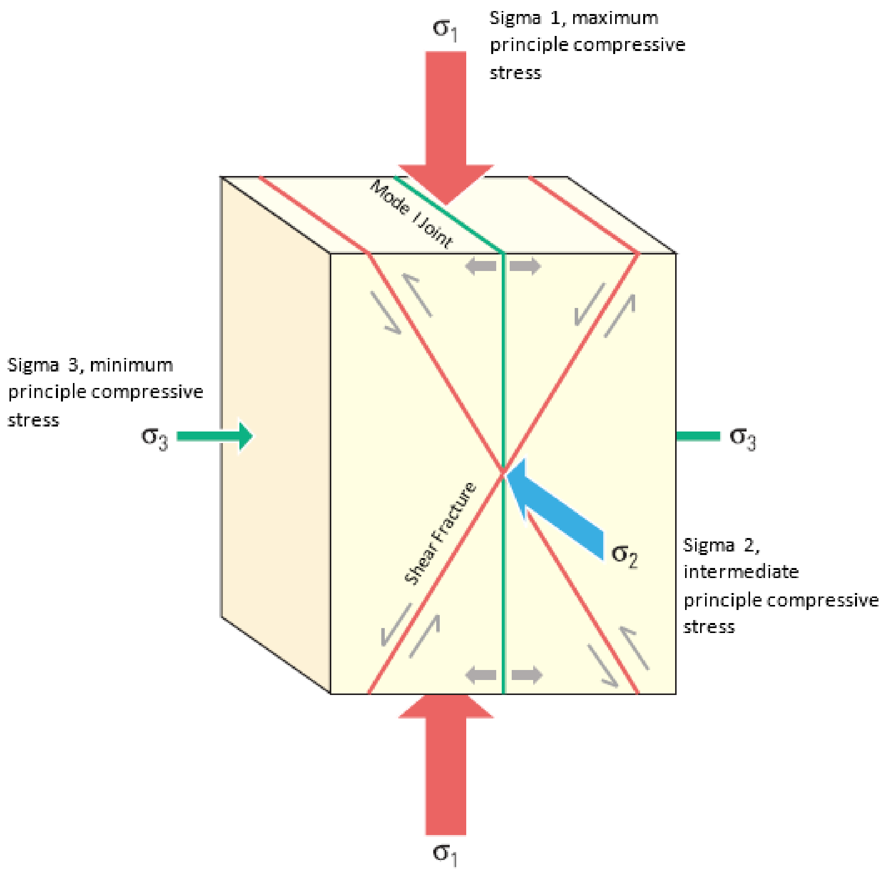

Figure 35. Model for principle stresses and the formation of fractures. This diagram shows the three principle directions of stress and their relation to fracture type and orientation. σ_1 Represents the maximum compressive principal stress, σ_3 the minimum compressive principal stress and σ_2 the intermediate stress. The resultant fractures are shown in green and red with their displacement denoted by directional arrows. The vertical fracture (green) is a mode I joint that forms perpendicular to σ_3. Note that the horizontal direction perpendicular to σ_3 is the direction of maximum horizontal compressive stress (S_{Hmax}). This means that strike of the joint can be used to determine both S_{Hmax} and S_{Hmin} and essentially orient the stress field (modified from Bratton et al., 2006).

Classification of joints

Fractures can be categorized based on their mode. The mode describes the displacement relative to the fracture plane. Figure 36 illustrates the three types of modes: mode I fractures represent displacement perpendicular to the fracture face, mode II represents shear movement horizontal and parallel to the fracture face and mode III represents shear movement vertical and parallel to the fracture face. Each mode corresponds to a unique type of stress. Mode I opening fractures, referred to as joints, are the focus of this study and they can be used as reliable stress indicators. Mode II fractures have the same sense of displacement as strike-slip faults and mode III fractures have the same as dip-slip faults.

Mode I joints usually form as a group or systematic “joint set”. The genesis of this joint set can usually be traced to a single event. These joints can be further classified into many different types based on geometry or processes involved with formation. The following tables displays some of these classifications.

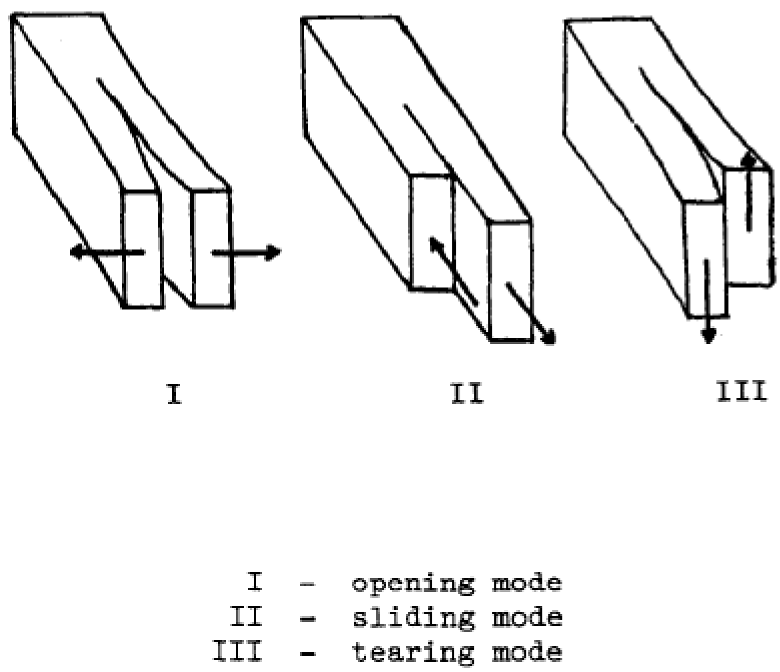

Figure 36. Diagram of fracture modes. Note that mode I is the only mode formed from tension (stress applied in opposite directions). while the other two modes involve shearing along the fracture plane and could result from shear stress (mode II) or compression (mode III). (from Kulander et al., 1979).

Table 1. (Following page) This table describes different joints classified by their geometry. To classify joints in this way we look at their “dihedral angles”, or the angles at which they intersect with each other. For individual joints it only matters whether they are parallel or not. Parallel sets of joints are called systematic while non-parallel joints are nonsystematic. The angle that distinct systematic joints sets intersect is classified as orthogonal, intersecting at 90^0, or conjugate, intersecting between 30^0 and 60^0.

Joints Classified by Geometry		
Joint Type	Description	Origin / other information
Systematic Joints	Planar, parallel, with regular spacing and consistent or gradually changing orientation. Can be grouped into “joint sets” based on similar orientation. A “joint system” is made up of two or more distinct joint sets.	Form at depth or near surface in response to far-field stresses or local deformational events.
Nonsystematic Joints	Irregular in form, spacing and orientation.	Form in locally perturbed stress fields. Typically, too complex to extract any useful information.
Cross Joints	Joints that occur in between the joints of a systematic joint set.	These can be systematic or nonsystematic and can be described as orthogonal and conjugate joints depending on the angle of intersection.
Orthogonal Joints	Systematic joints that intersect other joint sets at 90^0 angles.	A secondary joint set that forms when the stress relaxation caused by the initial set locally changes S_H to the opposite direction
Conjugate Joints	Systematic joints that intersect other joint sets at 30^0 to 60^0	Two joint sets that formed in a different stress regimes.
Columnar Joints	Nonsystematic joints that form in a hexagonal shape and form elongate columns	Typically, associated with lava flows. Produced by thermal stress during cooling.
Desiccation cracks	Nonsystematic joints that typically form in a hexagonal shape in drying clay/mud.	Caused by the dehydration and shrinkage of clay.

Since most joints are planar features their geometrical classification can be based on their “dihedral angles”, or the angles at which they intersect with each other. These angles are important because of what they tell us about the formation of the joints. For example, thoroughgoing joints that form parallel to each other (systematic joint set) likely have a shared origin. Or, if a set of cross-joints terminating at 90^0 (orthogonal joint set) to another thoroughgoing set, we can assume that the thoroughgoing set represents the far-field stress regime while the secondary set does not. This is because the first set formed in the initial state of tectonic stress allowing relaxation in the direction of maximum compression, effectively flipping the direction of stress towards the opposite direction near the joint. This leads to the formation of a set of cross-joints propagating in a direction perpendicular to the initial set. In other words the orientation of the orthogonal set was influenced by the initial set of joints rather than the far-field stress regime.

On the other hand, a conjugate set of joints, intersecting at 30^0 to 60^0 may indicate the presence of two distinct periods of tectonic stresses. Their truncating relationships, or which joint set halts the growth of the other joint set, if present, can be used to identify the sequence of formation. As an example, Engelder & Geiser (1980) used the orientation of two conjugate joint sets in the Appalachian Plateau to infer a chronological progression of paleostress fields and produce a kinematic model for the evolution of the New York Plateau. In addition to identifying the geometrical relationship of joints, it is equally important to determine how they formed. Table 2 describes some classifications of joints based on the processes that formed them.

Table 2 (following page). Joints classified by the way in which they formed. Note that tectonic joints indicate joints that can be traced to some tectonic event; other types of joints, including hydraulic or release joints, could also be present.

Joints Classified by Formation		
Joint Type	Description	Origin / other information
Tectonic Joints	systematic or nonsystematic joints formed in response to some tectonic event. Can also form as shear fractures.	Form when the tensional strength of a rock is exceeded by stresses generated by a tectonic event. Also caused by local deformational event like faulting or folding.
Neotectonic Joints	Tectonic joint formed in a late Cenezoic stress field, with an orientation that is approximately parallel with the principle axes of the contemporary stress field (Engelder, 1989)	Forms near surface (<500m) in a relatively recent stress field (Engelder 1985) in the direction of greatest horizontal compressive stress. Results from unloading during exhumation.
Hydraulic Joints	Joints formed at great depths when the maximum direction of stress is vertical. These joints are vertical and propagate in the direction of maximum horizontal compressive stress	Form at depth as vertical loading increases the pressure of trapped pore fluid to the point that it exceeds the tensional strength of the rock creating a tensional fracture (joint). Often results in the formation of veins.
Exfoliation Joints	Joints parallel to the ground that form as the vertical load is removed during exhumation.	Form near surface during exhumation as vertical stress is alleviated.
Unloading / Release Joints	Joints that form from cooling and contraction during uplift	As the overall compressive stress is lowered the rock compensates by expanding. Because the sediment has become lithified and brittle this expansion is achieved through fracturing.
Cooling Joints	Contraction of the rock through thermal stress leads to columnar jointing in igneous rocks.	Typically forms in cooling lava flows. The common example is basaltic columns.

Some joints are classified with respect to the deformation events that caused them, including faulting or folding. The direction of joints created by these events will, in general, be representative of the perturbation of the stress field in the region immediately surrounding the deformational event rather than any far field stresses. Rawnsley et al., (1992) showed that joints near faults are often aligned either perpendicular or parallel to the fault plane. Joints that form over folds can be classified into five groups displayed in figure 37 (Segall and Pollard 1983); such joints usually form in conditions where σ_1 is more or less horizontal.

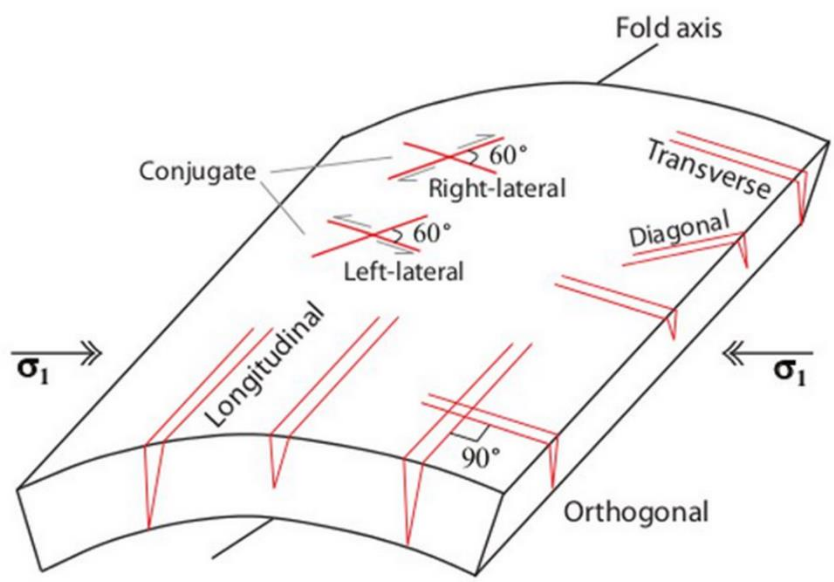

Figure 37. Classification of fractures over a folded structure. The fracture types include: longitudinal, diagonal (oblique), transverse (cross), orthogonal and conjugate. These fractures are categorized based on the relation of their orientation to the fold axis of the structure (Modified from Singhal, B.B.S. and Gupta, R.P., 2010, second ed.).

Surface Morphology

The surface morphology describes the unique pattern of striations and arcuate ripples recorded on the fracture face during formation. These are tiny undulations left behind as the fracture propagates outward experiencing tiny variations in speed and direction as it encounters microscopic inhomogeneities in the rock matrix and stress field (Kulander, 1979). An example can be seen in figure 38. This results in a somewhat predictable series of patterns and shapes that provide information on the formation of the joint. Unfortunately, joints in the Weches Formation do not appear to preserve any discernable surface morphology. This may have to do with the mechanical properties of the claystone.

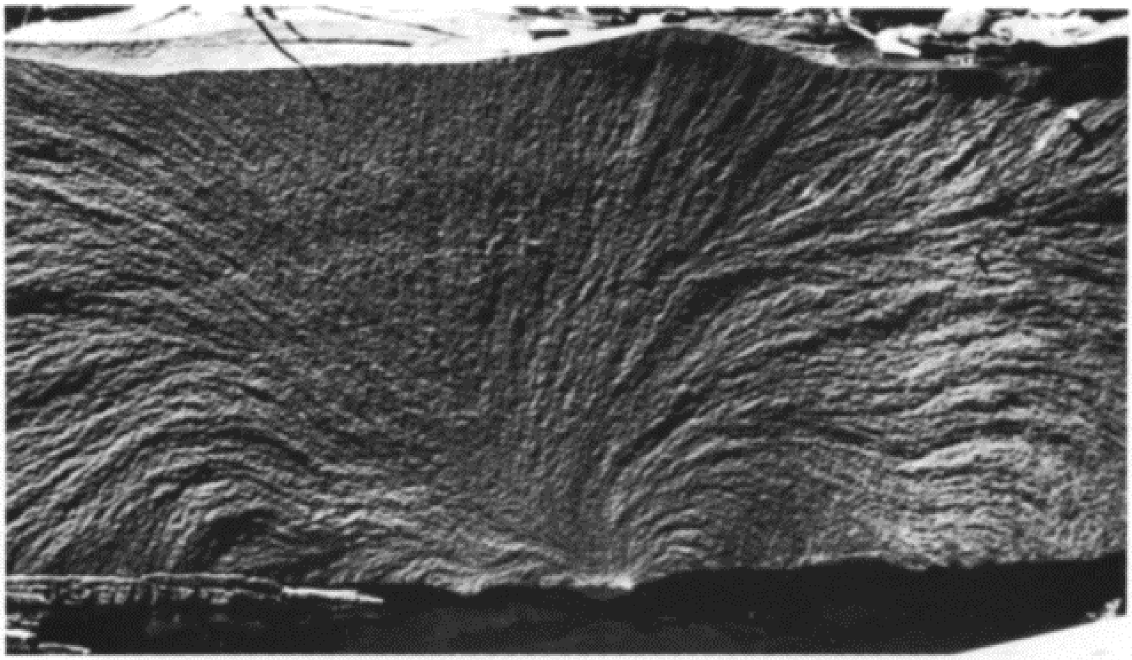

Figure 38. Surface morphology of a fracture face. Shown here is a plumose pattern of a fractured siltstone. The fracture propagated initially from the bottom center point moving outward in an arcuate path. Modified from Helgeson and Aydin 1991.

CHAPTER 6: METHODOLOGY

Introduction

Field data was obtained from 14 different sites near the East Texas towns of Jacksonville, Nacogdoches, Alto and Milam, and in road cuts on the highways connecting these cities (locations shown in figure 1). Access was granted into three different quarries that were mining the Weches Formation: one near Milam (Big 4 Inc.'s "McGee Pit"), one north of Rosevine (Attoyac Construction LLC) and one two miles east of Alto (currently privately owned). Other outcrops were found where the Weches was exposed in road cuts or where a cliff of Weches was created when the toe of a slope was cut away in order to site a business. The possible locations were greatly limited because the Weches is a slope former and because the warm, humid climate of East Texas results in dense vegetation cover. However, an effort was made to spread out data points to better analyze gradual changes in regional trends. Observations that were the point of focus in this study include:

- Style of jointing (purely tensional, purely shear, or a combination of both through reactivation)
- Trends in joint direction (local or regional groupings of similar strike)

- Presence of joint sets (sets of regularly spaced similarly striking joints Nature of joint intersections
- Presence of nearby geologic events.

Pincus (1951) laid out a general guideline for the collection, statistical treatment, and analysis of fracture orientation data. This was the basis for the method used in this study.

Collection

Orientations of joints at each site were measured using a Brunton compass. 540 readings of strike and dip were taken in total. Close examination of the outcrop and fracture faces with a short description of each joint was recorded. Field data for all sites is presented in the Appendix. The description of joints included length, quality, presence of infilling material, and any notable features like striations, en-echelon pairs and spacing. Even though displacement across joints is minimal, close examination of joint face was sufficient to document the fracture mode. Quality of the joint was based on how well the joint face was exposed and how weathered it was. A simple system of “poor”, “ok”, or “good” was used to denote the quality. This was done to indicate the reliability of each joint’s orientation measurement. Detailed descriptions and diagrams of each outcrop site were recorded. In order to remain objective in data collection, all joint surfaces were recorded except when the fracture face was: (1) too irregular to delineate a plane, (2) too small to be considered significant (less than a few inches long), (3) too far out of reach to accurately measure, or (4) too weathered or detached from the section. It is typical for layers of sedimentary rocks to contain different sets of joints (Narr and Suppe, 1991), but because the different members of the Weches have gradational contacts and are very similar it was decided not to assign joints to the Therrill, Viesca and Tyus members. The spacing between joints of similar orientation was recorded, however joint spacing is believed to be dependent on rock material and unit thickness, not necessarily providing insight into stresses (Narr and Suppe, 1991). In addition, the thickness and induration of the Weches is highly variable from location to location which could possibly make joint spacing a misleading characteristic. In order to avoid a change in method during data collection these guidelines were planned in advance and all data points were gathered by the writer and thesis advisor.

Analysis

Data from each site was plotted on a stereonet and rose diagram to visualize trends in joint direction. The rose diagrams were also plotted on their respective locations on the map to determine regional geographic trends and proximity to other geologic features.

Determining the origin and diagenesis of the fractures was done by examining fractures interfaces for crosscutting relationships to decipher relative ages. Even though joints sets form essentially instantaneously, they continue to grow and interact with each other which can create confusion when trying to determine crosscutting relationships. Even so, younger joints should terminate against older joints more often than not. This is because an extension fracture cannot propagate across a free surface such as another extension fracture (Bahat, 1991). However, certain factors can lead to a mutually cross-cutting joint system. For example, if cementation occurs in the first formed joint or if pressure is high enough across the older joint a younger joint can propagate across (Twiss and Moores, 1992). On the other hand, the relationship between fractures and other events – folds or mineralization for example – are straightforward. If the joint persists through folded strata without being affected by it then the joint is younger than the folding event, and if the joint contains a secondary mineral then the mineralization took place after the fracture occurred.

Extensive ironstone layers in the Weches, also affected jointing so the origin of these layers and their interaction with joints is given special attention in this study. Close inspection of the nature of vein filling material provides further insight into the history of the joints. The results were then synthesized and their relation to localized or widespread tectonic events as the driving factor in development of fracturing was explored. Because of the possibility of the "overprinting" effect of local faulting and gradual differences in regional stress, in conjunction with the lack of good exposures of the Weches Formation, the total data set cannot be plotted together for analysis. Instead, a series of relevant stereonets and rose diagrams were created.

Sources of error

Fractures that form in response to stress in near-surface rocks may be different from those in the deep subsurface. Haimson (1980), Zoback et al. (1980), and Zoback and Zoback (1980) observed shallow horizontal stresses (less than 100 m) much different from deeper stresses measured at the same site. They attributed these differences to the effects of erosion, weathering, and local topography. Outcrops accessed in this study might also be susceptible to these effects creating results that might vary significantly from joints created by regional stresses. For example, tree roots growing into the formation, creep or slump at the edges of road cuts, or repeated expansion/contraction of the formation during rain events might affect the joints or create new ones. These factors effecting local fractures and joints can dissociate surface rocks from the tectonic stress field. However, Tullis (1981) observed that near-surface horizontal stress directions are likely to be similar to those at depth if enough measurements are taken to mitigate the variation of localized effects. The 540 measurements, in addition to a practical field assessment of the state of the outcrop, should be sufficient to overcome these potentially erroneous results.

Because data collecting sites for this study are commonly located on highways or city roads, and because many such roads are often oriented N-S or E-W, that fact could result in a bias in the collected data. This effect is illustrated in figure 39. Therefore, an effort was made to balance out this potential bias by taking measurements at as many north-south oriented streets and west-east oriented as possible. As a result, six sites are on road cuts striking roughly north – south and four sites striking roughly east-west. This is not an issue at the outcrops located in quarries or meandering river beds.

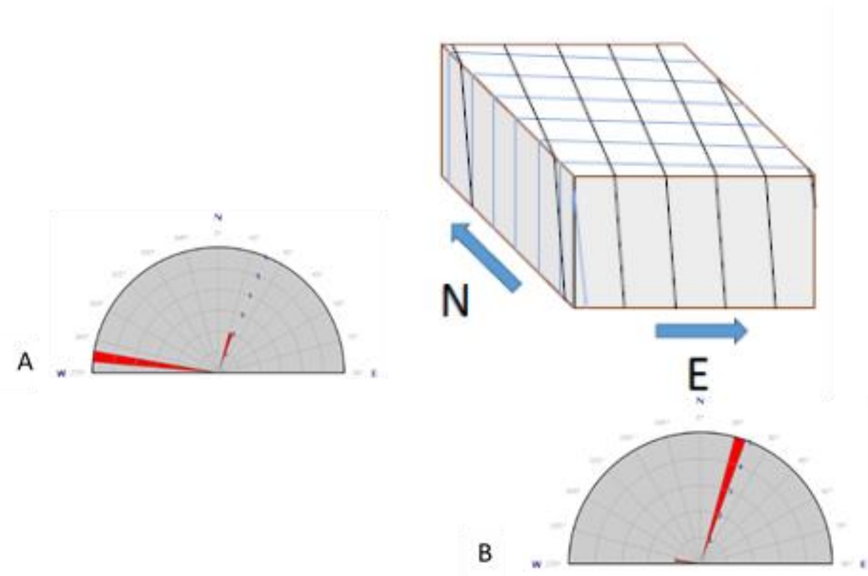

Figure 39. Illustration of the effect of outcrop orientation on the attenuation of joint trends. 'A' displays the strikes on the western facing outcrop and 'B' the south facing outcrop. Note that when the joint set is parallel to the outcrop only a few readings of randomly oriented fractures could "mask" the parallel joints set.

CHAPTER 7: FIELD RESULTS

Introduction

Joints in the study area are typically steeply dipping (70^0 – 90^0) and often iron filled. Slickenlines are uncommon but visible on a few fracture planes; however, their bearings show random orientation indicating unloading movement during erosional exposure. The study area includes a large portion of East Texas, but three groupings or trends of joint orientations were observed. The three major groupings of orientations are as follows:

- N75^0-85^0W (referred to as J1a) located in the eastern portion of the study area.
- N75^0-85^0E (referred to as J1b) located in the central area of the study area
- N40^0E (referred to as J2) Located in the northern area of the study area

These three trends are shown on figure 40. The majority of joint strikes from a given outcrop in the study area fall into one of these trends. These are systematic joint sets with common spacing that are not restricted to any one outcropping, but instead span several miles. The 1 and 2 in the naming scheme represent the possibility of two unique tectonic events driving origins of fracture development. This signifies that while J1b and J1a are distinct joint sets, it appears they may share a similar tectonic origin that will be discussed later in the paper. The average direction all joint strikes in the Weches Formation within the study area is approximately N87^{0}E. This trend was derived by plotting all strikes on a single stereonet. This average trend masks the three trends listed above, but it approximately matches the trend labeled j1b.

Trends in orientation

Set J1a

The J1a set can be found in locations furthest to the east (13, 6, and 4) from Chireno to near the Louisiana border. This is a set of steeply dipping joints oriented N75^0–85^{0}W. They are commonly spaced six to 8 feet (2.4 meters) apart and are iron filled when in contact with, or in the vicinity of an iron bed. Sites 13 and 6 were in quarries while site 4 was in a road cut. The Weches Formation in the quarries of sites 13 and 6 was much harder and better indurated than other outcrops and had a much lower density of nonsystematic joints, which resulted in less random scatter in the stereonets. Figure 41 shows the systematic nature of the joints at site 6. Sites 13 and 6 had fewer iron layers compared to other locations which allowed joint terminations (the ends of joint planes) to taper off rather than stop abruptly at bedding contacts. The geometry of these joint terminations can give insight into the nature of stress the rock underwent. At sites

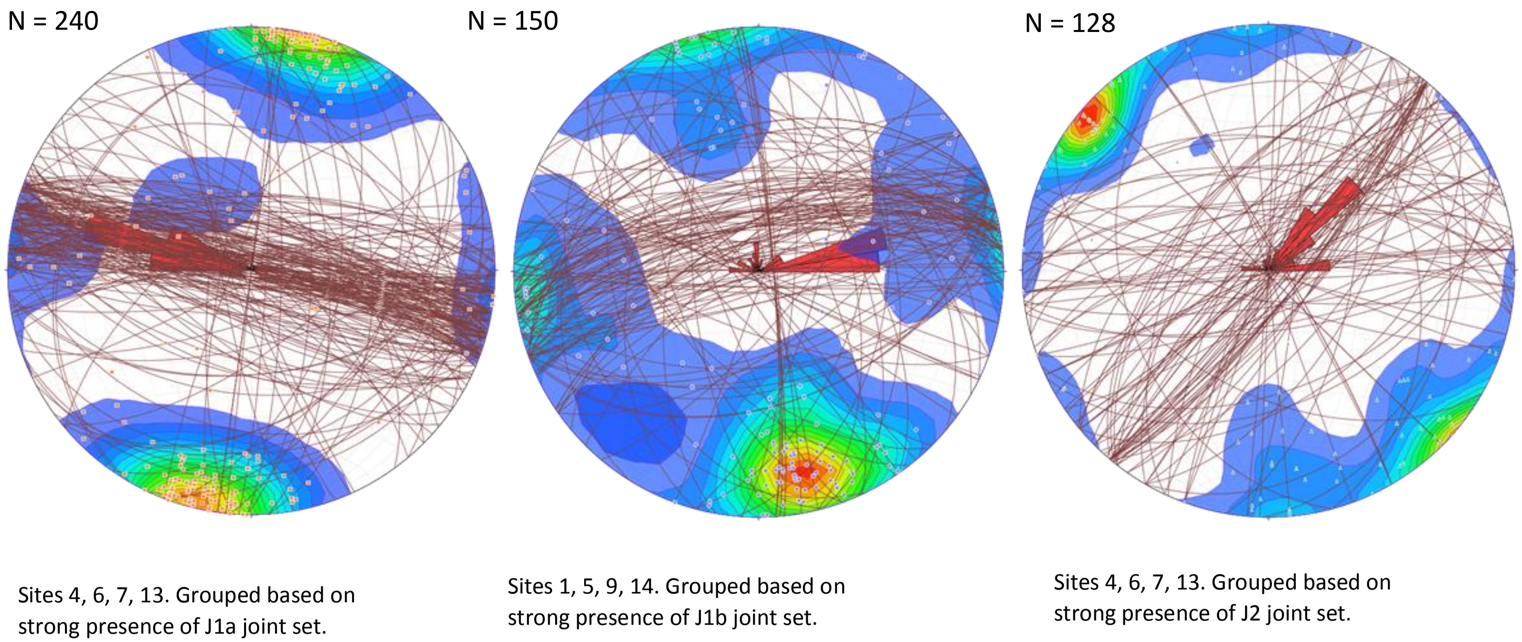

Figure 40. Joint orientation data from individual sites divided into three groups based on the dominant joint set present from left to right: J1a, J1b and J2. The strike of joints is represented by the dark-red arcs with dots representing poles. Poles are contoured to illustrate the grouping of similarly striking and dipping joints with higher clusters appearing as more red. Note that each grouping contains a secondary set of orthogonal joints approximately 90^0 from the main set. Sites 3 and 8 are omitted from the groupings because of their lack of a systematic pattern

13 and 6, joints oriented N70^0-75^{0}W can be seen terminated with hackle marks and then slightly changing direction, from top to bottom, to a more westerly direction of N85^{0}W through a lithologically homogeneous section shown in figure 42. In addition, several small faults and one large normal fault trending were found at site 13 with an average bearing approximately N75^0 - 85^{0}W. The possible impact of faults in the area is explored in the following chapter.

30 miles (50 km) west of location 13 on Highway 21, location 4 reveals the same J1a joint set along with a secondary set directed roughly north – south. This secondary set is arrested by the J1a set and intersects with it at 90^0 angles. Based on this crosscutting relationship and angle of intersection, this set is believed to be orthogonal to the J1a set.

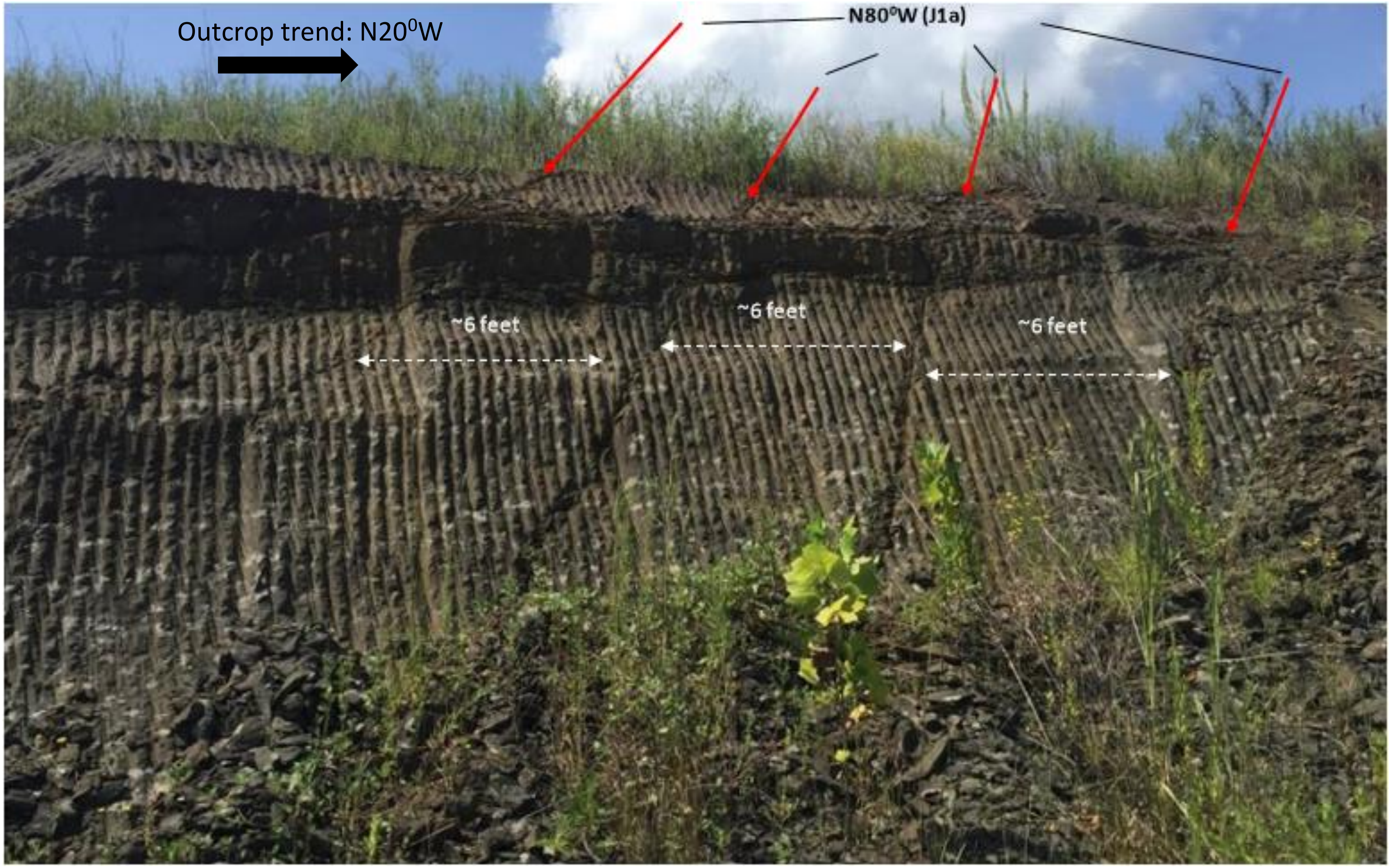

Figure 41. Outcrop of Weches Formation in a quarry at site 6 showing N80^{0}W systematic joints. Note the ordered nature of the joints. Parallel strike, consistent spacing and steep dip are all good indicators for being a set of systematic opening mode joints. These properties were common at the majority of outcrops at this site, while the density of jointing varied. Grooves in the outcrop wall are created by the machinery used to cut into the rock.

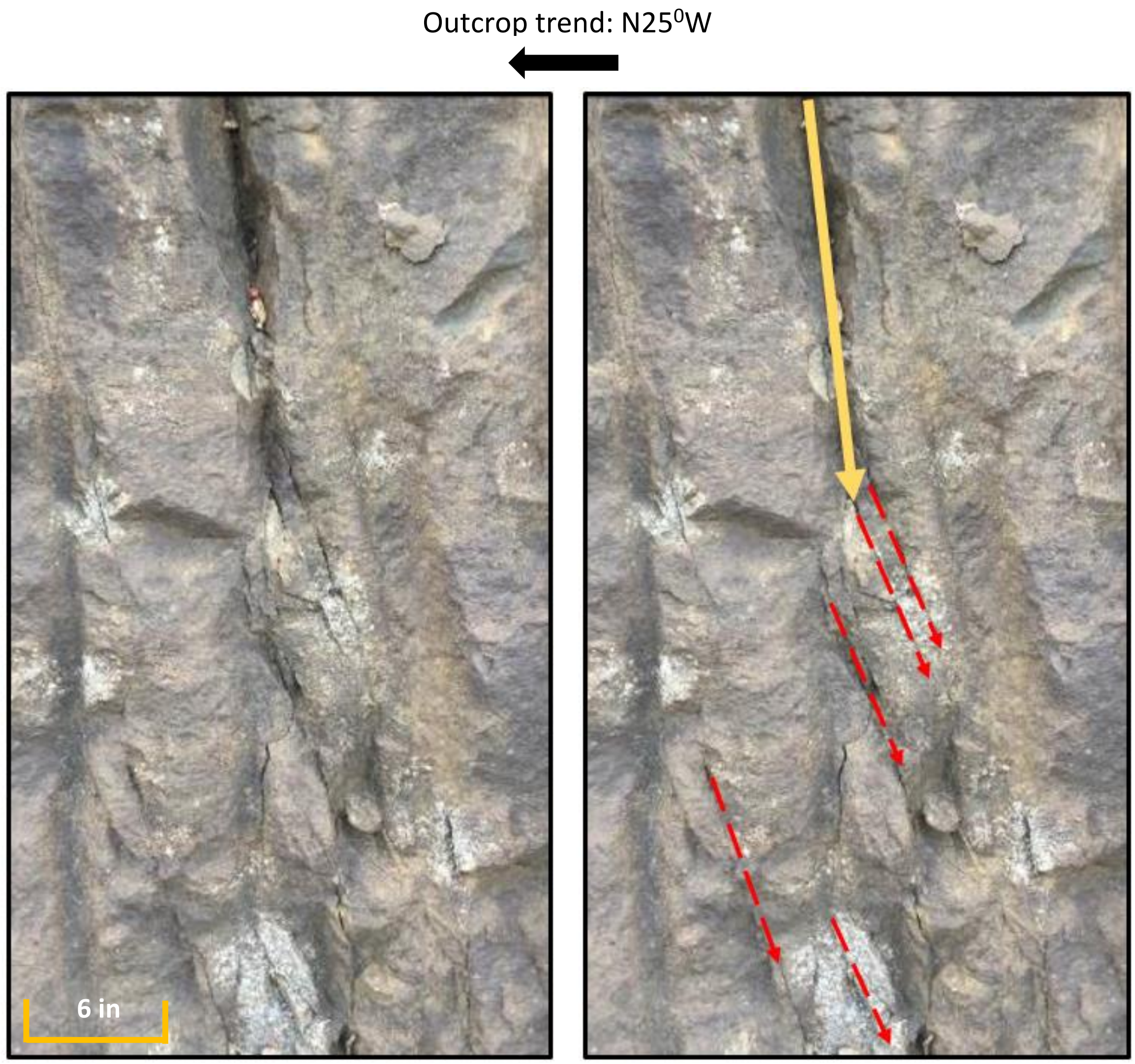

Figure 42. Rotation and segmentation of J1a joints at site 13. In the image on the right joints are highlighted in red. The upper section trends N75W and then twists in a zone of hackles into a N85W direction, likely as the result of nearby faulting.

Set J1b

Twenty miles (30 km) west of location 4 are a series of outcrops in the city of Nacogdoches, where the orientation of joint strikes is slightly different. The outcrops trending north-south (site 1 and 5) show a joint set similar to J1a but are oriented more easterly. This J1b set has a strike N $75^0 - 85^0$ E with a dip of about 75^0 to 90^0 N and a spacing of about 8 – 10 feet (2.5 - 3 meters). Jointing at site 1 is extremely complex and has the densest assemblage of superimposed joints of any site. This is shown in figure 43, which shows the prominent manmade cliff at this site. Another joint set in Nacogdoches is visible only in the bed of Banita Creek at site two. This joint set, referred to as J2, trends N40^0E, dipping very steeply. Likely due to weathering, this set is not well defined here but becomes more apparent at outcrops farther to the north. This set is also completely lacking at sites one and five. This may be because, while the outcrops at these sites are around forty to 50 feet (15 meters) long, they are oriented nearly parallel to this joint set making it a much less common occurrence and more likely to be broken off during weathering. Incidentally the owner of the business located in front of the outcrop at site five (parallel to the J2 set) where a manmade cliff of the Weches exists, mentioned that truckloads of clay have to be moved out from behind the shop where blocks of the Weches fall off.

About 5 miles (8 km) west of Nacogdoches a road cut reveals the J1b joint set with an orthogonal set of northerly oriented joints. Comparing site nine to four which is located roughly 23 miles (37 km) east and about 6 miles (10 km) north, clearly illustrates the subtle shift in direction from the J1a to J1b joint set. About 25 miles (25 km) west of Nacogdoches, just outside of Alto, a quarry no longer in operation is the location of site 14. This area was heavily covered in vegetation but outcrop surfaces were relatively fresh. The same J1b joint set prevails at this site.

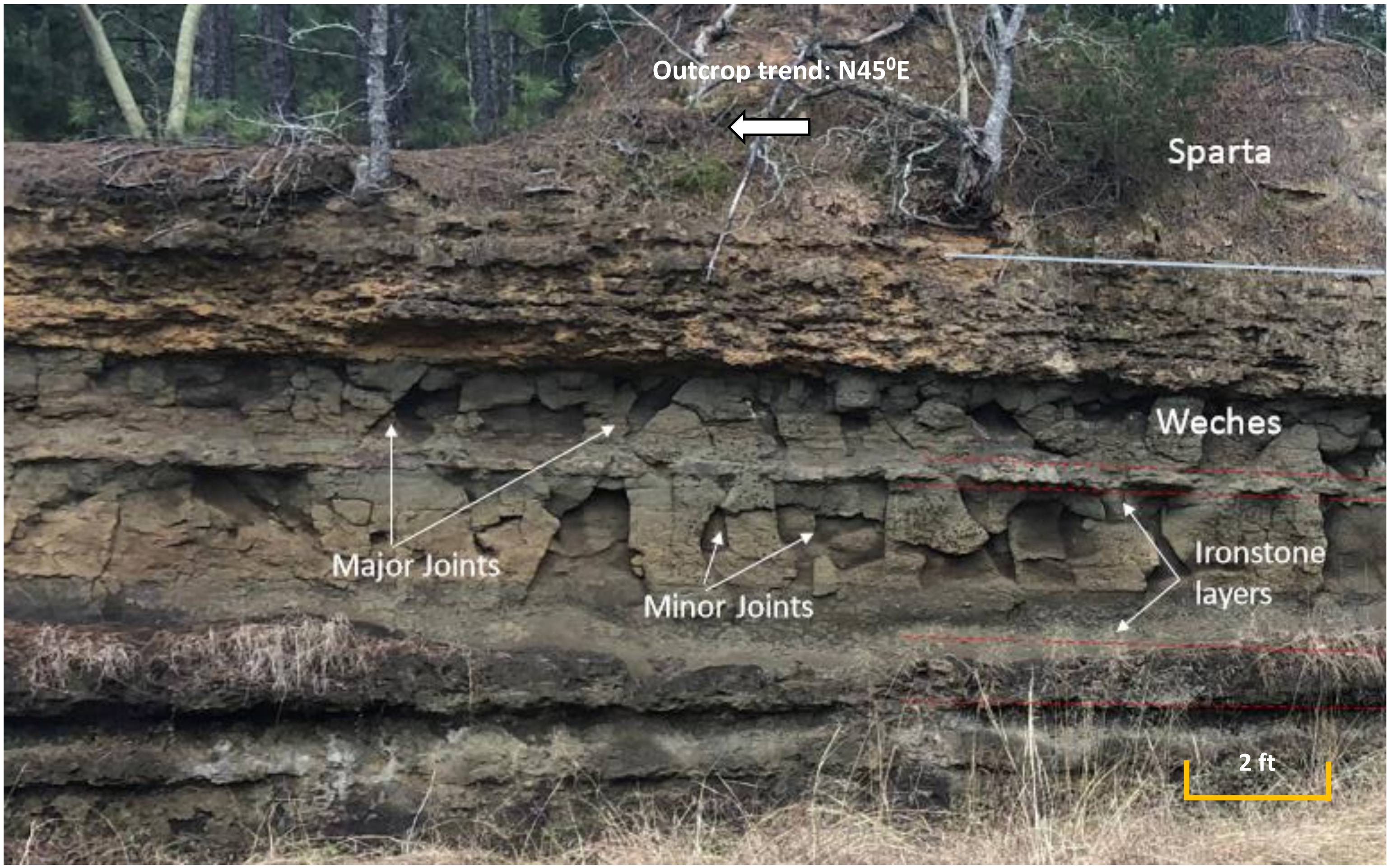

Figure 43. Highly fractured outcrop of Weches on South St, Nacogdoches, Texas at site 1. Upper contact with Sparta is visible as well as ironstone layers and major and minor joints. Joints are categorized into major and minor on the basis of length quality and systematic nature. Note that most joints are truncated by ironstone layers.

Set J2

Moving North from Alto, joints from the J2 set become the most common at outcrop. Sites 10, 11, and 12 are outcrops in road cuts located along US-69. These sites move from south to north through the Elkhart-Mt Enterprise Fault Zone. An example of one of these outcrops is shown in figure 44. This is a picture taken from site 10 which is an outcrop north of Jacksonville on the east side of US-69 and is typical for this area. The J2 joint set trends N40^{0}E and dips steeply. These joints are typically well preserved and have consistent spacing. The J2 joint set happens to be parallel with the trend of nearby faults. These are the faults on the western flank of the Mt-Enterprise Fault zone and the northeastern flank of the Elkhart Graben as well as subsurface central basin faults. Interestingly, site 7 which is just north of Jacksonville, contains none of the joints from the J2 set, but instead almost entirely what appears to be approximately either the J1b or J1a set. About 2 miles (3.2 km) north, at site 10 this same oriented joint set is visible commingling with the J2 set. At this location, crosscutting relationships are not clear cut with evidence for both joint sets terminating against one another. The J2 set is typically filled with iron concretion here with the J1b set less commonly so. Many of the iron veins and concretions in these northeastern outcrops are exceptionally large.

Stereonet and Rose Diagram Analysis

When the data is compiled into stereonets the trends discussed are clearly displayed. Figure 45 shows the strike and dip data of every measured joint grouped by outcrop and compiled into stereonets and rose diagrams. With a few exceptions it is obvious that each outcrop displays prominent grouping of joint directions. Even though it is possible for randomly oriented joints to show a preferred orientation by chance, there trend would not correlate from outcrop to outcrop as they do in this case. The respective position for each stereonet is shown in map view in figure 46. Observing the trends in map view we see that the trends tend to be tied to certain areas. Figure 40 shows the grouping of these sites with similarly trending joint strikes. The result is three trends of joint strike directions which can be divided into three different regions.

Figure 44. Outcrop of Weches Formation from Site 10 showing systematic J2 joints. The highlighted joints are trending roughly N40^{0}E, 88^0 S and are spaced about 3-5 feet apart. The clay layers are a greenish tan color and are poorly indurated. The Ironstone layers are a reddish brown and form ledges because they are more resistant. The joints terminate at the iron layers.

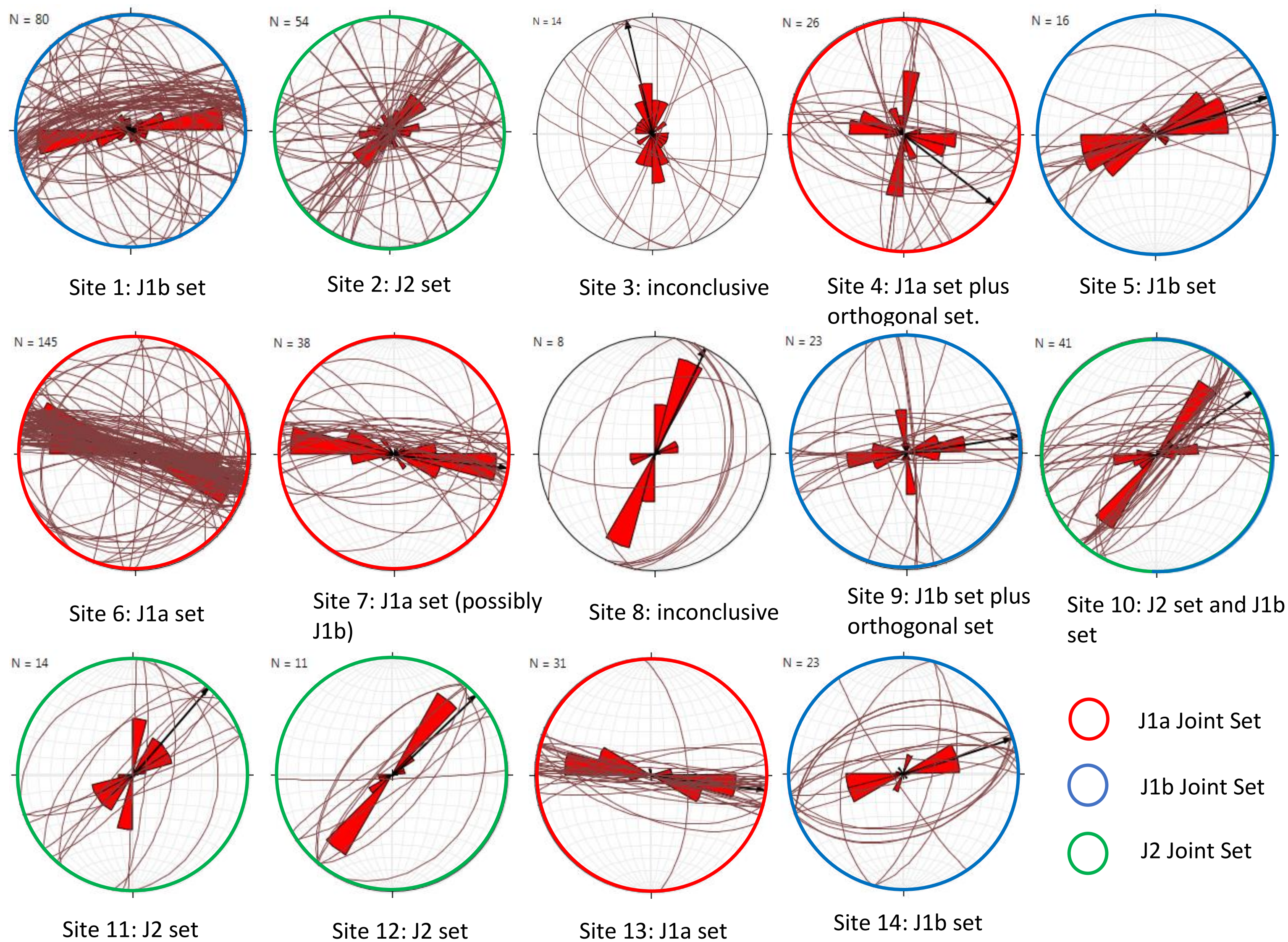

N = 80
Site 1: J1b set
N = 54
Site 2: J2 set
N = 14
Site 3: inconclusive
N = 26
Site 4: J1a set plus orthogonal set.
N = 16
Site 5: J1b set
N = 145
Site 6: J1a set
N = 38
Site 7: J1a set (possibly J1b)
N = 8
Site 8: inconclusive
N = 23
Site 9: J1b set plus orthogonal set
N = 41
Site 10: J2 set and J1b set
N = 14
Site 11: J2 set
N = 11
Site 12: J2 set
N = 31
Site 13: J1a set
N = 23
Site 14: J1b set
J1a Joint Set
J1b Joint Set
J2 Joint Set

Figure 45 (Previous Page). Stereonets from each outcrop location. Arcs on the stereonet represent the strike of joints. Rose diagrams are superimposed in the center of the stereonet which help illustrate the trend of joint strikes. “Petals” of the rose diagram represent 10^0 increments of joint strike. Each strike direction is grouped into the nearest degree increment and the petal increases in size for each subsequent data point added. This results in the petals with the most assigned data points being largest. Note that the majority of sites have a strong grouping of strike directions. The outer circle of the stereonets are colored based on the dominant joint set present.

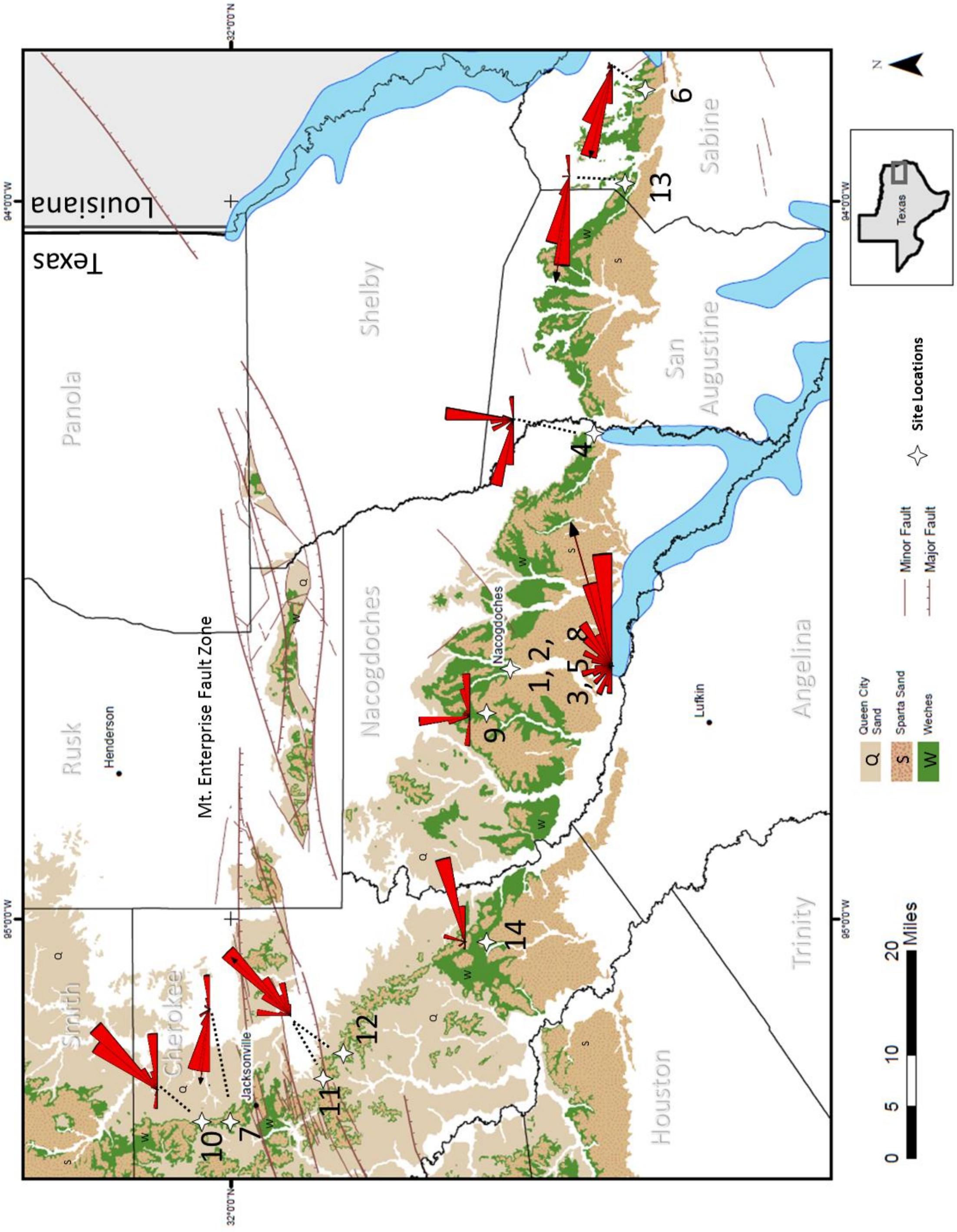

Figure 46. Map view of site locations and half circle rose diagrams of joint strikes.

CHAPTER 8: DISCUSSION

Introduction

The following section will explore four main topics: the nature of the joints in the Weches Formation, the timing of their creation (relative to each other and to the tectonic events surrounding them), what caused the joints to form and what they tell us about the stress regime in East Texas.

Nature of joints in the Weches Formation

Recall that there are three types of fractures: (1) opening mode, (2) horizontal sliding mode and (3) non-horizontal tearing mode. The majority of fractures in the Weches Formation appear to be purely opening mode. There are three main lines of evidence for this: (1) no offset of fossils or sedimentary layers crosscut by fractures (example shown in figure 47a), (2) steeply dipping systematic fractures (typical for opening mode fractures), and (3) the presence of veins with growth normal to fracture plane. While there are slickenlines present on some joint faces, the trends of these features are not systematic or consistent and are likely caused by sliding joint blocks that fall off during weathering.

Iron Veins

The majority of joints greater than a few inches in length in the Weches Formation contain an infilling of precipitated, oxidized iron creating a rusty, yellowish- to reddish-brown zone adjacent to the joint about one millimeter to several centimeters (.04 – 1 inch) in thickness. The width of the actual iron vein varies from 0 to usually no more than 1- 2 mm, but Fe- bearing fluid moving through the joints penetrated the soft, porous Weches clay on either side of each joint and created the distinctive rusty zone that parallels most of the joints. With this in mind, it is important to examine the morphology of the mineral fill because it gives insight into the formation of the joint.

Veins are fractures filled with a secondary mineral deposited by fluid entering the space. Ramsay (1980) described the structural relationship of vein filling material and jointing with a mechanism called crack-seal. Veins are formed as the joint dilates and water is able to flow through and deposit minerals on the walls. Once the joint is fully sealed with the infilling material it is likely another joint will form within the vein allowing further dilation. This sequence of cracking and sealing can last for millions of years. An example of this can be found in certain fractures in the Travis Peak formation which started around 48 Ma and lasted up until present day (Laubach et al., 2014).

The mechanism behind vein formation in the Weches is not always this straightforward. Some examples of the veins are shown in figures 47 and 48. Where iron precipitation is present there is typically a zone of repeating, closely formed, parallel fractures. At first glance this property seems like an example of crack-seal formation, where continued stress buildup causes repeated fracturing along joints “sutured” by mineral precipitation. However, veins at site five in Nacogdoches seem to indicate otherwise. Figure 47a shows fossils being crosscut by one of these veins without being displaced on either side of the “original” joint face. If this was a crack-seal formation the original joint face would crosscut the fossil and then would proceed to expand outward in repeated phases as each successive void is filled with secondary minerals leaving no trace of the fossil within the vein. Instead the fossil is present through the vein and is cut by multiple joints within. This makes crack-seal impossible, at least in this example. Caputo and Hancock (1999) studied a similar mechanism to crack-seal which they termed “crack-jump”, where mineral filled joints form in close parallel succession, but outside the original vein. This mechanism is likely the explanation for this feature. In other cases, like that of figure 48b, the vein appears to clearly have expanded outward during repeated ruptures with the center-most (therefore youngest in this case) joint being unsealed, leading to antitaxial, crack-seal vein growth. This form of vein growth is illustrated in figure

49. Either way, the repeatedly fractured nature of veins in the Weches indicate the introduction of secondary minerals in a purely opening mode fracture.

Because crack-seal and crack-jump mechanisms formed the Fe veins within the original joints it is logical to assume that, in geologic time scales, vein-fill and joint formation are almost synkinematic, with infilling occurring slightly later as extension across the joint was reactivated with the same sense of stress during exhumation. Veins and fractures are often related to confining pressures that occur deep in the crust because under these conditions natural hydrofracturing occurs when fluid pressure, concentrated in flaws in the rock, surpasses the tensional strength of the material (Secor, 1969). However, the Weches Formation was never buried to a significant depth, and the joints and the iron veins both occurred at shallow depth. The iron material in the veins appears to be identical to the material in the ironstone beds which are pervasive, continuous, flat-lying layers of ferruginous material, typically limonite or allied forms (Eckel, 1938). The joints in the Weches typically terminate at these iron beds, though in some cases the ironstone is also jointed. The interaction with these ironstone beds is important because it can constrain the timing of jointing.

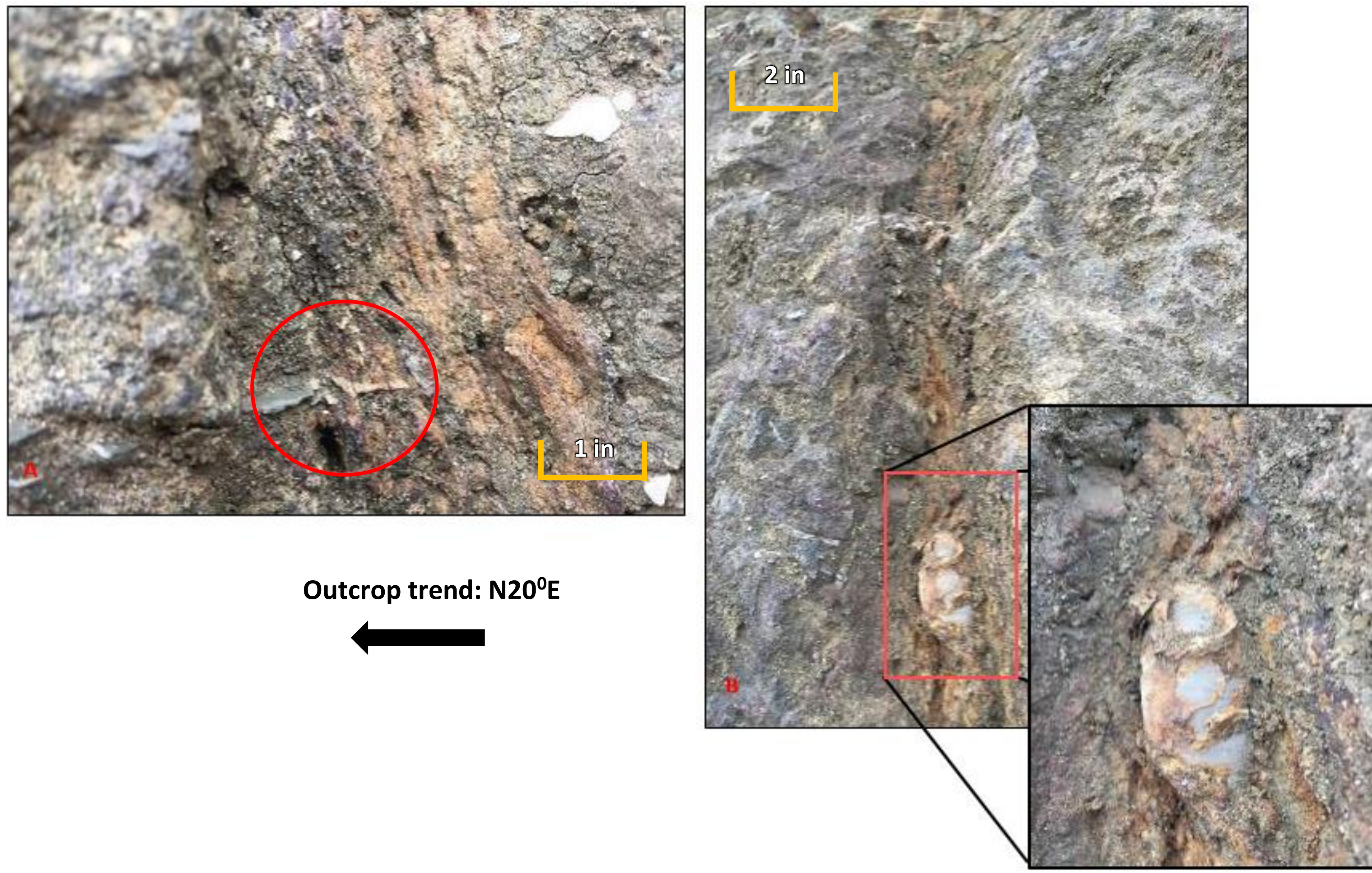

Figure 47. Veins crosscutting fossils at site 5 Nacogdoches (A) *Clypeasteroida (*sand dollar) fractured by joints through an iron vein. (B) Undeformed gastropod inside an iron vein also at site 5.These illustrate the fact that the veins are not shear fractures and that they are not always formed via crack-seal mechanism.

Figure 48. Iron bearing extensional veins in the Weches Formation. (A) “crack-jump” vein from site 5. (B) Crack-seal vein from Banita Creek (site 2) showing repeated jointing and resealing with the centermost joint (youngest) unsealed. (C) Vein from site 6 showing two episodes of cracking and resealing.

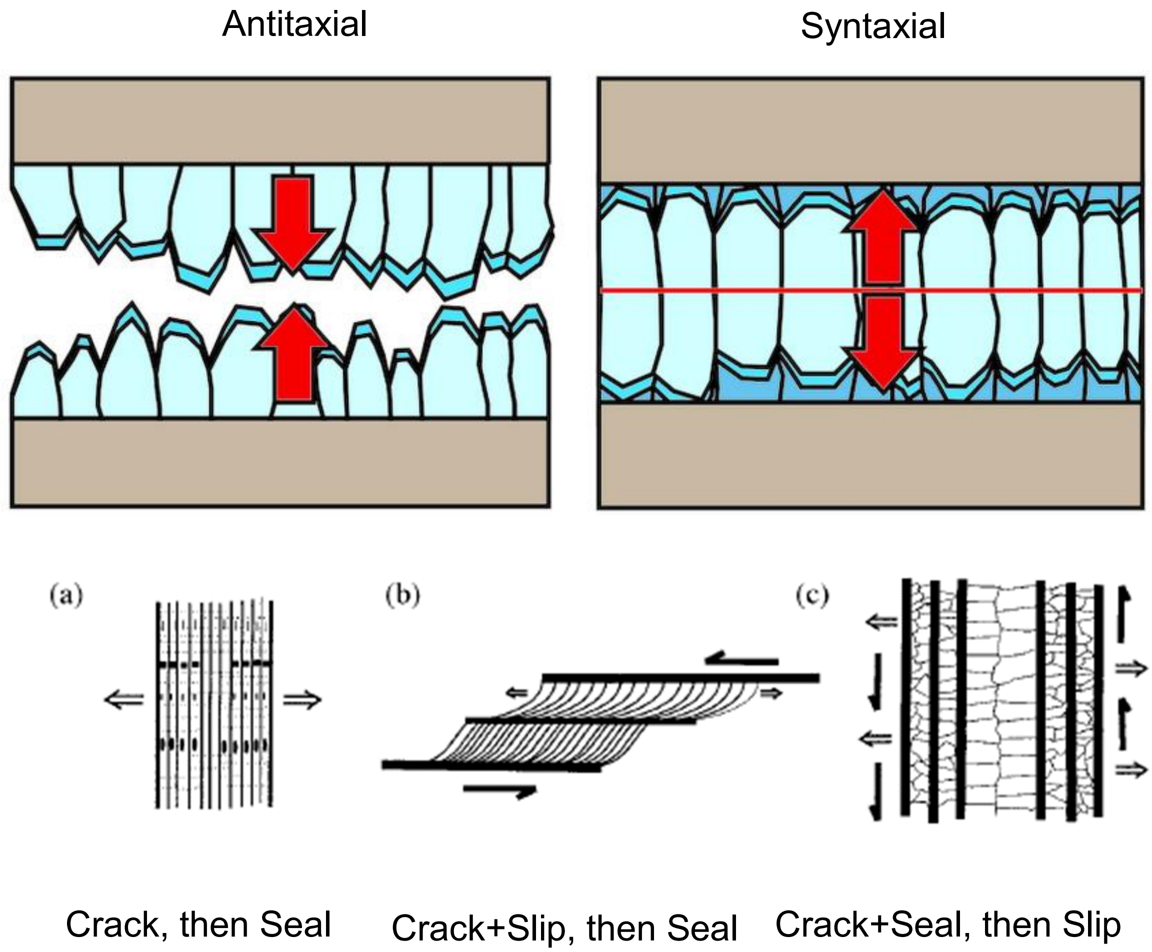

Figure 49. Types of vein growth. Antitaxial veins grow inward from the initial fracture face while syntaxial veins growth outward from the initial fracture face. (a), (b) and (c) show different ways the vein seals and then cracks repeatedly. Most veins in the Weches Formation display antitaxial crack-seal vein growth. Figure 47b is a good example of this. (Modified from (upper) McNamara, 2016 and (lower) Pettit et al., 1999).

Ironstone Layers

Several studies have interpreted the ironstone beds as secondary, late diagenetic features that formed post-deposition when the unit was close to the surface, due to movement of iron-rich groundwater during erosional exhumation (Eckel, 1938; Jones, 1969; Ledger 2007). Joints that stop at the iron ledges must be contemporaneous with or younger than formation of iron ledges based on cross-cutting relationships. They could not have all been younger since it is likely that the joints were necessary for the creation of the iron beds. This is because the Weches Formation is mostly a low permeability clay unit and jointing would have been necessary to provide conduits for the migration of groundwater required for iron deposition and oxidation. Figures 43 and 44 are good examples of a typical outcrop of Weches containing ironstone layers.

The caveat to using crosscutting relationships between the iron beds and jointing is the question of what lithology existed in the space that these iron beds currently occupy. These iron beds would probably not have formed layers with sharp contacts covering hundreds of square feet (or even square miles) without some preexisting sedimentary layer facilitating concretion. They did not form in horizontal fractures since there would need to be evidence for syntaxial crystal growth or crack-seal features as the concretion grew outward. Instead, primary iron bearing minerals that led to the formation of iron concretions precipitated first out of the seawater as the Weches was being deposited (Ledger 2007). Certain beds in the Weches must have either contained sediment that was more conducive to secondary generation of iron or been more porous so as to encourage water saturation. Foos (1984) concluded that there were multiple stages of mineral alterations, including alteration of kaolinite to berthierine and the precipitation of siderite, prior to the formation of goethite and limonite above the water table. The possibility of the existence of layers in the Weches (representing what would later become the iron beds after interaction with surface water) that were significantly different lithologically from other layers is important because it would provide an interface – pre-ironbeds – where joints would be terminated. Several studies have shown that layer interfaces disrupt joint propagation and that joints selectively confine to certain lithologies (Helgeson and Aydin, 1991). It is difficult to gauge the original lithology of the iron layers because they have become so altered.

Another line of evidence that might have indicated that the joints predate the iron beds is that fractures preferentially form in rock layers with lower tensional strength. This means that stiffer layers will typically fracture first (Fossen, 2016). This may seem counter intuitive but take for example a piece of glass and a piece of plastic, if they are cemented together and an increasing tensional force is applied, the glass will break first. Its stiffness does not allow it to deform elastically like the plastic and because being bound together means they experience the same amount of strain, the stress builds up in the glass before the plastic causing it to fracture first, even though the glass is structurally much stronger. This can happen in shale-limestone layers where the limestone fractures before the shale because of its higher stiffness (Fossen, 2016). The iron beds are undoubtedly stiffer than the claystone. In other words, if the iron layers were present during the fracture forming event, the fractures would preferentially propagate in the iron beds before the clay, however, the vast majority of the iron layers are unfractured. Despite this, it is doubtful that the restriction of jointing to the clay layer predates iron bed concretion because (1) the iron layers are not as continuous as they may appear from outcrop to outcrop and (2) The jointing occurred very shallowly when the clay’s tensional strength may have decreased after being fully lithified and cemented and experienced expansion as removal of overburden was occurring.

Hackle Marks

Hackle marks can be described as a segmented section of a joint that occurs as a joint rotates during propagation. An illustration of this feature is shown in figure 50 This feature was observed at site 13 which is the in the J1a region of joints and site 5 which is in the J1b region of joints. These features are shown in figure 48 and 51. Hackle marks and fracture segmentation can occur in response

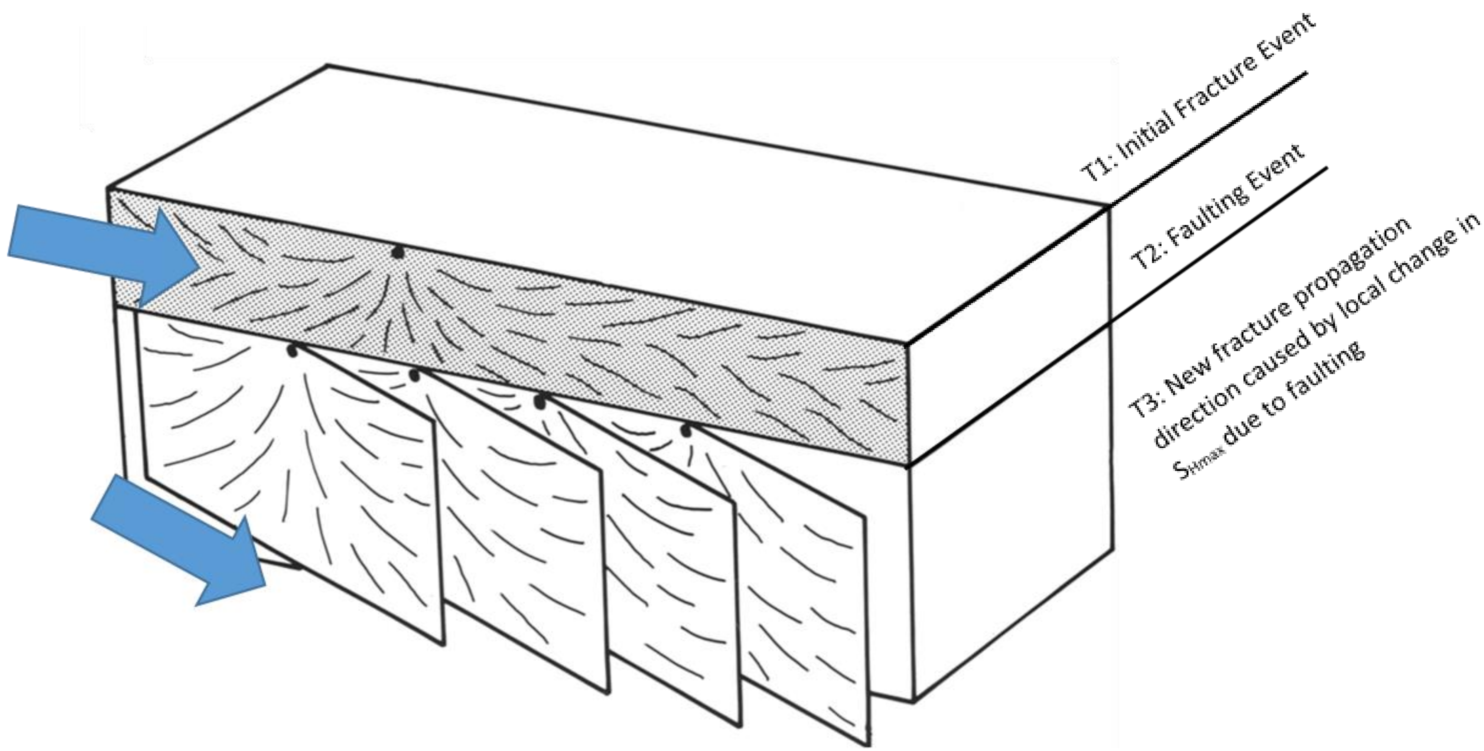

Figure 50. Cross-sectional schematic showing sequences of hackle mark formation. T1) Initially, a planar joint forms at the top of the section and moves downward , following the path of S_{Hmax}, as the tensional strength of the rock is exceeded. T2) Local deformational event occurs causing a perturbation in the stress field and a new S_{Hmax} direction. T3) Joint continues propagation as a segmented section in the new direction of S_{Hmax} (Kulander et al, 1979). Modified from Helgeson and Aydin, 1991.

to a minor rotation in the primary horizontal stress direction. The segmentation and change in direction allow the joint to continue propagation perpendicular to the direction of least compression (Pollard and others, 1982). Rather than a change in the far field stress regime this rotation is likely the result of the nearby fault. The main normal fault observed at site 13 trends N84^{0}W 55^{0}S, the same direction the hackle marks trend. Figure 48 shows that the rotation in joint direction occurred at the base of the first joint. This is important to note because when a joint becomes segmented and rotates in another direction the direction of the segmented section is the youngest direction (Kulander et al, 1979). In other words, the hackled joint section (N85^{0}W) and the similarly oriented fault occurred after the initial jointing. The upper section of the joints trend N75^{0}W which happens to be similar to another large normal fault nearby which trends N71^{0}W, 56^{0}S.

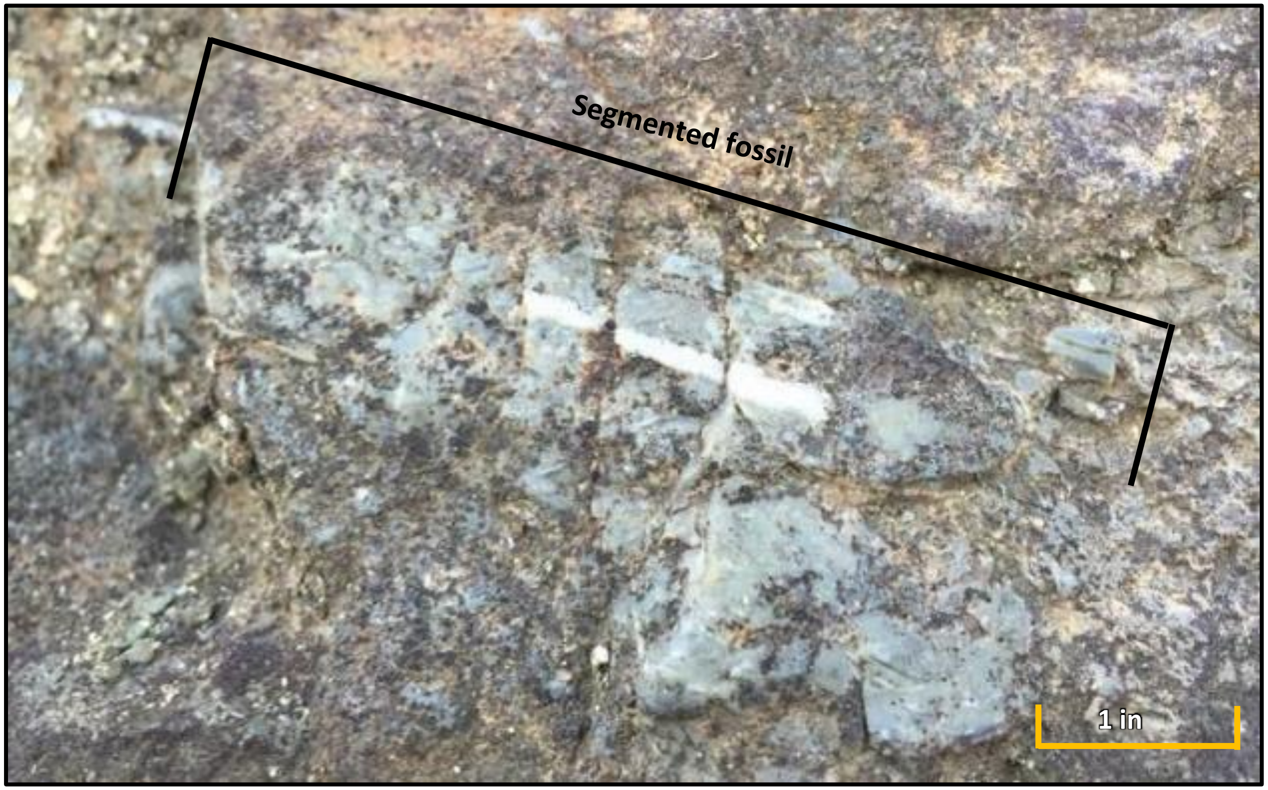

Figure 51. Segmented J1b joints through a fossil oriented N70E. This image was taken from site 7 which is in the J1b region of $N80^0E$ directed joints.

Relative ages of jointing

In order to correlate jointing to some geologic event it is necessary to first determine their relative ages by cross-cutting relationships. This can be a difficult proposition because of the little to no amount of offset that occurs across fracture surfaces and the fact that intersecting joint sets can form with only slightly different orientations. Engelder and Geiser (1980) studied jointing in the Appalachian Plateau and found two differently aged joint sets with a difference in strike as little as $18 – 30^0$. They found that there was a set of joints with a predominate orientation that coincided with the trend of fold hinges formed during Appalachian shortening while a second set of joints formed irrespective of this trend. This was interpreted as two stages of jointing, one forming during the Appalachian shortening and one forming later as the stress trajectory had changed slightly. While sets of intersecting joints with only slightly different orientations are possible in sedimentary rocks, it is highly unlikely for adjacent faults.

After determining the presence of joint sets, crosscutting relationships determine their relative ages. Even though some joints sets may form instantaneously, they continue to grow and interact with each other which can create confusion when determining crosscutting relationships. Even so, the older joints should truncate the younger joints more often than not.

Crosscutting relationships

Orthogonal Joints

Field work indicates that the main joint sets in the Weches Formation are, with some exception, isolated from one another. Apart from sites 3 and 8, systematic joint sets are present at each outcrop. Many of these outcrops, however, also contain cross joints with differing strikes – some systematic some nonsystematic. Refer to tables 1 and 2 for the joint classifications. The nonsystematic joints are of little importance and likely occurred at the surface due to weathering. The systematic cross joints are ones that are bounded between the main joint set but maintain consistent orientation. In every case these cross joints appear to be perpendicular to the main joint set which would classify them as orthogonal joints. Recall that orthogonal joints form in the reoriented stress field created immediately nearby the initial joint set. This means they can be ruled as inconsequential in terms of regional tectonic stress information. These groupings of joints perpendicular to the main joint set become clear when orientations are plotted in stereonets. This can be viewed in figure 45 in the field results section of this paper and is especially evident in sites 9 and 4.

Conjugate Joints

The presence of conjugate joint sets, or two or more joint sets intersecting at angles between 30^0 and 60^0, is rare in studied outcrops of the Weches Formation. However, there is evidence that, in in some cases, the J1b or similarly oriented set coexists with the J2 set in the northwestern section of the study area. Examples of their crosscutting relationships can be seen in figures 52 and 53. Site 10 and especially site 7 show a strong presence of a conjugate set of joints trending roughly east-west. The J2 joints in this area do not consistently arrest the J1b joints but tend to be the thoroughgoing joint more often than not. This relationship is shown in figure 52. Because an already existing joint would have had to be present in order to prevent a subsequent joint from propagating further, the thoroughgoing joint must be older. The relationship in this area is not quite this simple, however. The J2 set does appear to have formed initially before the J1b set however there are examples of the J2 joints being halted by the J1b. This relationship is shown in figure 53. If we assume that joints from the J2 set form as a result of the similarly trending faults in the central basin and northeastern flank of the Elkhart graben based on proximity and similar orientation, then we must corroborate the timing of the two.

The Elkhart Graben has been active since the Early Cretaceous and has offset Quaternary terraces, implying movement as recent as 37,000 years ago (Jackson, 1988). Collins et al., (1980) measured offset of up to 66 cm in the Weches Formation exposed in the Trinity River caused by Elkhart Graben faulting. Central basin faults are believed to have a similar origin and timing (Jackson, 1988). In other words, the Elkhart Graben and Central Basin Faults have been active on and off throughout the history of the Weches. This fits well with the assumption that the J2 joints formed in the stress field that lead to these faults. At the same time, a period of inactivity in faulting could have allowed stress to buildup in the more N80^{0}E direction, the common stress field for the majority of East Texas, forming conjugate J1b joints periodically. This could explain the presence of both J2 and J1b joint sets and the lack of one dominant set consistently truncating the rest.

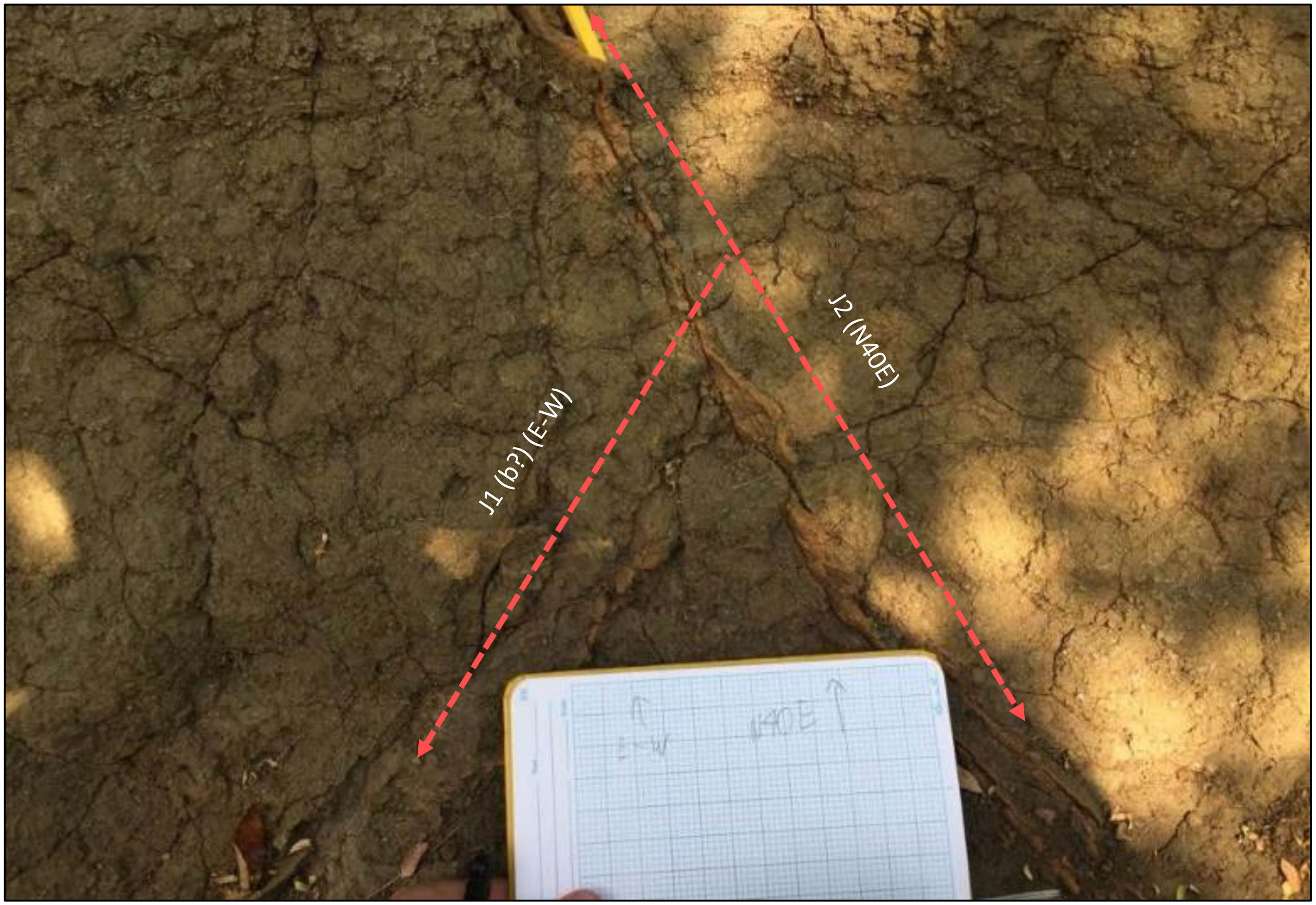

Figure 52. Intersection of J2 and J1(b?) set at outcrop. The J2 set abuts the J1b set indicating that the J2 joint formed first. Their dihedral angles indicate that they are not orthogonal joints but are conjugate. This tells us that the secondary joint (J1b in this case) likely formed as a result of a remote stress field rather than the nearby perturbed stress field caused by the initial joint. In this example both joints have iron infilling.

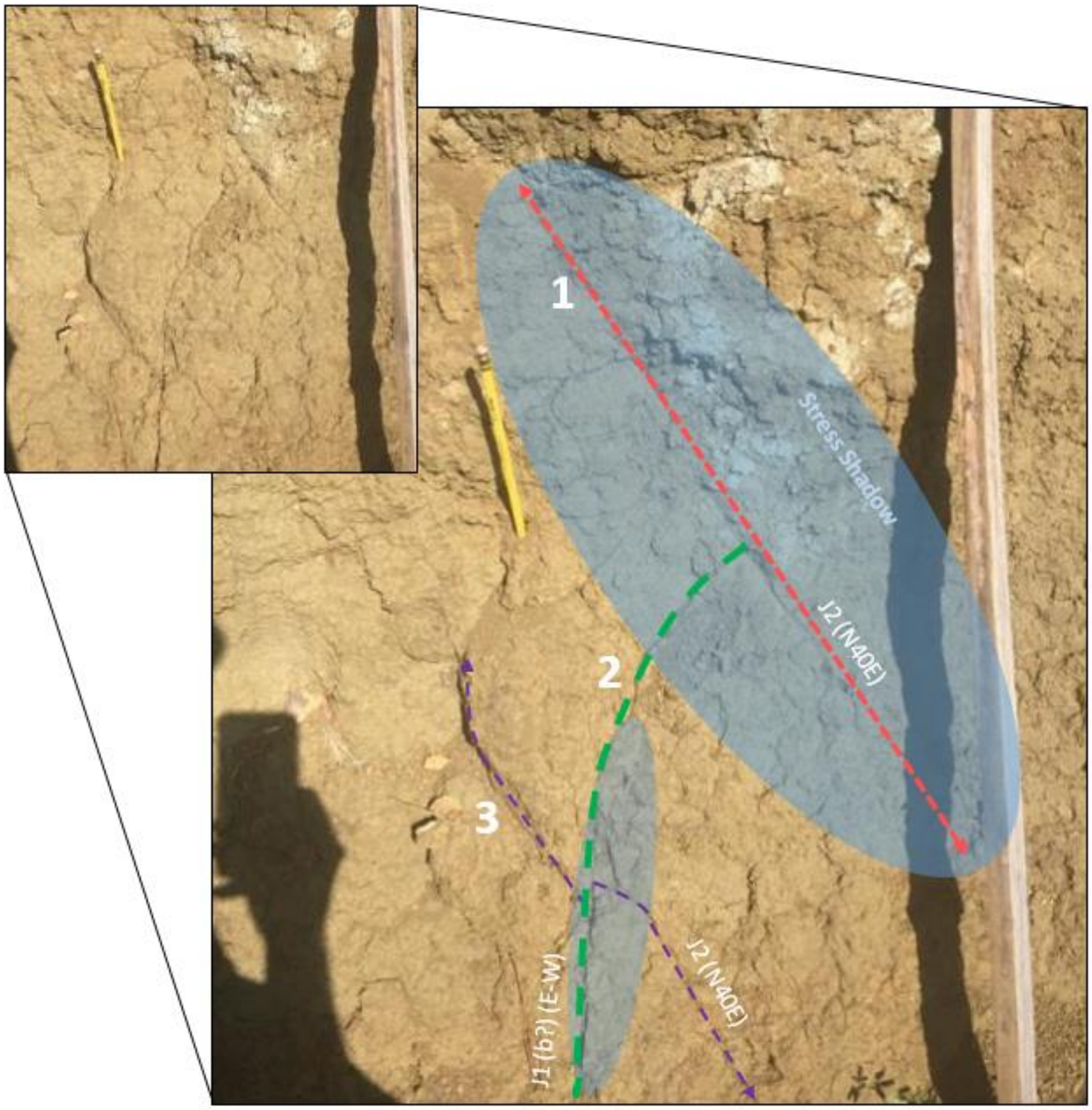

Figure 53. Interpretation of outcrop example of intersections of J2 and J1b joints. A pencil is there for scale. In this example from site 10, there appears to be three jointing events based on abutting relationships in the following succession: red (J2), green (J1b) and purple (J2). The green and purple lines show how the joints initiating off adjacent joints propagate at ~90^0 and then curve in another direction. These curves show the influence of joint propagation transitioning from local stress perturbation created by the initial joint to far-field stress (tectonic activity) as it moves away. When the first joint is formed a sphere of influence – called the "stress shadow" (shown as blue bubbles in this figure) – is created. Any joints moving through this region will be influenced by this localized stress field rather than the far field stress. This succession of jointing may be a result of the intermittency between faulting in the East Texas Basin and the overall extension towards the Gulf Coast Basin.

Age of joints based on interaction with the ironstone layers

As mentioned earlier, several studies have interpreted the ironstone beds as secondary, late diagenetic features forming near the surface. Because the propagation of a joint is often terminated between lithologically different interfaces, these ironstone layers are essentially paleo-indicators for the timing of jointing. Joints formed before the ironstone layers would persist through the iron section, while joints forming afterwards would terminate along the interface.

At outcrops where ironstone layers are present, the vast majority of joints are either terminated by the ironstone layers or their propagation path is somehow disrupted by them. Figure 54 shows the relationship between joints and ironstone layers in a cliff at site 1. Therefore, the joints likely formed after the ironstone layers and thus during exhumation near the surface. This is also supported by the fact that the Weches was not likely subjected to high enough tectonic pressures at depth to generate hydraulic joints. This is because the Weches was not buried to a significant enough depth (except possibly near the depocenter of the East Texas Basin) and was not subjected to any significant amount of folding. The prevalence of well preserved fossils showing no signs of deformation support this as well.

In summary, all three of the systematic joint sets observed in outcrops of the Weches Formation found in the study area appear to be late-forming features (Neogene) occurring during exhumation. Because the J1a and J1b joint sets were not observed sharing the same location their ages relative to each other remain a mystery. The J2 and J1b joints do coexist in some outcrops in the northern region of the study area and appear to have formed in periodic successions, based on crosscutting relationships, indicating their ages are relatively similar.

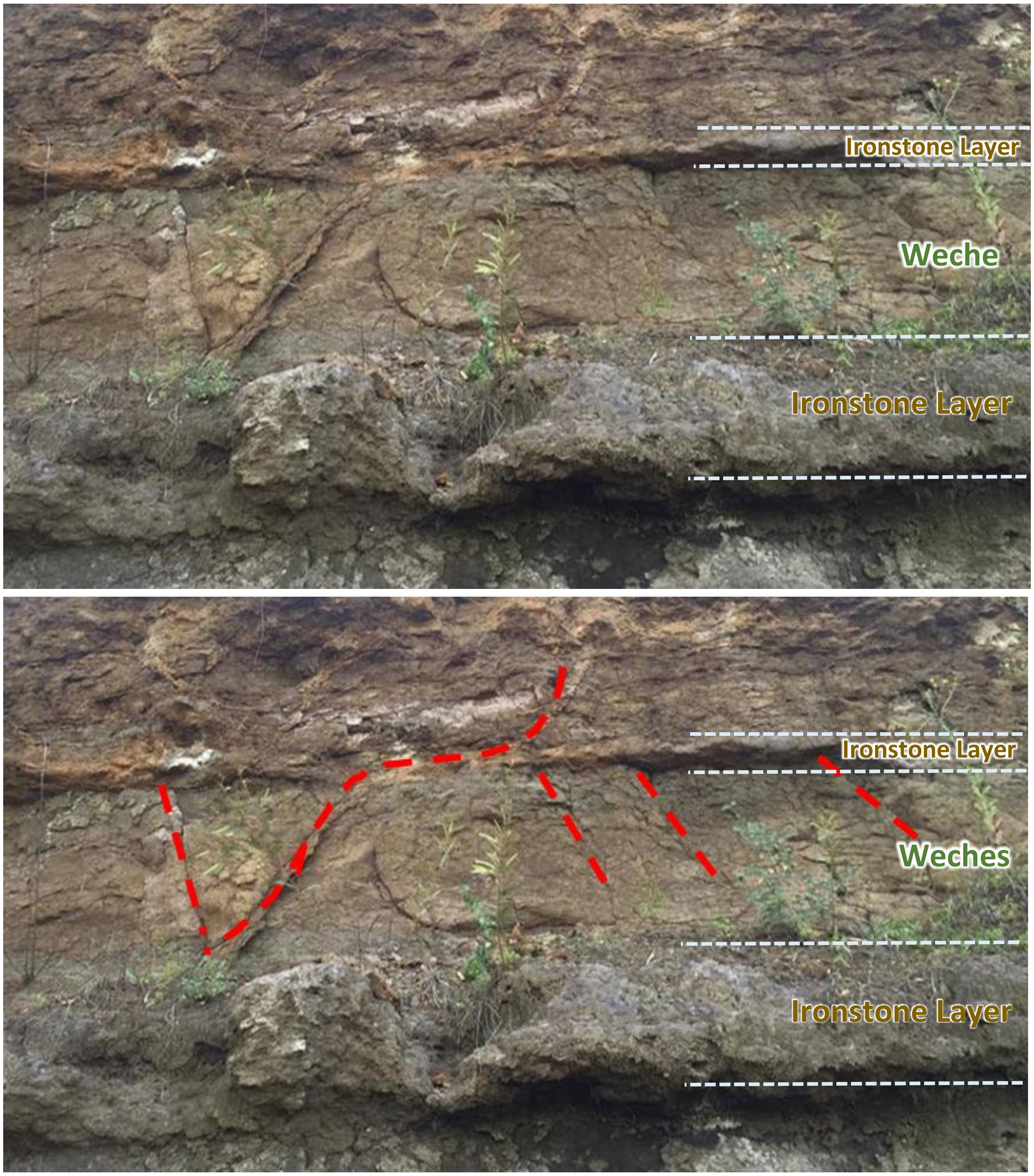

Figure 54. Crosscutting relationships of joints and ironstone layers. The joints in this image are either terminated by the ironstone layer or their propagation path is disrupted by it. This most likely means that the ironstone layers existed before the joints formed. Because the ironstone layers formed during exhumation the joints must have as well.

Relation to the stress regime in East Texas

The accepted average modern stress regime in east Texas based on results from direct stress measurements, borehole breakout data, hydraulic fracture tests, earthquake data, and recent movement along the Elkhart-Mt. Enterprise Fault Zone suggest a modern maximum horizontal stress that trends east-northeast and is relatively consistent throughout East Texas (Gough and Bell, 1982; Laubach, 1989; Snee and Zoback, 2016). Stress maps showing the state of stress in East Texas are shown in figures 31 and 32.

Systematic, vertical, mode I fractures should, in theory, propagate in the direction of maximum horizontal compressive stress (S_{Hmax}) that they formed in. Because the field data indicates that the joint sets measured in this study do meet these criteria (see section: Nature of joints in the Weches Formation) their strike should indicate the direction of S_{Hmax} with the S_{Hmin} being in the perpendicular direction. Assuming the joints in this study are resulting from contemporary tectonic stresses, then these orientations could provide information on a modern stress regime. Recall that three separately oriented joint sets confined to three different regions have been observed. Figure 55 displays these joint set trends in map view. Based on their orientations, at least three stress provinces with subtle differences in direction may be inferred. The following paragraphs will explore the possible stress regimes.

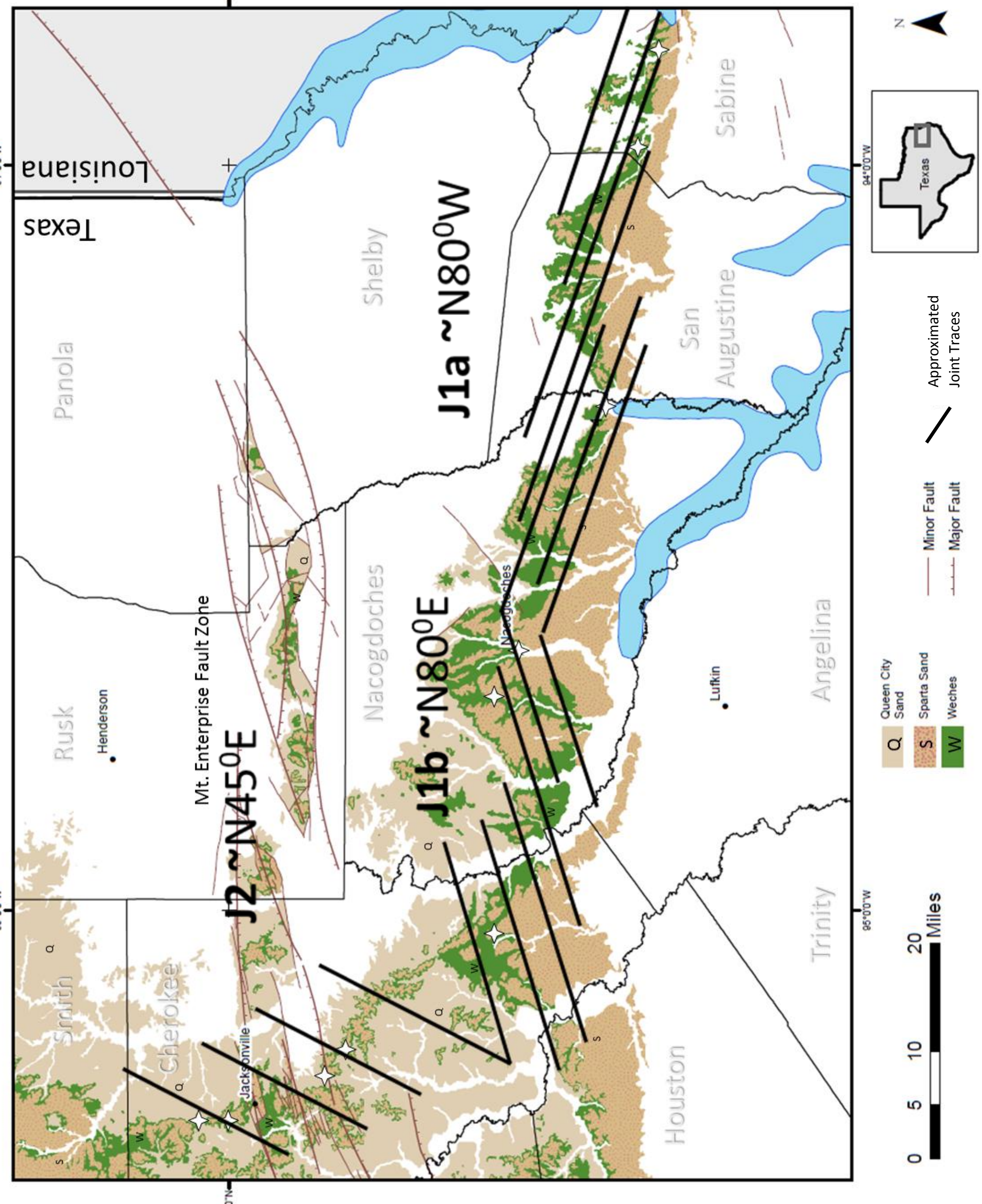
J1a ~N80⁰W
J1b ~N80⁰E
J2 ~N45⁰E
Mt. Enterprise Fault Zone
Texas
Louisiana
Panola
Shelby
Sabine
San Augustine
Rusk
Henderson
Nacogdoches
Angelina
Lufkin
Smith
Cherokee
Jacksonville
Trinity
Houston
Queen City Sand
Sparta Sand
Weches
Minor Fault
Major Fault
Approximated Joint Traces
0 5 10 20 Miles
32°0'0"N
94°0'0"W
95°0'0"W

Figure 55. (On previous page): Approximation of joint traces extended to illustrate the regional trend. The joint sets (J1a, J1b and J2) group into three provinces. J1a trends N80^{0}W and is located to the east, J1b trends N80^{0}E and is located centrally and J2 trends N40^{0}E and is located to the northwest of the study area. These three provinces could indicate regional differences in recent to present-day stress regimes across East Texas. Note that these joint traces have been extrapolated lengthwise into areas where data was not taken to better illustrate the pattern, however measurements were restricted to Weches outcrops. Geologic units shapefile from USGS geologic database of Texas.

Joint set J1a

East of Nacogdoches County the predominant systematic joint set is approximately N80^{0}W (figure 52). This is roughly 20^0 different than the typical measurement for S_{Hmax} in East Texas which is around N65 – 80^{0}E (Snee and Zoback, 2016). This change in direction may delineate a change in stress province where the greatest horizontal stress direction is to the northwest. This stress direction information is unique to this study and is not shown in stress maps of east Texas. Almost all published data on maximum horizontal stress directions in Texas show east-west to northeast-southwest orientations throughout. Despite this, several small normal faults (bearing N75^0 - 85^{0}W) were mapped at site 13. These faults are believed to be kinematically related to the J1a set.

It is possible for joints to be precursors for faulting as well as occurring during and after faulting. All joints at site 13 appear to have occurred post-faulting based on the fact that: the joints do not curve towards the fault, do not increase in frequency approaching the fault, and the unit is completely unjointed on one side of the fault. These factors all point to post-fault jointing (Peacock, 2000). Because these joints are oriented similarly to the faults it is safe to say they are kinematically related, although the cause of these faults is unknown. Even though the dip of the joints is much steeper, Hancock (1985) noted that joints are often concordant with dip-slip faults, but usually have different dips. Because the same features exist at site 6 and 5 it is possible there is a similar fault in the vicinity. although none were found.

Interestingly, recent measurements of a 2012 earthquake recorded near Timpson, roughly 30 miles (48 km) north of Chireno (site 4, figures 1 and 2), indicated slip had occurred on a NW trending strike-slip fault (Snee and Zoback, 2016). They found this to be puzzling for two reasons: because it had occurred in an area believed to have NE trending S_{Hmax} and because NE trending faults exist nearby. This is problematic because any NE trending faults should be the first to slip in a NE oriented stress field. Elevated pore pressure can cause unfavorably oriented faults to slip, however they determined that the change in pore pressure required to allow this to happen was beyond what hydraulic injections could achieve. It is much more likely that a fault better oriented for failure in the current stress field will create an earthquake, regardless of injection-related pressure changes (Snee and Zoback, 2016). In other words, a NW trending S_{Hmax} is more favorable for slip on a NW trending strike-slip fault. One explanation mentioned in the study was that there was a dramatically varying local stress field near the fault. Because a NW S_{Hmax} is also favorable for the formation of the NW trending joints in the Weches Formation to the south, further research into determining the cause of the change in stress field near Timpson could be informative.

The J1a joints measured in this study indicate a clock-wise rotation in direction of maximum horizontal stress starting about 20 miles (32 km) east of Nacogdoches, in Chireno, continuing to the Louisiana border (figure 55). The orientation of the J1a joint set indicate that the east side of Nacogdoches County to San Augustine and Sabine Counties has a maximum horizontal stress direction of N75^0-85^{0}W. The possible causes of this change in stress field are discussed in following section.

Joint set J1b

20 miles (30 km) west of Chireno the predominant systematic joint set shifts by about 20^0 from N80^{0}W to a new orientation of approximately N80^{0}E. This trend fits well with previously published fracture analyses and stress tests. For example, a fracture analysis in East Texas was conducted by Laubach, (1989) where they found predominantly east-northeast trending natural extension fractures in the Travis Peak Formation. Their subsurface joint data bears striking

results to the data found at outcrop in this study. The relationship can be seen in figure 56. They attributed this trend to south-southeast directed tectonic extension resulting in an east-northeast directed S_{Hmax} that numerous stress tests have confirmed (Snee and Zoback, 2016; Gough and Bell, 1982; WSM Team, 2016; Heidbach et al., 2016). It is unsurprising that the J1b set is an east-northeast trending joint set which delineates a maximum horizontal stress in the same direction. It is also no coincidence that this set is parallel to faults in the Mt. Enterprise Fault Zone, which is believed to accommodate continued extension in the Louann and post-Louann strata, and to the extensional faults which persist parallel to the Gulf coast and accommodate Gulfward-extension (Jackson, 1982). In other words, the J1b joint set represents the roughly east-west maximum horizontal stress province resulting from the south-southeastern directed tension from the Gulf. The majority of Nacogdoches County and Cherokee County are therefore of a tensional province directed north-northeast which is typical for the East Texas region.

Natural fractures from this study taken at outcrop:

n = 540

Mean = **N87^{0}E**

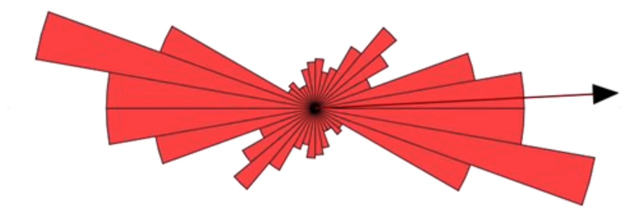

Travis peak fractures up to 1,800 feet in depth in Nacogdoches County (Laubach, 1989):

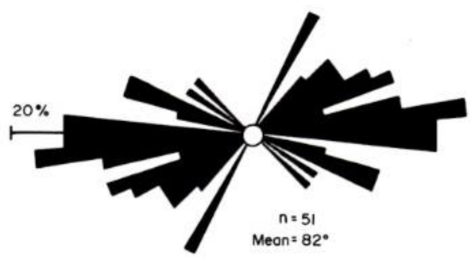

Figure 56. Rose diagram of all joint strike data in comparison with a separate study of joint orientations in East Texas. The upper diagram, (A) shows all joint strikes from this study plotted in 10^0 increments. (B) shows orientations of 51 natural joints in the Travis Peak formation in East Texas in 5^0 increments from Laubach (1989). Joint data from b was taken from two wells in northern Nacogdoches County. There are obvious parallels between the two sets of data with the difference in mean strike direction being only 5^0. Note that (B) was taken from dipmeter readings in a wellbore readings from depths of up to 1,800 feet while (A) was taken from outcrops at the surface.

Joint set J2

In the upper part of Cherokee County and the lower part of Smith County the J2 joint set, with an average trend of N40^{0}E is most prevalent. Joints from both the J2 and the J1b sets are present in these counties; and while the J2 set is the dominant joint set, there is evidence for both sets abutting each other (see figure 53), indicating that the stress field might have varied through time alternating between the N40^{0}E and N80^{0}E direction. The strike of the J2 joints appear to closely resemble fault strikes in the Elkhart Graben Fault Zone and in the central part of the East Texas Basin. They also exist in the direct vicinity of these two fault systems. These faults are tied directly to salt structures in the East Texas Basin.

The cross-cutting relationships with the ironstone layers also apply to joints in the northern region. This means they should reflect the stress field caused by recent events. The Elkhart Graben has affected Claiborne units as young as the Yegua Formation and has been active as recently as 37,000 years ago (Jackson 1982). Jackson (1982), also stated that the faults in the central basin shared a similar origin to the Elkhart Graben faults based on fault geometry. This makes it more likely that salt mobilization in the East Texas Basin could be affecting a contemporary stress regime, possibly in localized areas rather than regionally. The strike of the J2 joint set indicates that the maximum horizontal stress in the immediate vicinity of the central basin rotates to a north-northeasterly direction.

Three Stress Provinces

Three separately trending and regional joint trends have been mapped. Assuming the joints in these sets have propagated in the direction of S_{Hmax} then they should be representing three different stress provinces. Based on this principle, the directions for S_{Hmax} are as follows: N40^{0}E in near the East Texas Basin, N80^{0}E in the central part of the study area and N80^{0}W east of Nacogdoches. These stress provinces inferred from the joint sets found in this study are shown in figure 57. Figure 58 shows the comparison of these stress provinces to previous stress data. Except for the J1a province, these orientations of the stress regime fit fairly well with stress data published in previous studies of the East Texas area. The following section will explore the possible causes of the formation of each joint set.

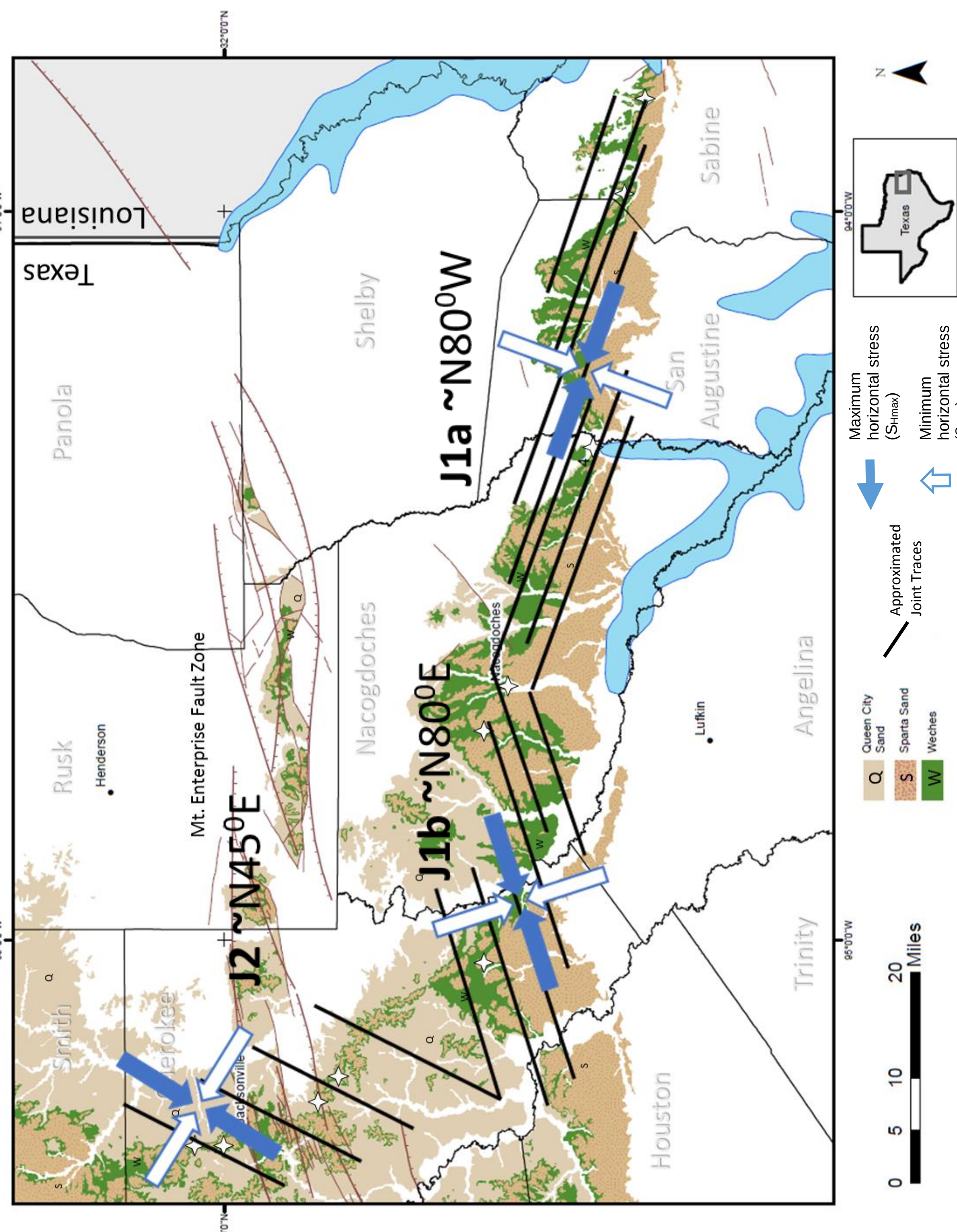
J1a ~N80⁰W
J1b ~N80⁰E
J2 ~N45⁰E
Mt. Enterprise Fault Zone
Texas
Louisiana
Panola
Shelby
Rusk
Henderson
Nacogdoches
San Augustine
Sabine
Angelina
Lufkin
Smith
Cherokee
Jacksonville
Trinity
Houston
Q Queen City Sand
S Sparta Sand
W Weches
Approximated Joint Traces
Maximum horizontal stress (SHmax)
Minimum horizontal stress (SHmin)
Texas
N
0 5 10 20 Miles
32°0'0"N
95°0'0"W
94°0'0"W

Figure 57. (On previous page): Approximation of stress regime based on observed joint set trends. Systematic, vertical, mode I fractures should, in theory, propagate in the direction of maximum horizontal compressive stress (S_{Hmax}) that they formed in. Assuming the joint sets measured in this study meet these criteria (field data indicates that they do) then their strike should indicate the direction of S_{Hmax} with the S_{Hmin} being in the opposite direction. The blue and white arrows indicate this inferred direction based on the joint set trends, with the blue arrows representing S_{Hmax} and white representing S_{Hmin}. Geologic units shapefile from USGS geologic database of Texas.

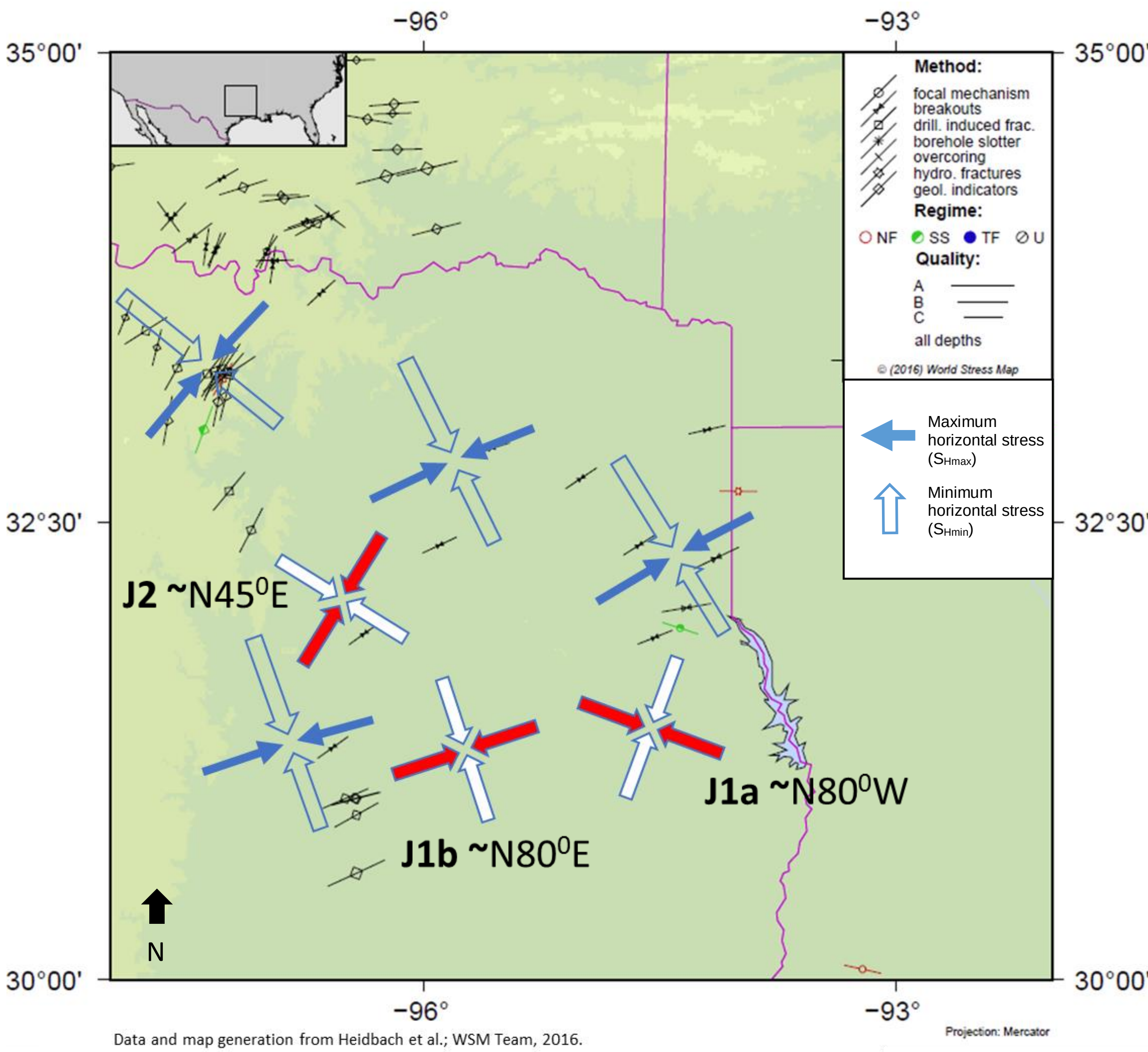

Figure 58. Stress provinces as indicated by joint sets in the Weches Formation in comparison to stress data from previous studies. Colored arrows represent directions of S_{Hmax} while uncolored arrows represent S_{Hmin}. Red arrows represent the stress directions inferred from the joint sets observed in this study while blue arrows are an approximation based on the previous stress data shown here. Stress directions inferred from the J1b and J2 joint sets more or less matches previously measured regional trends, while the J1a has a less typical orientation. Data and map generation from (Heidbach et al.; WSM Team, 2016).

Causes of jointing

Possible influences based on time and location constraints

Because the Weches Formation was deposited in the Eocene, all events following this epoch must be considered as possible causes of jointing. There are several main tectonic influences that were contemporaneous with Eocene Weches deposition: continual crustal extension caused by Gulf of Mexico Basin subsidence, salt-driven extension into the East Texas basin, and possibly Laramide compression from the west. Structurally, in East Texas, these influences collectively resulted in the Mexia-Talco Fault Zone, the Elkhart-Mt. Enterprise Fault Zone, central basin faults in the East Texas Basin, and uplift of the Sabine Arch. During the early history of the Weches, none of those events may have caused any jointing in the Formation because: This is because (1) brittle deformation would be more likely if the rock was lithified through compaction or cementation which typically takes place after burial and (2) there is little evidence of fracturing during burial or at depth. This is not to say that these early events should be ignored, because any residual stress that may have built up earlier in the unit's history could have direct control over the orientation of fractures that formed later during exhumation (Fossen, 2016). However, the lack of structures other than jointing in the Weches Formation suggests that early stresses were not of intense enough magnitude that residual stress was trapped and later affected the rocks. Instead, it is more likely that recent to present day regional tectonic and/or localized stresses control the orientation of joints. This would rule out events of the Early Eocene and before as causes of jointing. This includes Mexia-Talco faulting and possible Laramide northeast directed compression; the latter event may have been responsible for the Sabine block uplift. The episode of compression and uplift of the Sabine block is postulated to have only lasted until about 45 mya which is when the Weches Formation was deposited (Adams, 2009). Subsequent uplift of the Sabine Arch did occur during the Oligocene and Miocene; however, the rest of the Gulf Coast Plain was uplifted along with it due to loading and subsidence in the Gulf of Mexico Basin (Ewing, 2009; Jackson and Laubach, 1988). This is not to say that the Sabine Uplift has no effect on the present-day stress regime; just that it likely did not directly affect the orientation of jointing in the Weches Formation in the surrounding area. On the other hand, indirectly, the presence of a large inhomogeneity in the crust could still have some bearing on how on the strata is being stressed by disrupting the S_{Hmax} in the surrounding area. This is because topography in general, which was created by the uplift of the Sabine Arch, can affect the state of tectonic stress in the surrounding area (Liu and Zoback, 1992).

The proposed influence of Laramide compression is tied to basement rocks and its ability to significantly impact the stress regime of the overlying Cenozoic strata in East Texas seems unlikely, but not impossible. The following paragraphs present the most likely tectonic events resulting in each of the three joint set trends observed in East Texas. Figure 59 is the basis for these theories and illustrates the relationship of the joint trends to regional structural features by proximity and orientation. This figure overlays the major joint trends on a subsurface structural map.

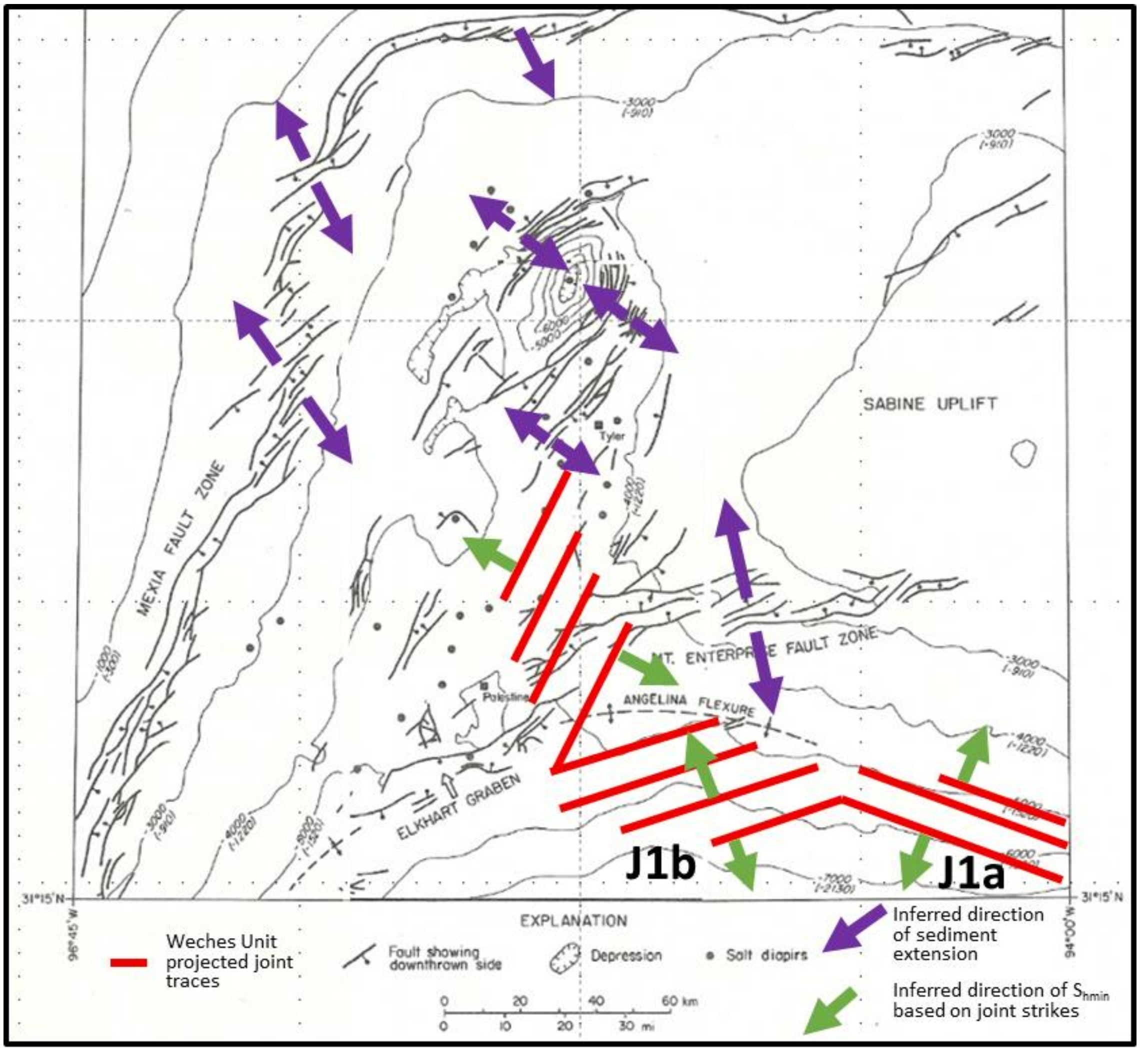

Figure 59. Subsurface structural map showing fault traces and structure contours. Main average joint traces in the Weches Formation are shown as heavy red lines on the map with green lines representing the inferred direction of S_{Hmin}. Inferred directions of extension related to regional structural elements are shown as purple arrows. The three sets include: J1a trending N80^{0}W, J1b trending N80^{0}E and J2 trending N40^{0}E. The trends of the subsurface structures seem to coincide with the trends of measured joint orientations, which suggests that the kinematics of the two are related (modified from Dix and Jackson, 1981).

Gulfward Extension and the J1b joint set

The J1b set is centrally located in the study area and trends N80^{0}E. Gulfward directed, Cretaceous to Tertiary extension caused by Gulf Coast Basin subsidence has had a strong influence this joint set. Zoback and Zoback (1980) have shown that the resultant tensional province created by this Gulfward subsidence extends as far north as the Mexia-Talco Fault Zone and southward to the present-day coast. This southward extension has been shown to have produced a S_{Hmax} of roughly east-west in East Texas. Because joints form in the direction of maximum horizontal stress one would expect to see east-west directed joints and, indeed, the cumulative average direction of all recorded joints in the Weches Formation is N87^{0}E. These analogous orientations, paired with the strong possibility that jointing is at least a Paleogene event, possibly up to the present, supports this idea. The J1b set which trends N80^{0}E best illustrates this stress regime, paralleling the growth faults to the south as well as the Mount Enterprise fault system to the north (figure 60).

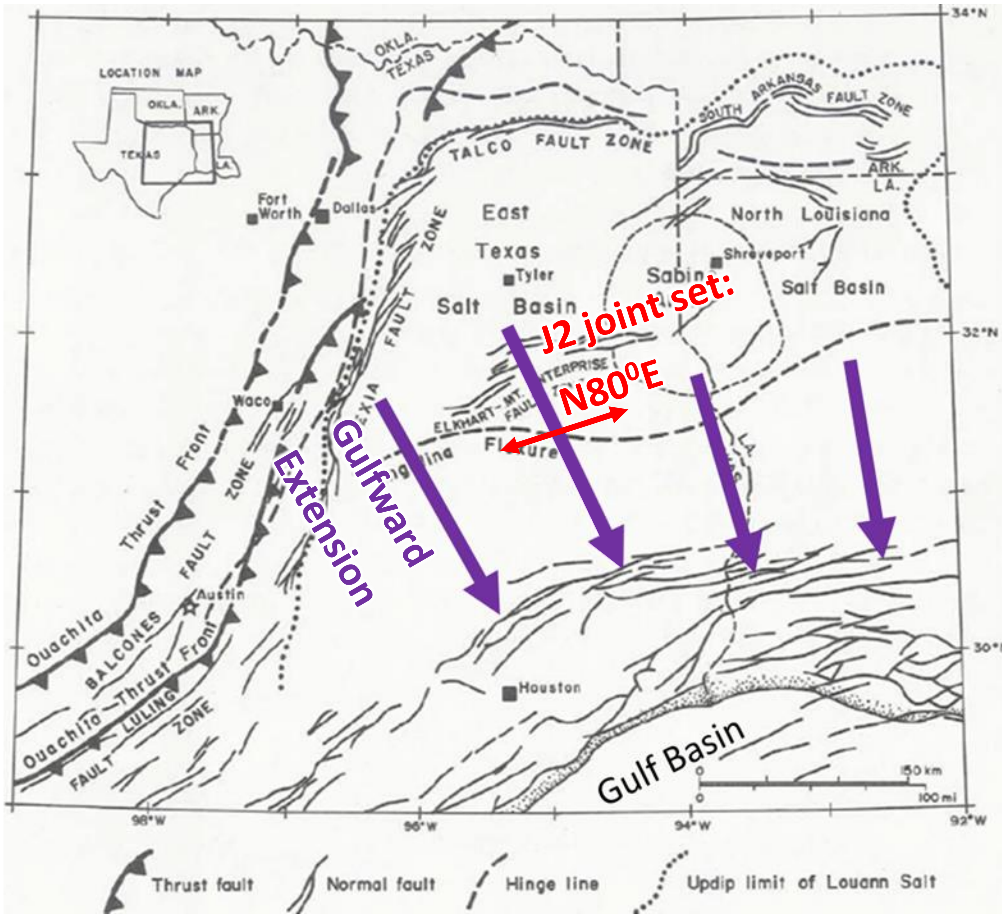

Figure 60. Relation of the J2 joint set to the regional SSE gulfward extension. The purple arrows represent the direction of extension based on previous studies of regional S_{Hmax} and trend of faults accommodating gulfward extension (gulf coast faults and Mexia Talco Faults). The red arrow represents an approximation of joint strikes from the J2 set. Note that they are perpendicular to each other. This is because the joints form perpendicular to the S_{Hmin}, or the direction of extension (modified from Jackson, 1982).

Salt Movement and the J2 joint set

The J2a joint set is located in the northern region of the study area and trends approximately N40^{0}E. In addition to Gulfward tension, halokinesis in the East Texas Basin has encouraged basinward sediment movement as salt from the bottom of the basin was evacuated vertically. Recent fault movement in the Elkhart-Mt. Enterprise Fault Zone to the northwest of Nacogdoches County accommodating this basinward tension is likely affecting the modern stress regime (Collins et al., 1980). This change in stress regime along the flanks of the East Texas basin and the nearby central basin faults is evident in the joint patterns. The J2 set, which trends N40^{0}E, parallels central basin faults and some faults in the Elkhart graben system which formed because of salt migration. The J2 joints appear to be kinematically related to these faults based on orientation and position. This relationship can be seen in figure 61. Further research is necessary to determine if these joints formed pre-, syn-, or post-faulting.

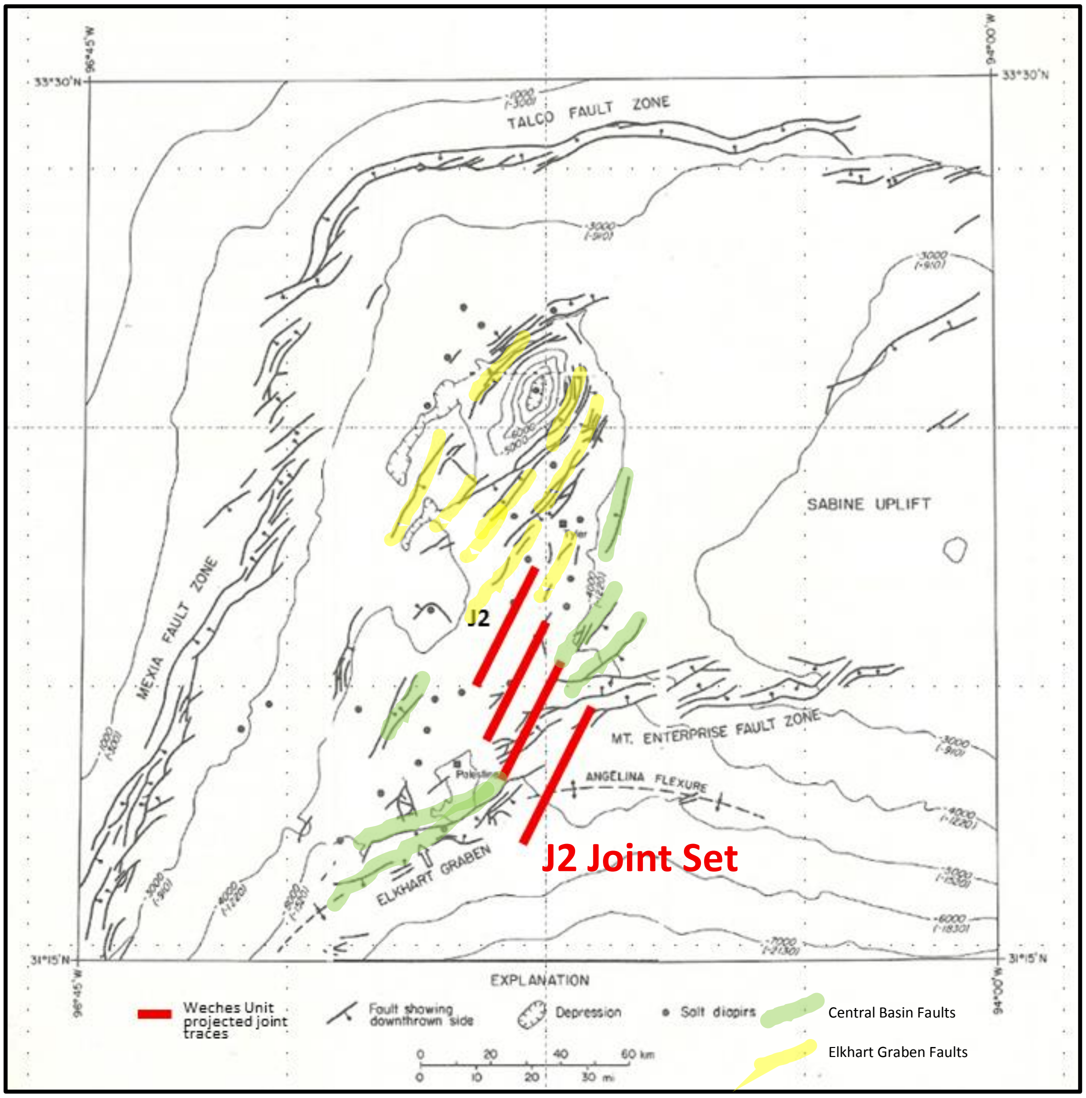

Figure 61. Subsurface structural map highlighting relationship of J2 joint set to central basin faults and Elkhart Graben Faults. Note that the Central Basin Faults, highlighted in yellow, are subsurface faults which form as a result of salt structures in the basin. The central basin faults and the Elkhart Graben Faults are both tied to salt movement within the East Texas Basin. Because of the similar orientation and proximal location to these fault zones the J2 joint set is believed to have formed from a similar origin (modified from Dix and Jackson, 1981).

Multiple causes of the J1a joint set

The J1a joint set is located in the eastern region of the study area and trends approximately N80^{0}W. This marks a change from the J1b joint set trend of N80^{0}E to approximately 20^0 in the clockwise direction (figure 57), which suggests a change in tectonic influence driving the direction of jointing. This J1a strike direction may indicate a greatest horizontal stress direction between N75^0-85^{0}W for Nacogdoches County to San Augustine and Sabine Counties. The three most likely possibilities for this trend are as follows:

(1) Much like the south dipping growth faults that parallel the coast, the joints could be rotating in response to the curvature of the Gulf of Mexico (figure 62). The trend of growth faults can be seen changing from northeast to east-west near the same latitude that the J1b set changes to J1a. While the gulf coast does not quite trend towards the northwest, the paleo-topography of the coast does.

(2) The Sabine Arch is influencing the stress regime. The J1a joints parallel the southern flank of the Sabine Arch. Published borehole fracture data, however, do not show any disruption in joint orientation or stress direction of lower Cretaceous sediments around the center and northern flank of the Sabine uplift (Gough and Bell, 1982; Snee and Zoback, 2016), nor are

there any Cenozoic faults that can be tied to the Sabine uplift. One explanation is that the amount of stress generated from uplift may not have been enough to fracture the rock at depth, but uplift, in conjunction with other stresses that occur during exhumation, could be enough to produce joints (Fossen, 2016). This could be proven by taking stress tests in wellbores however; to our knowledge, there are no stress tests that have been published in the area south of the Sabine Arch.

Rather than directly creating the jointing it is also possible that the lateral relief around the uplifted block is somehow affecting the stress regime. The paleo-topography around the Sabine Arch creates a sloping trend down to the coast that parallels the J1a set which can be seen in figure 62. These joints could be forming in response to extension in this direction of lateral relief.

(3) The NW trending joints may be kinematically related to a proposed compressional regime that may have caused wrench faulting in the basement rocks. There are no nearby mapped fault systems that parallel this N80^0W trend except for the ones mapped in this study located at site 13 which strike between N74^0W and N85^0W. When viewed in the context of basement faults the J1a set parallels the strike slip faults that run NW to SE through Texas. Figure 55 juxtaposes the joint trends measured in this study onto theorized basement fault configuration, proposed by Fowler (1964). The similarity in

trend of NW trending basement faults and the J1a joint set is apparent. In fact, all three joint sets can be linked to a trend of one of these basement fault configurations in Texas. This relationship is illustrated in figure 63. It may not seem likely for basement faults to produce visible strain in the sedimentary rocks above, but White et al., (1995) showed that intense zones of joints can develop in cover rocks above basement faults that are reactivated.

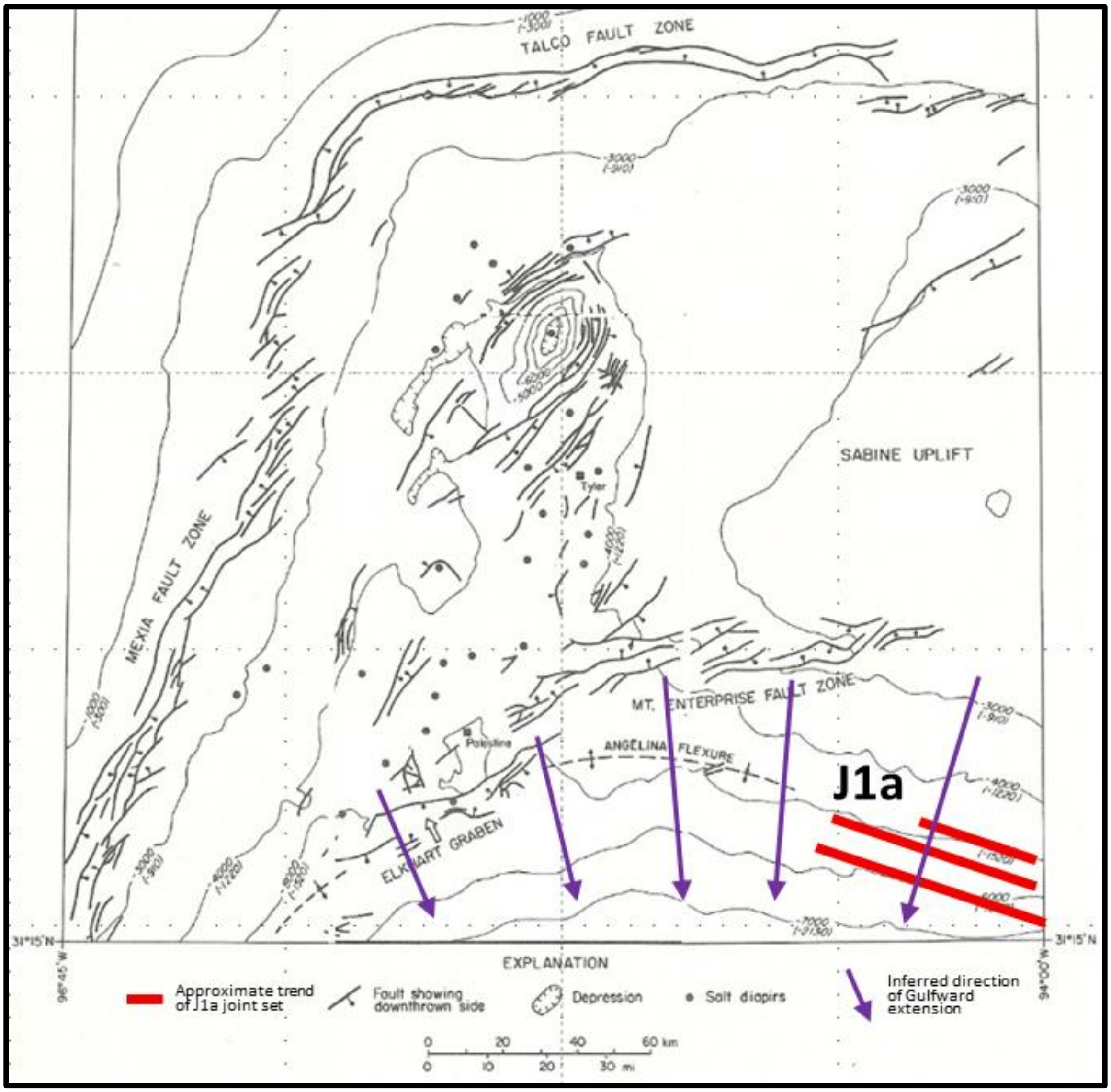

Figure 62. Trend of the J1a joint set in relation to the curving Gulf coastline. The red lines represent the approximate trend of the J1a joint set (N80^{0}W) while the purple arrows represent the direction of sediment extension into the gulf based on the curvature of the coast. Note that the trend of the J1a joint set here is parallel to the elevation lines. This may be because the coastline is curving around the depocenter of the Gulf of Mexico Basin. This is a subsurface map of the surface with contour lines (in feet and meters below sea level) representing the base of the Austin Chalk Formation (top of the Eagle Ford Formation) which is around 4000 feet below Claiborne sediments (i.e. the rock group containing the Weches Formation) (modified from Dix and Jackson, 1981).

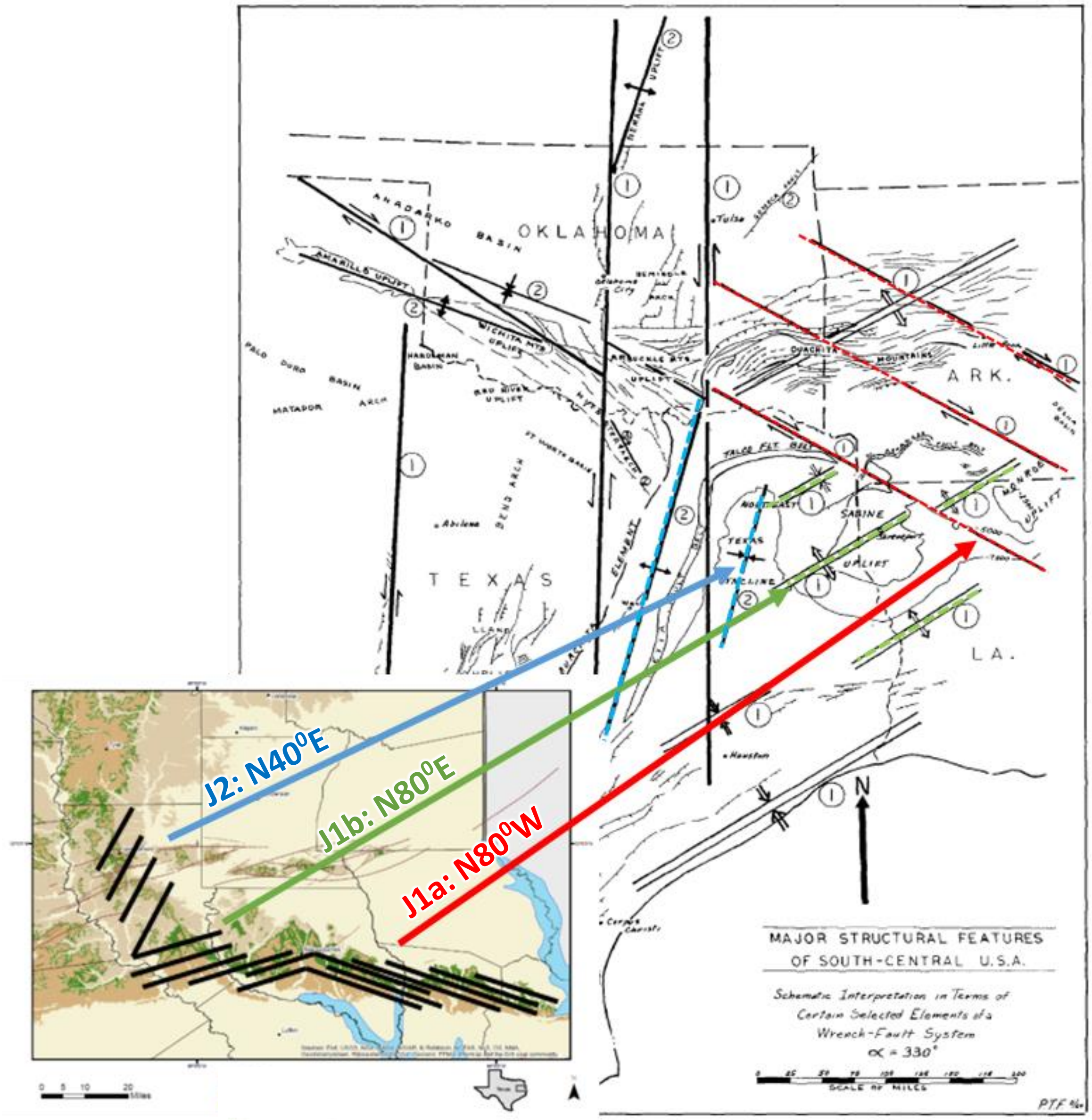

Figure 63. Illustration of possible basement fault configuration in relation to measured joint orientations in the Weches Formation. Colored arrows show the match between joint sets and proposed basement structures. The J1a set appears to match up with the NW oriented strike slip faults while the J1b and J2 sets also appear to parallel basement fault trends, modified from Fowler (1964).

CHAPTER 9: CONCLUSION

Field work in this study has revealed that the Weches Formation in East Texas has at least three regional sets of steeply dipping, opening mode joints, as listed below in geographic order from east to west and as shown in figure 49.

1) J1a – Eastern-most joint set located south of the Sabine Uplift with an average trend of N80^{0}W.

2) J1b – Centrally located joint set near Nacogdoches County with average trend of N80^{0}E.

3) J2 – Northwesterly located joint set near the eastern flank of the East Texas Basin and running parallel to the Elkhart Graben with an average trend of N40^{0}E.

The J1a set that extends as far east as Milam and west until at least Chireno. The J1b set then begins somewhere between Nacogdoches and Chireno, Texas and continues west until at least Alto. North of Alto the J2 set is the dominant joint set which extends north to at least Mt Selman.

East Texas stress regime

It is likely that jointing in the Weches Formation in East Texas was not generated at depth but rather originated during removal of overburden and with orientation influenced by the tectonic stress at the point of initiation. This conclusion was arrived at based on crosscutting relationships between the systematic joints with the secondary, late forming ironstone layers. While it is possible that the joints could have formed because of residual paleostress, all evidence seems to indicate that these joints delineate a recent (Neogene) to present-day stress regime.

The cumulative average direction of greatest horizontal stress according to orientation of all fractures in the Weches is roughly E-W (N87^{0}E), but consists of at least three orientation provinces: (1) a north-northeast directed province in the immediate vicinity of the East Texas Basin (J2 joint set: N40^{0}E), (2) the east-northeast directed province in Nacogdoches and Cherokee counties and likely the majority of East Texas (J1b joint set: N80^{0}E), and (3) the west-northwest directed province which begins about 20 miles (32 km) east of Nacogdoches and continues to the Louisiana border (J1a joint set: N80^{0}W).

Tectonic influence

The wide geographic area covered by the observed joint trends is indicative of tectonic influence. The variety of orientated joint sets and the lack of comingling between them indicates that this influence changes laterally rather than changing temporally, because the latter would have resulted in overlapping major joint trends. When these joint traces are drawn in map view and extended out (shown in figures 49 and 64), it becomes clear that each trend appears to occupy its own space and presumably representing three different stress provinces. Each of these trends are indicative of changes in the principle tectonic influence affecting that area.

J1a Joint Set: N80^{0}W

This set represents a change in stress direction south of the Sabine Arch. Three causes for this change in stress regime are considered:

1) Rotating in response to the curvature of the Gulf of Mexico / paleocoast.

2) Sabine Arch influencing the stress regime due to the lateral relief produced by uplift (joints parallel the southern flank of the arch)

3) Stress being transferred from active basement faulting to the overlying Cenozoic strata.

Hackle marks at the terminations of joints in site 13 (located in the J1a province) represent a subtle counter-clockwise rotation in stress direction related to nearby faulting. Hackle marks were occasionally observed at sites 5 and 6 and more commonly at location 13. several faults were mapped at site 13 oriented between N75^{0}W and N85^{0}W. The mechanism creating this faulting is a topic for further research as it might help explain the possible change in direction of the stress regime in this area.

J1b Joint Set: N80^{0}E

The J1b set is continuous throughout the central region and western regions of the study area. It likely represents the expected direction of S_{Hmax} in East Texas based on its orientation in relation to the south-southeasterly extension of Cenozoic strata into the Gulf of Mexico Basin and to the Mt Enterprise faults and down-to-the-coast faults that accommodate this extension.

Because of the similar spacing and isolation of each joint set, it is determined that the J1a set and the J1b set represent a changing direction in stress from the east to west. This set also shows hackle marks and a similar amount of counter-clockwise rotation (10 - 15^0) in the easterly direction. Again, this could suggest a subtle change in the horizontal direction of stress locally as the result of a nearby fault, although no fault was found. It is unlikely that this is related to the rotation in the sites to the east.

J2 Joint Set: N40^{0}E

Based on proximity and similar orientation to nearby faults, the joints in the J2 joint set are believed to be linked to the salt related movement in the East Texas basin. Tension is created in the Weches Formation as salt movement encourages basinward creep of overlying sediments. Because the J2 province also contains J1b joints, this basinward tension must experience periods of quiescence. During these times the stress field created by the gulfward subsidence becomes the dominant field allowing back and forth generation of J2 and J1b oriented joints.

Summary

A field-based study of joint orientation and characteristics in the Weches Formation was undertaken to develop a better understanding of the stress regime in East Texas. The joints in the formation are often systematic with ordered spacing and orientation over large distances. It is postulated that these features are of a late origin likely forming due to flexure and removal of overburden during exhumation of the unit. These joints likely formed in response to the maximum horizontal direction of stress at the time of formation.

Joints are typically steeply dipping ($70^0 – 90^0$) and iron filled. Crack-seal formation, steep dip and a lack of shear movement suggests these fractures were predominantly opening mode joints. Slickenlines are uncommon but visible on a few fracture planes; however, their bearings show random orientation indicating unloading movement during erosional exposure. Limonite veins are present throughout the formation and were likely the result of more recent groundwater flow and Fe-precipitation, since alteration of the siderite in the Weches Formation to goethite and limonite has been shown to be a late stage diagenetic process facilitated by water flow and leeching of iron from greensands. Crosscutting relationships of joints with late diagenetic ironstone beds within the Weches indicates a late origin for joints which likely forming during exhumation. These sets are not localized to individual areas but stretch over distances of up to 90 miles (145 km). The fracture orientations are believed to be the result of Neogene to present day neotectonic stress states.

Based on the average orientation of all fractures in the Weches (N87.1^0E ± 3.8^0) the average cumulative direction of greatest horizontal stress is approximately N87^0E. This direction is consistent with previous studies of east Texas. However, previous stress data is sparse in the study area and closer inspection reveals a more complex stress regime. Three main average stress provinces were mapped in east Texas (figures 51 and 54): (1) a N80^{0}W directed province (called J1a) moving towards Louisiana which may be related to lateral relief around the southern flank of the Sabine Uplift, the curve of the stress regime paralleling the coastline and/or paleo coastline around the Gulf Coast basin depocenter, or basement faults, (2) a N80^{0}E directed province (called J1b) caused by Gulfward extension and, (3) a N40^{0}E directed province (called J2) in the immediate vicinity of the East Texas Basin which is heavily influenced by the perturbation of the stress regime near salt-structures.

Further gathering of fracture data should reveal a clearer picture of subtle changes in the East Texas stress provinces, as well as information about joint origins, ground water flow, tectonic history and the potential for future fault development. Surface fracture studies may provide an important analog for subsurface fracturing in units that are significant hydrocarbon traps. Additional research into the relatability of natural fractures at outcrop to borehole fracture readings at depths should be explored. Assessment of natural fractures in outcrops may provide information about modern stresses in areas where core is unavailable. This study provides information about fracture patterns in the Weches Formation in East Texas that may be of use to civil engineering and construction projects, seismologists interested in earthquake development, petroleum geologists or mineralogists exploring hydrocarbons or minerals and environmental geologists interested in groundwater migration.

APPENDIX A

Spreadsheet of data from outcrops. This includes all information gathered from outcrop descriptions and fracture measurements in the field. The categories describing this information are explained in the key.

Key:

JI	Joint intersection (trend of the intersection two joint planes);
JL	Joint lineation (linear feature found on the joint plane i.e. slickenlines);
JP	Joint plane (orientation of the joint planes described by strike and dip);
T	Type or category of joint; major or minor (see method section for details)
Size	Vertical length of joint visible at outcrop;
II	Iron infilling;
PS	Spacing between parallel joints;
Quality	quality of the joint face (based on amount of weathering, curvature); SA = Special attributes (any notable features that don't fit into the other categories)
P	Plunge (angle of inclination a linear feature has from the horizontal position)
B	Bearing (map direction that a linear feature is dipping)
S	Strike (the path that a planar feature (fracture) follows in the horizontal direction)
D	Dip (angle of inclination of a planar feature from the horizontal position)
DD	Dip Direction (Quadrant direction that an inclined plane is dipping)

Stop 1: 1019 South Street, Nacogdoches, Texas 75964													
La., Lo.: 31.596404, -94.661457													
Elevation: 303 (ft)													
Notes on outcrop	**JI**		**JL**		**JP**			**T**	**Size**	**II**	**PS**	**Quality**	**SA**
	P	B	P	B	S	D	DD	M/N	(ft)		**(in)**		
Outcrop exposes about 15 (ft) of	35	S55E	59	S80W	N20W	61	SW	M	2			GOOD	
Weches Formation with three					N56E	75	NW	M	5				
continuous iron ledges present. Sparta					N70E	63	SE	M	7				
contact is marked by thick iron deposit					N84E	75	NW	N			6		
at the top of the outcrop.			53	N22E	N83E	71	NW	N	2				
					N79E	85	NW	N				POOR	
Located between El Indigo Tire Shop					N54W	88	SW	N			7		
and MetroPCS					N65W	87	SW	N			1		
					N64W	87	SW	N			1		
Greenish brown fossiliferous clay					N64W	89	SW	N			1		
with abundant jointing. Poorly indurated.			35	N30E	N64W	36	NE	M	2			GOOD	
Sparta contact is visible at the top of	14	S35W			N40W	88	SW	M	1		8		
the outcrop					N77E	80	SE	M	5.5			POOR	
			54	N10W	N85E	46	NW	M	2		1	GOOD	
Outcrop trends ~N45E					N55E	75	NW						
	88	N05W			N85E	43	NW	M				GOOD	
J1b joint set is present at a spacing					N55E	79	NW	M	6			GOOD	

of about 8 - 10 (ft)	3	S25E			N35W	88	SW	N				GOOD	
					N44W	59	SW	N	0.66			GOOD	
	32	N80W			N70E	60	SE	M	6		36	GOOD	
					N70W	70	SW	M	4				
					N85E	75	NW	M	6	Y		GOOD	
					N85E	58	SW	M	5			GOOD	
					N65E	74	NW	N	2		1		
					N70W	64	NE	M	8	Y		GOOD	
					N70E	86	SE	M	4				
					N80E	65	NW	M	3		8	GOOD	
					N87E	55	NW	M	1				
					N56E	75	NW	N	0.5				
					N70E	73	NW	M	1.5				
					N78W	85	NE	M	1		6	GOOD	
	45	N40E			N75E	75	NW	M				GOOD	
					N05E	46	SE	N	1			POOR	
					N85E	60	NW	M	2		2	GOOD	
					N83E	70	NW	M	1		2	GOOD	
	20	N30W			N60W	45	NE	M	1			POOR	
					N45W	75	SW	N				POOR	
					N88W	70	NE	M	5		5	GOOD	
					N80E	75	NW	M	2		5		
					N80E	84	NW	M	5			GOOD	

				N81E	70	NW	M	4		8	GOOD	
37	N50E			N88W	72	NE	M	2.5		8	GOOD	
				N70E	64	NW	M	1			GOOD	
				N10E	60	NW	N					
50	N80E			N81E	62	NW	M			1		
				N15W	44	NE	N	0.66		12	POOR	
				N10W	85	NE	N				GOOD	
34	N55E			N76E	60	NW	M	4			GOOD	
				N55E	65	SE	N	0.5				
				N80E	70	N	M	3	Y	48	GOOD	
				N85E	70	N	M	3	Y	48	GOOD	
				N80E	68	N	M	0.8	Y		GOOD	
				N82E	63	N		0.66			GOOD	
				N90E	85	S		0.5			POOR	
				N80E	75	N	M	6			GOOD	
				N88E	76	N	M					
				N74E	74	N					POOR	
62	N60W			N87W	74	N	M	3		3	GOOD	
				N04W	68	S	N	0.33				
				N68E	70	N	M	2	Y	1.5		
				N72E	70	N	N				POOR	
				N32E	25	N	N	0.66				
67	N80E			N24W	57	N	N					

					N78W	87	N		0.5				
					N25W	70	N	N					
					N78E	80	N	M				GOOD	
	25	S82W			N69E	56	N	M	0.5	Y			
					N75E	75	N	M	2			POOR	
					N84E	69	N	N	2				
					N86W	48	N	N	1				
					N76E	70	N	M	3	Y		GOOD	
					N14W	59	N	N					
					N26W	25	S	N	0.1			POOR	
					N35W	57	N	N	0.8				
					N79E	64	N	N	1				
					N72E	66	N	M	2			GOOD	
					N75E	80	N	M	2		5		
					N70E	83	N	N					
					N81E	60	N	M	3				
					N80E	70	N	M	1.5				
					N79E	75	N	M	1		1.5	GOOD	
					N80E	74	N	M	0.66			GOOD	
					N38W	57	S	M	1				
Stop 2: 101 W Main Street													
La., Lo.: 37.133, -95.786													

Elevation: 262 (ft)													
Notes on outcrop	**JI**		**JL**		**JP**			**T**	**Size**	**II**	**PJ**	**Quality**	
	P	B	P	B	S	D	DD	M/N	(ft)	y = yes	**(in)**		
Weches is exposed in the Banita Creek					N20E	88	NW	M	3		3	GOOD	
river bed near the Pillar St bridge. Joints					N30E	87	SE	N	1		12	POOR	
can be measured when the river is dry.					N20E	85	NW	M	3		3		
The Weches also makes up the river bank					N24E	78	NW	M	5		1	GOOD	
on one side but joints are rarely present					N38E	72	NW	M	4.5		1	POOR	
here.					N39E	84	NW	M	2		4	GOOD	
					N45E	85	NW	N			4	POOR	
Lithology is similar to site 1, but					N46E	78	NW	N	0.5		1	POOR	
better indurated and more weathered					N38E	87	SE	M	6		4	POOR	
from river flow.					N40E	88	SE	N	3		4	POOR	
					N85E	89	SE	N	0.5			GOOD	
Joints orientations are scattered but					S75E	89	SW	N	0.3		2	GOOD	
a concentration of joints trending NE					S72E	80	SW						
(likeley J2) and a smaller concentration					N30W	86	NE	N	0.3			POOR	
of joints trending East North East (J1b)					N86W	80	SW	N	1		1		
					N83E	78	SE	N	0.3		1		
					N89E	68	NW	M	3			GOOD	
					N82E	70	SE	N	1.5		1	GOOD	

					N80E	72	SE	N	0.2			GOOD	
					N67E	50	SE	M	7	Y		GOOD	
					N50E	48	SE	M	5	Y		GOOD	
					N80W	60	NE	M	10			GOOD	
					N81W	45	NE	M					
					N50E	89	SE	N	1				
					N84W	56	NE	M				GOOD	
					N86W	87	NE	N	0.66			POOR	
					N40E	88	SE	N	0.5			GOOD	
					N65E	90		N	0.66			POOR	
					N50E	89	SE	M	4		2	GOOD	
					N52E	88	SE						
					N45W	89	SW	N				POOR	
					N45E	88	NW	M			2	POOR	
					N40E	87	NW	M				GOOD	
					N15W	40	S	N				POOR	
					N30W	85	N	M				GOOD	
					N60W	50	SW	M	10			POOR	
					N25E	90		M	6			POOR	
					N40E	85	SE	M	6	Y		POOR	
					N85E	89	NW	N	1	Y		POOR	
					N20E	89	SE	M	3		24		
					N05W	90		N					

					N70W	90		N				POOR	
					N75E	57	NE	M	4			GOOD	
					N20W	90		N	5	Y		POOR	
					N05E	90		N	7			POOR	
					N40E	88	SE	N	0.5			GOOD	
					N65E	90		N	0.66			POOR	
					N50E	89	SE	M	4		2	GOOD	
					N52E	88	SE	M	4		2	GOOD	
					N45W	89	SW	N					
					N45E	88	NW	M			2		
					N40E	87	NW	M			2	GOOD	
					N15W	40	S	N				POOR	
					N30W	85	N	M				GOOD	
Stop 3: 715 W Main Street													
La., Lo: 37.1328, -95.7855													
Elevation: 340 (ft)													
Notes on outcrop	**JI**		**JL**		**JP**			**T**	**Size**	**II**	**PJ**	**Quality**	
	P	B	P	B	S	D	DD	M/N	(ft)	y = yes	**(in)**		
Weches exposed in a highly weathered					N25E	68	SE	M	3			GOOD	
section of road cut. About 6 feet of the					N20E	80	SE	M	2		6	GOOD	
rock unit is exposed on the north side of					N30E	75	SE	M	5			POOR	
the road					N20E	85	SE	M					

No pattern is observable at this site,					N68W	78	SW	N					
likely because of the amount of foliage					N25E	85	SE	M	3				
cover and wezthering.					N80W	75	SW	M				GOOD	
					N45W	88	SW	N	0.5				
					N55E	80	NW						
					N50W	80	SW	M	0.66			GOOD	
					N10W	45	NE	M		Y	10	GOOD	
					N10E	45	SE	M					
					N20W	85	NE	N	0.33			GOOD	
					N02E	87	SE	N					
					N10W	40	SW	M	6	Y	5	GOOD	
					N12W	37	SW	M	1	Y	5	GOOD	
					N20W	35	NE	N	0.66				
					N20W	30	NE						
Stop 4: Hwy 21, Chireno, TX (near 22119)													
La., Lo: 31.506436, -94.344648													
Elevation: 248 (ft)													
Notes on outcrop	**JI**		**JL**		**JP**			**T**	**Size**	**II**	**PJ**	**Quality**	
	P	B	P	B	S	D	DD	M/N	(ft)	y = yes	**(in)**		
Weches is exposed on the north side of					N72W	74	S	N	1			POOR	
of the highway in a roadside ditch which					N70W	56	S	N	1				

trends N65E curving east. Because the					N75W	55	S						
road is downslope it exposes about 20					N05E	60	S	M		Y		GOOD	
feet of the rock unit. No Sparta Formation					N75W	65	N	M	4	Y		GOOD	
present.					N84E	55	S	M	5	Y			
There are atleast four iron ledges present					N88E	67	N	N				POOR	
with highly fossiliferous grey-green clay					N01E	80	S	N				POOR	
in between. Fossils are predominately					N10W	80	S	N			5		
bivalves (relatively well preserved).					N20W	83	S	N					
Burrows are also present.					N25W	87	S	N					
The dominant joint set is the J1a set and					N24W	85	S	N					
an orthogonal set trending about N05E					N80W	80	N			Y		POOR	
Spacing of the J1a set appears to be					N85W	85	N			Y		GOOD	
about 6-8 feet.					N85W	48	S			Y		OK	
					N04W	49	N	N				OK	
			62	S45W	N55W	62	S	N					
					N75W	78	N					OK	
					N06E	90		M		Y		OK	
					N10E	80	N					OK	
					N08E	90		N				OK	
					N08E	90		N				OK	
					N08E	90		N				OK	

					N88W	75	S	M				OK	
					N80W	85	N	M				OK	
Stop 5: 628 N University Dr, Nacogdoches TX													
La., Lo: 31.606270, -94.641599													
Elevation: 316 (ft)													
Notes on outcrop	**JI**		**JL**		**JP**			**T**	**Size**	**II**	**PJ**	**Quality**	
	P	B	P	B	S	D	DD	M/N	(ft)	y = yes	**(in)**		
Weches is exposed in a man made cliff					N50E	65	N	M		Y			
behind the Kline's and Wrap it up stores.					N79E	65	N	N					
About 50 (ft) of Weches is visible, however					N55E	89	N	M		Y			
only the bottom 10 feet or so is accessible					N45E	80	N	M		Y			
due to foliage cover. Outcrop trend: N19E					N65E	79	N	N			3		
Grey to black clayey fossilifoerous beds					N56E	85	N	N	0.5		3	GOOD	
alternating with hard red fossiliferous and					N70W	90		N		Y		POOR	
ferruginous beds.					N66E	83	N	M	2	Y		GOOD	
the east-northeast trending joints of the					N80E	84	N	N	0.66			POOR	
J1b set are present at a spacing of about					N74E	89	S	M			4	GOOD	
8 - 10 feet.					N84E	88	S	N				POOR	

These joints o(ft)en terminate in segmented					N75E	80	S	M	2	Y		GOOD	
sections of slightly different S. From					N75E	89	S	M	1				
the bottom up the S rotates north					N70E	90		N	0.5			POOR	
about 10 to 15 degrees.					N50W	40	N	M	1			GOOD	
Jonts near the top of the outcrop appear					N69E	87	N	N	0.66			POOR	
to S ~N80E but are out of reach.													
Stop 6: Big 4 inc Milam Pit													
La., Lo: 31.429348, -93.863285													
Elevation: 265 (ft)													
Notes on outcrop	**JI**		**JL**		**JP**			**T**	**Size**	**II**	**PJ**	**Quality**	
	P	B	P	B	S	D	DD	M/N	(ft)	y = yes	**(in)**		
This outcrop is in a quarry owned by Big					N70W	87	N	M	15	Y	18		
4 inc, located just outside of milam.					N76W	89	N	N		Y			
The Weches Formation is exposed near					N75W	88	S	N	3				
the contact between the overlying Sparta					N80W	87	S	M	15	Y			
Formation indicated by the telltale thick					N78W	88	S	M	16	Y			
(~6 feet) ferrugenous section with					N78W	89	S	M	1.5				
overlying clayey sandstone above.					N76W	88	N	N	2	Y			
					N69W	73	S	M	2	Y		GOOD	

The Weches here is better indurated than					N79W	83	N	M	20	Y	12		
outcrops to the west and is dark green					N78W	87	N	M	8	Y	12	GOOD	
made up almost entirely of glauconite					N80W	90		N	6			POOR	
pellets. There are small pockets of					N80W	85	S	M					
silicified skeletal fragments and nodular					N75W	86	N	M	15	Y		GOOD	
concentric iron concretions.					N60W	70	N	N		Y		GOOD	
Cross-bedding and Herribgone structure					N69W	81	N	M		Y	36	GOOD	
are present. Fossils are not well preserved.					N68W	85	N	M	15	Y	36	GOOD	
					N70W	84	N	M	3	Y	24	GOOD	
The only iron ledge present is at the					N69W	82	N	N	2			POOR	
Sparta contact. Most of the joints					N72W	87	N	M	10	Y	24	GOOD	
terminate at this contact and have iron					N70W	87	N	M	15	Y		GOOD	
infilling.					N64W	90		N	0.5	Y		GOOD	
Most of these joints are N75W, 80 N					N83W	88	N	N	8		18	POOR	
(J1a) that are atleast continuous through the entire exposed section					N80W	85	S	M	8		18	GOOD	
(~10 - 20 feet).					N85W	88	S	N	1	Y		POOR	
Joints in this set are consistently spaced about 3 feet apart.					N80W	88	N	M	20	Y		GOOD	
Other Northeasterly joints appear to be arrested by this major trend.					N75W	88	N	M	5	Y	6	GOOD	
					N75W	87	N	N	3	Y	6	GOOD	
					N76W	88	N	N		Y	6	POOR	

An adjacent quarry at a lower elevation was active and not available for study, however samples of the rock from this area were a much more fossiliferous brighter green claystone that was less indurated than the section near the Sparta contact.					N76W	87	N	M	10	Y		GOOD	
					N70W	86	N	M	6	Y			
					N74W	88	N	M	6	Y	10		
					N75W	88	N	M	20	Y	10	GOOD	
					N75W	88	N	M	20	Y		GOOD	
					N76W	89	N	M	20	Y			
					N85W	89	S	M	2	Y			
					N85W	89	S	M	2	Y			
					N85W	89	S	M	2	Y			
					N85W	89	S	M	2	Y			
					N85W	89	S	M	2	Y			
					N76W	87	N	M	8	Y	18	GOOD	
					N70W	89	N	N	3	Y	18		
					N80W	89	N	N	0.5	Y	6		
					N77W	88	S	N	0.5	Y	6		
					N85W	87	N	N	2	Y	10	GOOD	
					N85W	87	N	N	2	Y	10	GOOD	
					N85W	87	N	N	2	Y	10	GOOD	
					N85W	87	N	N	2	Y	10	GOOD	
					N70W	85	N	M	20	Y	36	GOOD	
					N71W	87	N	M	15	Y	36	GOOD	
					N70W	90	N	M	5	Y	36	GOOD	
					N86W	86	N	M	10	Y	10	GOOD	

					N85W	86	N	M	8	Y	6	GOOD	
					N86W	85	N	M	6	Y	6	GOOD	
					N56W	80	S	N	3	Y		GOOD	
					N55W	87	S	N	0.8	Y		GOOD	
					N48W	87	S	N	2	Y			
					N84W	85	N	M	15	Y		GOOD	
					N80W	74	N	M	30	Y	36	GOOD	
					N70W	80	N	N	6	Y	36		
					N88W	90		N	1	Y		POOR	
					N80W	88	N	N	1	Y			
	27	N89W			N32E	24	N	N	0.8	Y			
					N85W	87	S	N		Y			
					N74W	75	S	N	10				
	23	N58W			N80W	80	S	M	6	Y		GOOD	
					N50W	70	N	N	1				
	33	N88W			N36W	60	N	N	0.5	Y			
					N80W	85	S	N	3	Y			
					N70W	85	N	M	4		10		
					N75W	88	N	N	2	Y	10	GOOD	
					N85E	26	S	M	4	Y			
					N30E	25	N	N	0.66	Y			
					N80E	86	N	M	20	Y	6	GOOD	
	4	N89E			N79E	85	N	N	2	Y	6	GOOD	

					N62E	30	S	M	1			GOOD	
					N78W	82	N	M	6	Y	12	GOOD	
					N78W	84	N	M	10	Y	12	GOOD	
					N70W	80	N	M	10	Y	6	GOOD	
					N71W	80	N	M	3	Y	6	GOOD	
					N80W	88	S	M	8	Y			
					N69W	88	N	M	4	Y	12		
					N67W	80	N	M	5	Y			
					N70W	87	N	M	5	Y			
					N70W	71	N	M	4	Y			
					N71W	75	N	M	3	Y			
					N80W	76	N	M	10	Y	12		
					N76W	71	N	M	20	Y	12		
					N84W	68	N	M	5	Y			
					N75W	65	N	M	4	Y		POOR	
					N65W	65	S	N	0.8				
					N80W	81	S	M	8	Y			
					N74W	83	N	M	3	Y		GOOD	
					N21E	42	S	M	2	Y			
					N78W	85	S	M	2	Y		GOOD	
					N70W	88	N	M	6	Y		GOOD	
					N25E	27	S	M	4	Y			
					N64W	71	S	M	6	Y		GOOD	

	22	N31W			N68E	18	S	N	2	Y		GOOD	
	68	N78W			N50E	70	N						
					N05E	76	N	N	0.66	Y			
					N61W	76	S	M	5	Y			
					N19E	59	S	N	1	Y			
	67	N51W			N64W	73	S	N	1	Y			
					N51E	65	S	M	3	Y			
					N70W	81	S	M	3	Y	2		
					N70W	80	S	M	1.5	Y	2		
					N51E	41	S	N	1	Y		GOOD	
	35	N64W			N70W	78	S	N	0.8	Y			
	54	N85W			N54E	40	S	M	0.5	Y			
					N02E	63	S	N	0.5	Y			
					N57W	80	S	M	2	Y	24		
	54	N66W			N51W	65	S	M	3	Y			
					N01E	70	S	N	0.8	Y			
					N70W	74	N	M	5	Y		GOOD	
					N78W	76	N	M	2	Y		GOOD	
					N65W	82	S	N	2	Y			
					N64W	74	S	N	3	Y			
					N55W	32	N	M	2	Y			
					N75W	80	N	M	5	Y		GOOD	
					N70W	70	N	M	7	Y			

					N75W	75	N	M	8		18	GOOD	
					N73W	80	N	N	4		18		
					N80W	81	N	M	5			POOR	
					N88W	64	N	M	4	Y			
					N80W	81	N	M	4	Y			
					N67W	87	N	M	12	Y			
					N58W	88	N	N	1.5	Y		POOR	
					N71W	86	S	M		Y		GOOD	
					N89W	88	S	N	3	Y			
					N84W	84	S	N	0.8	Y			
					N70W	81	S	N	0.5	Y	6		
					N70W	80	S	N	0.8	Y	6		
					N72W	81	S	N	1	Y		POOR	
					N45W	67	N	N	0.5	Y		POOR	
					N74W	84	N	N	1	Y			
					N03E	85	S	N	1	Y		GOOD	
					N70W	72	N	M	2	Y		GOOD	
					N81W	88	S	N	1.5	Y			
					N21E	84	N	N	1	Y			
					N74W	88	S	N	0.66	Y	6	GOOD	
					N74W	88	S	N	0.66	Y	6	GOOD	
					N74W	88	S	N	0.66	Y	6	GOOD	
					N74W	88	S	N	0.66	Y	6	GOOD	

					N69W	87	S	M	2	Y	4	GOOD	
					N69W	87	S	M	2	Y	4	GOOD	
					N70E	22	S	N	1	Y			
					N74W	80	N	M	4	Y		GOOD	
Stop 7: US-69 Loves Lookout Park													
Jacksonville, TX 75766													
La., Lo: 32.030583, -95.281111													
Elevation: 650 (ft)													
Notes on outcrop	**JI**		**JL**		**JP**			**T**	**Size**	**II**	**PJ**	**Quality**	
	P	B	P	B	S	D	DD	M/N	(ft)	y = yes	**(in)**		
Around 40 feet of Weches is exposed in a roadcut just north of the turn in to					N76W	74	N	M	4			OK	
Loves Lookout Park, on the east side of					N62W	80	N	N	1	Y		POOR	
the road, trending N15E.					N80W	79	N	N	0.833	Y	2	OK	
Here the Weches is a beige - grey					N78W	80	N	N	0.66	Y		OK	
claystone interbedded with numerous					N74W	83	N	N	0.5	Y		OK	
iron beds throughout. No fossils present.					N86W	80	N	N	0.5	Y		OK	
Much of the section is inaccessible due to foliage.					N75W	82	N	N	0.5	Y		OK	
					N89W	70	N	N	1	Y		GOOD	
					N89W	70	N	N	1	Y		GOOD	
The dominant joint set is the J1a set					N89W	70	N	N	1	Y		GOOD	
typically spaced about 1 - 2 feet apart and bound by iron ledges.					N89W	70	N	N	1	Y		GOOD	

					N89W	70	N	N	1	Y		GOOD	
					N85W	74	N	N	0.5	Y		OK	
					N77W	76	N	M	5	Y		GOOD	
					N76W	74	N	N	3			POOR	
					N69W	70	N	N	4	Y		POOR	
					N85W	88	S	N	1			POOR	
					N85E	55	S	N	0.5			GOOD	
					N85W	74	N	N	2			POOR	
					N64E	87	S	N	0.5			POOR	
					N85E	85	N	N	0.833			POOR	
					N89W	65	N	N	0.833	Y		POOR	
					N80E	80	N	M	1.5			POOR	
					N80E	84	N	N	0.833			POOR	
	15	N76E			N75E	65	S	N	0.833				
					N40W	38	N	N	0.33			POOR	
					N88E	65	N	M	2			OK	
					N45W	87	N						
					N71E	74	S	M	1	Y		GOOD	
					N88E	74	N	M	0.833			POOR	
					N35E	43	S	N	0.5			OK	
					N71W	43	N	N	2.5			OK	
					N40W	79	N	N	0.5			POOR	
					N67W	78	S	N	0.33			GOOD	

					N74W	86	S	M	1			OK	
					N80W	85	N	M	1			OK	
					N81W	85	N	M	0.833			POOR	
					N75W	35	S	M	2	Y		GOOD	
Stop 8: 1200 E Main St and Timberlake St													
Nacogdoches, TX, 75961													
La., Lo: 31.599637, -94.644926													
Elevation: 309 (ft)													
Notes on outcrop	**JI**		**JL**		**JP**			**T**	**Size**	**II**	**PJ**	**Quality**	
	P	B	P	B	S	D	DD	M/N	(ft)	y = yes	**(in)**		
About 6 feet of Weches is exposed in a					N25E	25	S	N	0.5			POOR	
roadcut on the north side of the road.					N10E	40	S	N	2			OK	
					N16E	35	S	N	1.5			OK	
The unit here is heavily weathered with					N20E	38	S	N	1.5			OK	
extensive foliage cover. It is tannish to					N19E	36	S	N	1.5			POOR	
brown-grey fossiliferous sandy claystone					N85E	67	S	M	1.5	Y		OK	
that is poorly indurated except where it					N65E	40	N	M	0.833	Y		OK	
has hardened due to iron concretion													
Joint Planes here are inconclusive.													

There is a grouping trending roughly north													
however they are Dping at a low angle													
down the slope of the outcrop which could													
point to erosional influence													
Stop 9: 4865-5065 TX 21, Nacogdoches, TX 75964													
La., Lo: 31.622073, -94.721249													
Elevation: 390 (ft)													
Notes on outcrop	**JI**		**JL**		**JP**			**T**	**Size**	**II**	**PJ**	**Quality**	
	P	B	P	B	S	D	DD	M/N	(ft)	y = yes	**(in)**		
A roadcut on the north side of the road					N65E	80	N	N	1			OK	
exposed about 15 feet of Weches. Mostly					N71E	79	N	N	1			GOOD	
well indurated highly fossiliferous					N70E	84	S						
grey to green claystone interbedded with					N89E	90					1		
frequent iron ledges. Fossils are					N88E	90					1		
predominately well preserved bivalves and					N14W	87	N	N	0.833				
burrows. At the base of the outcrop the					N78E	90	S	N	1			POOR	
clay becomes a dark black-green and					N15W	40	S	N	0.66	Y		POOR	
poorly indurated, likely due to water flow					N80E	79	N	N	0.33			OK	

off the road.					N84E	85	N						
					N20W	75	S	M	0.833			OK	
The dominant joint set is the J1b set spaced					N88W	83	S	M	0.833		1	GOOD	
about 10 feet apart and an orthogonal set					N88W	83	S	M	0.083		1	GOOD	
with about 5- 6 feet spacing.					N81W	81	N	N				OK	
					N70E	81	N	M	0.5	Y		OK	
					N04E	78	S	N		Y		OK	
					N20E	88	S	N	1	Y		POOR	
					N88E	70	N	N	1.5			POOR	
					N82W	65	N	M	6	Y		OK	
					N05W	85	N	N	0.66		4	OK	
					N05W	85	N	N	0.66			OK	
					N05W	85	N	N	0.66			OK	
					N05W	85	N	N	0.66			OK	
					N05W	85	N	N	0.66			OK	
					N04W	84	N	N	0.833			OK	
					N85E	63	N	M	1.5			OK	
					N40E	75	S						
Stop 10: N 59 North of Jacksonville, 1 mile north of Burns Rd													
La., Lo: 32.058132, -95.283182													
Elevation: 636 (ft)													
Notes on outcrop	**JI**		**JL**		**JP**			**T**	**Size**	**II**	**PJ**	**Quality**	

	P	B	P	B	S	D	DD	M/N	(ft)	y = yes	**(in)**		
About 50 feet of Weches is exposed in a roadcut on the either side of the					N64E	45	S		1	Y		POOR	
road.					N85E	41	N	M	1	Y		POOR	
Weches here is a tannish-green claystone with abundant sand-sized					N65E	90		M					
pellets, frequent iron concretions and					N35E	80	S		2	Y		GOOD	
sparse fossils (mostly iron replaced bivalves and burrows).					N30E	66	N		0.5	Y		OK	
					N80E	75	N	M	0.833			GOOD	
Jointing is abundant					N85E	87	N	M	1.5			GOOD	
					N85E	88	N	M	1			OK	
There are two main joint trends: J1b and J2					N89W	35	N		0.5	Y		POOR	
					N70E	74	N		0.5	Y		POOR	
the J1b joints are commonly arrested by					N56E	85	N	M	2	Y		OK	
J2 sets.					N51E	75	N		3	Y		OK	
J2 joints are spaced regularly at 4 - 5 feet					N30E	60	S		0.5	Y		OK	
J1b joints have a more sporadic spacing.					N30E	88	S		2	Y		GOOD	
					N50E	70	N	M	3	Y	4in	GOOD	
					N50E	70	N	M	3	Y		GOOD	
					N82E	89	S		0.5			OK	
					N72E	79	N	N				OK	

					N80W	72	N	M	4	Y		GOOD	
					N25E	60	N		3	Y		OK	
					N30E	75	S		2	Y		OK	
					N35E	75	S		2	Y		GOOD	
					N70E	68	N	M	2	Y		GOOD	
					N40E	88	S	M	2	Y	2in	GOOD	
					N40E	88	S	M	2	Y		GOOD	
					N42E	80	S	M	3	Y		GOOD	
					N43E	75	S	M	4	Y		OK	
					N40E	80	S	M	5	Y		GOOD	
					N40E	80	S	M	5	Y		GOOD	
					N39E	79	S	M	5	Y		GOOD	
					N85E	55	N						
					N40E	87	S	M	5	Y		GOOD	
					N88W	82	N		0.833			OK	
					N86W	85	N		1.5			OK	
					N40E	85	S	M	5	Y		GOOD	
					N40E	84	S	M	5	Y		GOOD	
					N40E	84	S	M	5	Y		GOOD	
					N40E	84	S	M	5	Y		GOOD	
					N89E	67	N		1			OK	
					N39E	80	S	M	7	Y		GOOD	
					N39E	80	S	M	7	Y		GOOD	

					N39E	80	S	M	7	Y		GOOD	
					N38E	80	S	M	4	Y	1(ft)	GOOD	
					N38E	80	S	M	4	Y		GOOD	
					N38E	80	S	M	4	Y		GOOD	
					N82E	70	N	M	0.5	Y		GOOD	
					N82E	70	N	M	0.5	Y		GOOD	
					N40E	82	S	M	3	Y		GOOD	
					N40E	82	S	M	3	Y		GOOD	
Stop 11: N59 South of Jacksonville just east of Cherokee County Airport													
La., Lo.: 31.874265, -95.215188													
Elevation: 620 (ft)													
Notes on outcrop	**JI**		**JL**		**JP**			**T**	**Size**	**II**	**PJ**	**Quality**	
	P	B	P	B	S	D	DD	M/N	(ft)	y = yes	**(in)**		
20 feet of Weches is exposed on the east					N45E	79	S	M	20	Y		GOOD	Giant Vein (Fissure)
side of the curved highway. The Weches					N10E	62	S						
is heavily iron altered and veins are					N50E	88	S	M	7	Y		GOOD	
abundant. Some green clay is present, but					N70E	85	S	M	20	Y		GOOD	
the unit is mostly limonite.					N50E	58	N	N	1.5	Y		OK	
Veins at this outcrop are predominately J2					N38E	61	N	N	1	Y		OK	
J2 trending NE with a spacing of about					N05E	81	S	N	1	Y			

8 feet.					N02E	90			4				
					N70E	76	S		4	Y		OK	
					N75E	25	N		4	Y		OK	
					N40E	87	N						
					N41E	81	N					GOOD	
					N01E	27	S	N	3	Y		OK	
Stop 12: N 59 just south of Co. Rd. 1506													
La., Lo.: 31.868769, -95.208721													
Elevation: 648 (ft)													
Notes on outcrop	**JI**		**JL**		**JP**			**T**	**Size**	**II**	**PJ**	**Quality**	
	P	B	P	B	S	D	DD	M/N	(ft)	y = yes	**(in)**		
10 feet of Weches is exposed in a roadcut					N40E	65	S	M	1	Y		OK	
on the east side of the road. Here the					N30E	25	S	N	1	Y		POOR	
Weches is almost completely converted to					N40E	75	S	M	1	Y		OK	
limonite or clay stained red from iron					N60E	80	N	N		Y		OK	
weathering.					N55E	85	N		5	Y		POOR	
					N40E	82	N	M		Y		OK	
Joints are predominately J1 spaced about					N41E	81	N	M	3	Y		OK	
10 feet apart.					N56E	79	S	M	5	Y		GOOD	
					N40E	59	N	M	6	Y		GOOD	
					N39E	60	N	M	6	Y		OK	

					N88E	87	S	N		Y		OK	
Stop 13: Attoyac Construction LLC Quarry													
La., Lo.: 31.449025, -93.978194													
Elevation: 280 (ft)													
Notes on outcrop	**JI**		**JL**		**JP**			**T**	**Size**	**II**	**PJ**	**Quality**	
	P	B	P	B	S	D	DD	M/N	(ft)	y = yes	**(in)**		
Quarry owned by Attoyac Construction LLC					N85W	81	N	M	9			OK	
exposes Weches up to 60 feet thick. Iron					N89W	90		M	8.5			OK	
ledges are infrequent at this location.					N85W	90		M	8			OK	
lithology is similar to Site 6: predominately					N88W	90		M	8.5			OK	
glauconitic pellets with sparse fossils, well					N70W	90		M	6			OK	
indurated.					N87W	78	S	M	8			OK	
					N89W	84	S	M	8			OK	
Joints are typically N80W (J1a) with a					N74W	80	S	M	8			OK	
spacing of 7 - 8 feet with no II					N74W	90		M	6			OK	
and surfaces that are not well defined.					N75W	88	S	M	6			OK	
A total of four micro faults and three large					N86W	85	S	M	8			OK	
faults were observed in this area. All faults					N75W	80	S	M	8			OK	
are normal faults Dping to the north					N89W	85	S	M	8			OK	

except one large fault that Ds to the south					N76W	90		M	8			OK	
					N82W	88	S	M	8			OK	
					N75W	87	S	M	8			OK	
					N84W	88	S	M	8			OK	
					N85W	85	S	M	8			OK	
					N82E	80	S	N	1			OK	Fault Nearby: N54W, 50 N
					N04W	64	N	N	0.833			POOR	Listric base
					N89W	80	S	N	1			OK	Slickenlines: 50, N36E
					N75E	79	N	N	4			GOOD	
			74	N12E	N81E	74	N	N					
					N66W	61	S	N	2			OK	
					N70W	75	S	N	1			OK	
					N75W	60	S	N	2			OK	
					N70W	90		N				POOR	
					N75W	80	N						Joints here become highly irregular
					N85E	90						POOR	and brecciated
					N89W	85	N	M				OK	Large normal faults

													present: N84W, 55 S;
					N80W	89	N						N80W, 27 N; N55E 39 N
Stop 14: Hicks Rock mining pit Alto, Texas 75925													
La., Lo.: 31.645767, -95.057657													
Elevation: 648 (ft)													
Notes on outcrop	**JI**		**JL**		**JP**			**T**	**Size**	**II**	**PJ**	**Quality**	
	P	B	P	B	S	D	DD	M/N	(ft)	y = yes	**(in)**		
Privately owned quarry 2 miles east of Alto no longer active exposes up to					N90W	80	N	M	2	Y		GOOD	
formation is present delineated by the					N80E	73	N	M	2	Y		GOOD	
thick ferruginous layer common at this					N80E	73	N	M	2	Y		GOOD	
interface.					N34W	83	S	N					
					N79E	84	S	N				POOR	
covered by foliage but iron infill is					N70E	88	S	N				POOR	
common, preserving the fracture faces.					N70E	75	N	N		Y		OK	
					N79E	75	N	N	1			POOR	
Where not weathered the Weches is a					N15E	55	S	M	5	Y		GOOD	
bright green fossiliferous claystone with sparse iron beds and joints.					N89E	56	N	M	7			OK	
					N70E	45	S		5.5	Y			
Joints at this location are most common along the Sparta contact					N70E	45	N	N	1	Y		OK	

and typically dip gently, seemingly					N75E	55	S	N					
without a preference for north or south					N70E	45	N						
					N75E	50	S	M	4	Y		GOOD	
The S of joints resembles that of the					N80E	52	S	M	6	Y		OK	
J1b set, however the dip is generally gentler than previously					N70E	41	N	M	6	Y		GOOD	
observed joints from this set.					N70E	41	N	M	6	Y		GOOD	
					N70E	41	N	M	6	Y		GOOD	
					N15E	70	S		2	Y		GOOD	
					N85E	69	N	N	4	Y		GOOD	
					N69E	45	S	N	2			OK	
					N15E	47	N	N	1			POOR	

APPENDIX B

Spreadsheet of the type of outcrops studied and trend of the outcrop face.

Outcrop Type	Site #	Trend of outcrop
Man-made Cliff	1	N45E
Stream Bed (Banita Creek)	2	Meanders in an approximately N direction
Road Cut	3	N80E
Road Cut	4	N65E
Road Cut	5	N20E
Quarry	6	Not applicable
Road Cut	7	N15E
Road Cut	8	N30E
Road Cut	9	N65W
Road Cut	10	N10W
Road Cut	11	N-S to N40W (curved road)
Road Cut	12	N30W
Quarry	13	Not applicable
Quarry	14	Not applicable

REFERENCES

Abbott, P. L., The Edwards Limestone in the Balcones Fault Zone, South-central Texas. Thesis. University of Texas at Austin, 1973. Ann Arbor: U Microfilms International, 1983. Print.

Adams, R. L., 2009, Basement tectonics and origin of the Sabine Uplift: Gulf Coast Association of Geological Societies Transactions, v. 59, p. 3-19.

Ahr, Wayne M. 1979, Claiborne Sediments of the Brazos Valley, Southeast Texas. Houston Geological Society 12-13. AAPG Bulletin. Web.

Andrews, T. G. Jr., 1975, The streptoneurian gastropods of the Weches Formation from Nacogdoches County, Texas and vicinity. Copywright 1976. M. S. Thesis, Stephen F. Austin State Univ., Nacogdoches Texas. 432p.

Bahat, Dov. 1991. Tectonofractography. Springer.

Baumgardner, Robert W., Jr. 1987, Landsat-Based Lineament Analysis, East Texas Basin and Sabine Uplift Area, Bureau of Economic Geology 167 1-26. Print.

Berg, Robert R, 1979, Houston Geological Society. Stratigraphy of the Claiborne Group 5-11. AAPG Bulletin.

Bratton, T., et al. 2006. The Nature of Naturally Fractured Reservoirs. Oilfield Review. 23 pp

Brown, R. O., Forgotson, J. M., & Forgotson Jr, J. M. 1980, Predicting the orientation of hydraulically created fractures in the Cotton Valley Formation of East Texas: Society of Petroleum Engineers Paper 9269. Richardson, Texas.

Buffler, R. T., J. S. Watkins, F. J. Schaub, and J. L. Worzel, 1980, Structure and early geologic history of the deep central Gulf of Mexico basin, in R. H. Pilger, Jr., ed., The origin of the Gulf of Mexico and the early opening of the central North Atlantic Ocean: Department of Geology, Louisiana

State University and Louisiana Geological Survey, Proceedings of symposium, March 3-5, 1980, p. 3-16.

Choung, H., 1975, Paleoecology, stratigraphy, and taxonomy of the foraminifera of the Weches Formation of east Texas and the Cane River Formation of Louisiana: M.S. thesis, Louisiana State University, Baton Rouge, 278 p.

Collins, E.W., 1995, Structural framework of the Edwards aquifer, Balcones fault zone, central Texas: GCAGS Transactions, v.45, p. 136–142.

Collins, E.W., D.K. Hobday, and C.W. Kreitler, 1980, Quaternary faulting in East Texas: The University of Texas at Austin, Bureau of Economic Geology Geological Circular 80-1.

Collins, S. E. 1980. Jurassic Cotton Valley and Smackover reservoir trends, east Texas, north Louisiana, and south Arkansas. AAPG Bulletin, 64(7), 1004-1013.

Collins, E. W., and Luneau. B. A., 1986, Fracture Anyalyses of the Palo Duro Basin Area, Texas Panhandle and Eastern New Mexico: Geological Circular 86.6, 1-7.

Coon L. A., 1956, Tertiary-Cretaceous Growth of the East Texas Basin: Gulf Coast Association of Geological Societies Transactions Vol. 6, 85-90 p.

Crocker, C., 1995, Composition and environment of the Weches Formation, Nacogdoches, Texas, in C. D. Sumner, and C. Mazur (Guidebook Compilers), Eocene of east Texas, Nacogdoches and Rusk counties: Southwestern Association of Student Geological Societies, Nacogdoches, Texas, p. 7-9.

Csontos, R.M., 2007, Three dimensional modeling of the Reelfoot Rift and New Madrid seismic zone [Ph.D. dissertation]: Memphis, Tennessee, University of Memphis, 92 p.

Curtis, N. M., Jr., 1955, A paleoecological study of the Viesca member of the Weches Formation, Smithville, Texas: Journal of Paleontology, v. 29, p. 263-282.

D. I. Gough, J. S. Bell, 1982, Stress orientations from borehole wall fractures with examples from Colorado, east Texas, and northern Canada, Canadian Journal of Earth Sciences, 19:1358-1370

Davies, D. K., Ethridge, F. G., & Berg, R. R., 1971. Recognition of barrier environments: AAPG Bulletin, 55(4), 550-565 p.

Dix, O. R., and Jackson, M. P. A., 1981, Statistical analysis of lineaments and their relation to fracturing, faulting, and halokinesis in the East Texas Basin: Bureau of Economic Geology, University of Texas at Austin.

Dumble, E. T. 1920, The Geology of East Texas: University of Texas Bulletin 1869, 388 p.

Eargle, H. 1968, Nomenclature of Formations of Claiborne Group, Middle Eocene Coastal Plain of Texas. Washington: U.S. Govt.

Eckel, E. B., 1938, The brown iron ores of eastern Texas: U.S. Geol. Survey Bull. 902, 157 p.

Engelder, T., Geiser, P.A., 1980. On the use of regional joint sets as trajectories of paleostress fields during the development of the Appalachian Plateau, New York. Journal of Geophysical Research 85, 6319-6341.

Engelder, T. 1987. Joints and shear fractures in rock. In: Fracture Mechanics of Rock (edited by Atkinson, B. K.). London, Academic Press, 27-69

Ervin, C.P., and McGinnis, L.D., 1975, Reelfoot Rift: Reactivated precursor to the Mississippi embayment: Geological Society of America Bulletin, v. 86, p. 1287–1295

Feray, Daniel Edward, 1948, Relation of the foraminera to the sedimentary characteristics of the Weches Formation in Texas. Unpublished Ph.D. dissertation, University of Wisconsin. 209p.

Ferrill, D. A., D. W. Sims, D. J. Waiting, A. P. Morris, N. Franklin, and A. L. Schultz, 2004b, Structural framework of the Edwards aquifer recharge zone in south-central Texas: Geological Society of America Bulletin, v. 116, p. 407–418.

Ferrill, D. A., & Morris, A. P., 2008, Fault zone deformation controlled by carbonate mechanical stratigraphy, Balcones fault system, Texas: AAPG bulletin, 92(3), 359-380 p.

Finley, R. J., and Gustavson, T. C., 1981, Lineament Analysis Based on Landsat Imagery, Texas Panhandle: The University of Texas at Austin, Bureau of Economic Geology, Geological Circular 81-5, 37 p

Fisher, W.L., 1964. Sedimentary patterns in Eocene cyclic deposits, northern Gulf Coast region. Kansas Geological Survey Bulletin, 169, pp.151-170.

Fischer, M. P., and Polansky, A., 2006, Influence of flaws on joint spacing and saturation: Results of one-dimensional mechanical modeling, J. Geophysical Research, 111

Foley, L. L., 1926, Mechanics of the Balcones and Mexia faulting: Am. Assoc. Petroleum Geologists Bull., Bull., v.10, p. 1261-1269.

Foos, A. M., 1985, Mineralogy and geochemistry of limonite from the Lone Star iron ores, east Texas: Proceedings of the International Clay Conference, Denver, Colorado, p. 227-230.

Foote R.Q., Massingill, and Wells R. H., 1988, Petroleum geology and the distribution of conventional crude oil,Natural gas, and natural gas liquids, East Texas basin: Department of the Interior U.S. Geological Survey, Open-File Report 88-450K

Fossen, Haakon. 2016. Chapter 7: Brittle Deformation, Structural Geology, 2nd ed., Cambridge University Press.

Fowler, P.T., 1964, Basement faults and Smackover structure: Gulf Coast Association of Geological Societies Transactions, v. 14, p. 179-190.

Galloway, W. E., Ganey-Curry, P. E., Li, X., & Buffler, R. T. 2000, Cenozoic depositional history of the Gulf of Mexico basin: AAPG bulletin, 84(11), 1743-1774.

Garner, R.D., and H.H. Roberts. 1990, A Higher Resolution Stratigraphic and Sedimentological Study of the Subsurface Queen City Formation (Eocene), Nacogdoches and Angelina Counties, Texas. N. p., Print.

George W. Viele. 1989, "The Ouachita Orogenic Belt." The Appalachian-Ouachita Orogen in the United States. Boulder, CO: Geological Society of America. pg. 555-562

Ghosh, Protip K., 1972, Use of Bentonite and Glauconites in 4OK-40Ar Dating in Gulf Coast Stratigraphy: unpublished Doctoral dissertation, Rice Univ., Houston, 136 p.

Gleason, J.D., Gehrels, G.E., Dickinson, W.R., Patchett, P.J., and Kring, D.A., 2007, Laurentian sources for detrital zircon grains in turbidite and deltaic sandstones of the Pennsylvanian Haymond Formation, Marathon assemblage, west Texas, U.S.A.: Journal of Sedimentary Research, v. 77, p. 888–900.

Godley, R. F., 1998, Depositional cyclicity in the Weches Formation, Sabine County, Texas: M.S. thesis, University of Southwestern Louisiana, Lafayette, 303 p.

Gough, D. I., and Bell, J. S., 1981, Stress orientations from oil-well fractures in Alberta and Texas. Canadian Journal of Earth Sciences, 18, 638-645 p.

Granata, W. H., 1962, Cretaceous structural development of the Sabine Uplift area: Gulf Coast Association of Geological Societies Transactions, v. 12, p. 117-119.

Granata, W. H., Jr., 1963, Cretaceous stratigraphy and structural development of the Sabine Uplift area, Texas and Louisiana, in Report on selected North Louisiana and South Arkansas oil and gas fields and regional geology: Shreveport Geological Society Reference Report, v. 5, Louisiana, p. 50-95.

Haimson. B.C., 1970, Near-surface and deep hydrofracturing stress measurements in the Waterloo quartzite, International Journal of Rock Mechanics and Mining Sciences & Geomechanics, Volume 17

Haimson, B. C., 1972, Earthquake related stresses at Rangely, Colorado. In The 14th US Symposium on Rock Mechanics (USRMS). American Society of Civil Engineers, New York, NY, pp. 680-708.

Halbouty, M. T., and J. J. Halbouty, 1982, Relationships between East Texas Field region and Sabine Uplift in Texas: American Association of Petroleum Geologists Bulletin, v. 66, no. 8, p. 1042-1054.

Halbouty, Michel T., 1991, East Texas Field--USA East Texas Basin, Texas. TR: Stratigraphic Traps II A024: 189-206.

Hancock, P.L., 1985. Brittle Microtectonics: principles and practice. Journal of Structural Geology 7, 437-457.

Heidbach, Oliver; Rajabi, Mojtaba; Reiter, Karsten; Ziegler, Moritz; WSM Team 2016: World Stress Map Database Release 2016. GFZ Data Services.

Hodgson A. Robert 1961. Regional study of jointing in Comb Ridge - Navajo Mountain Area, Arizona and Utah.

Holditch, S. A., Robinson, B. M., and Whitehead, W. S., 1987, The analysis of complex Travis Peak reservoirs in East Texas: Transactions, Low Permeability Reservoirs Symposium, Society of Petroleum Engineers Paper 16427, p. 381-399.

Hsieh, J. C. C., and C. J. Yapp, 1999, Stable carbon isotope budget of CO2 in a wet, modern soil as inferred from Fe (CO3)OH in pedogenic goethite: Possible role of calcite dissolution: Geochimica et Cosmochimica Acta, v. 63, p. 767-783.

Hubbert, M.K. and Willis, D.G. 1957. Mechanics of Hydraulic Fracturing, 210. Petroleum Transactions, AIME.

Huggett, J.M., A.S. Gale, and D. McCarty, 2010, Petrology And Palaeoenvironmental Significance Of Authigenic Iron-Rich Clays, Carbonates And Apatite In The Claiborne Group, Middle Eocene, NE Texas. Sedimentary Geology 228.3/4 119-139. Academic Search Complete.

Jackson, M. P. A., and C. J. Talbot, 1986, External shapes, strain rates, and dynamics of salt structures: Geological Society of America Bulletin, v. 97, p. 305-323.

Jackson, M. L. W., and S. E. Laubach, 1988, Cretaceous and Tertiary tectonics as cause of Sabine Arch, eastern Texas and northwestern Louisiana: American Association of Petroleum Geologists Bulletin, v. 79, no. 9, p. 1114.

Jackson, M. L. W., and S. E. Laubach, 1991, Structural history and origin of the Sabine Arch, East Texas and Northwest Louisiana: Texas Bureau of Economic Geology Geologic Circular 91-3, Austin, 47 p.

Jackson, M. P. A., 1982, Fault tectonics of the East Texas Basin: Texas Bureau of Economic Geology Geologic Circular 82-4, Austin, 31 p.

Jobe, Kelly, E. B. Ledger, Patricia Sharp, and M. C. Crocker, 1993, Radiostratigraphy and Heavy Mineral Content of the Weches Formation (Eocene), Nacogdoches County, Texas. Gulf Coast Association of Geological Societies Transactions 43: 145-48. AAPG Bulletin.

Klitgord, K.D., Popenoe, P., and Schouten, H., 1984, Florida: A Jurassic transform plate boundary: Journal of Geophysical Research, v. 89, p. 7753-7772.

Kreitler, C. W., Collins, E. W., Davidson, E. D., Dix, O. R., Donaldson, G. A., Dutton, S. P., Fogg, G. E., Giles, A. B., Harris, D. W., Jackson, M. P. A., Lopez, C. M., McGowen, J. H., Muehlberger, W. R., Pennington, W. D., Seni, S. J., Wood, D. H., and Wuerch, H. V., 1981, Geology and geohydrology of the East Texas Basin: a report on the progress of nuclear waste isolation feasibility studies: The University of Texas at Austin, Bureau of Economic Geology Geological Circular 81-7, 207 p.

Kulander, B. R., Barton, C. C., & Dean, S. L., 1979, The application of fractography to core and outcrop fracture investigations: Morgantown Energy Technology Center, report prepared for US Department of Energy, METC/SP-79/3, 174p .

Laubach, Stephen E. 1989, Fracture Analysis of the Travis Peak Formation, Western Flank of the Sabine Arch, East Texas. Bureau of Economic Geology 185: 1-55.

Laubach, Stephen E., Jon E. Olson, and Julia F.w Gale, 2004, "Are Open Fractures Necessarily Aligned with Maximum Horizontal Stress?" Earth and Planetary Science Letters 222.1 191-95.

Ledger, E. B. 2006, Occurrence of Arsenic and Iron in the Weches Formation of Texas. Gulf Coast Association of Geological Societies Transactions 56, 411-420p.

Liu, L., and Zoback, M.D., 1992, The effect of topography on the state of stress in the crust: application to the site of the Cajon Pass scientific drilling project: Journal of Geophysical Research, v. 97, no. B4, p. 5095-5108.

Lund Snee, J.-E., and M. D. Zoback (2016), State of stress in Texas: Implications for induced seismicity, Geophys. Res. Lett., 43

Mainster, M. A., & Coppinger, W. W. 1996, Fracture analysis of Austin Chalk exposures in and around the Olmos creek basin, San Antonio, Texas. Rocks landscapes and man: urban geology of the San Antonio area, 96-2, 71 p.

Mann, C. John, and Thomas, William A., 1968, The Ancient Mississippi River: Gulf Coast Association of Geological Societies Transactions 18, 187-204 p.

Marshall, J. L., 1983, Geochemistry of iron-rich sediments on the outer continental shelf off northern New South Wales: Marine Geology, 51, p. 163-175.

McClay, K., and Bonora, M., 2001, Analog models of restraining stepovers in strike-slip fault systems: AAPG bulletin, 85-2, 233-260 p.

McGookey, D. P., 1975, Gulf Coast Cenozoic sediments and structure: an excellent example of extra-continental sedimentation: Gulf Coast Association of Geological Societies Transactions Vol. 25, 104-120 p.

Michael R. Hudec, Ian O. Norton, Martin P. A. Jackson, Frank J. Peel 2013 Jurassic evolution of the gulf of Mexico salt basin AAPG Bulletin, v. 97, no. 10, p. 1683–1710.

Muehlberger, W.R., Tauvers, P.R., 1989. Marathon fold-thrust belt, west Texas. In: Hatcher, R.D., Thomas, W.A., Viele, G.W. (Eds.), The Appalachian-Ouachita Orogen in the United States. The Geology of North America, v. F-2. Geological Society of America, Boulder, CO, pp. 673–688.

Murray, Grover E., 1961, Geology of the Atlantic and Gulf Coastal province of North America: New York , Harper and Brothers, 692.

Narr, W. and J. Suppe 1991, Joint spacing in sedimentary rocks: Journal of Structural Geology, v. 13, p. 1037-1048.

Payne, J. N., 1968, Hydrologic significance of the lithofacies of the Sparta Sand: U.S. Geological Survey Professional Paper 569-A., p. A3— A5,

Peacock, David. (2001). The temporal relationship between joints and faults. Journal of Structural Geology. v. 23, p. 329-341.

Phillips, John, 1855, Manual of Geology, Practical and Theoretical. R. Griffin and Company, London, 1856, British Assoc. Report, 369.

Pindell, J., and J. F. Dewey, 1982, Permo-Triassic reconstruction of western Pangea and the evolution of the Gulf of Mexico/Caribbean region: Tectonics, v. 1, p. 179–211.

Pindell, J.L., 1985. Alleghenian reconstruction and subsequent evolution of the Gulf of Mexico, Bahamas, and proto-Caribbean. Tectonics 4, p. 1–39.

Pollard, D. D., & Aydin, A., 1988, Progress in understanding jointing over the past century. GSA Bulletin, v. 100-8, p. 1181-1204.

Ramsay, J. G. 1980, The crack-seal mechanism of rock deformation. Nature 284, p. 135-139.

Rawnsley, K.D., Rives, T., Petit, J.-P., Hencher, S.R., Lumsden, A.C., 1992. Joint development in perturbed stress ®elds near faults. Journal of Structural Geology 14, p. 939-951.

Ricoy, J. U., and Brown, L. F., Jr., 1977, Depositional systems in the Sparta Formation (Eocene), Gulf Coast Basin of Texas: Gulf Coast Association of Geological Societies Transactions, v. 27, p. 139-154.

Rodgers, D. A., 1984 Mexia and Talco Fault Zones, East Texas: Comparison of Origins Predicted by Two Tectonic Models. East Texas Geological Society Publication: The Jurassic of East Texas, p. 23-31.

Rowan, M.G., M.P.A. Jackson, and B.D. Trudgill, 1999, Salt-related fault families and fault welds in the northern Gulf of Mexico: American Association of Petroleum Geologists Bulletin, v. 83, No. 9, p. 1454-1484.

Salvador, A., 1991a, Origin and development of the Gulf of Mexico Basin, in A. Salvador, ed., The Gulf of Mexico Basin: Geological Society of America, The Geology of North America, v. J, p. 389–444.

Sellards, E.H., Adkins, W.S., and Plummer, F.B., 1932, The geology of Texas: University of Texas, Bureau of Economic Geology Bulletin 3232, v. 1, p. 1007.

Seni, S. J., and M. P. A. Jackson, 1983, Evolution of salt structures, East Texas diapir province, part 2: patterns and rates of halokinesis: American Association of Petroleum Geologists Bulletin, v. 67, p. 1245-1274.

Seni, S. J., and Jackson, M. P. A., 1984, Sedimentary record of Cretaceous and Tertiary salt movement, East Texas Basin: times, rates, and volumes of salt flow and their implications for nuclear waste isolation and petroleum exploration: The University of Texas at Austin, Bureau of Economic Geology Report of Investigations No. 139, p. 89.

Singhal, B.B.S. and Gupta, R.P. 2010, second ed. Applied Hydrogeology of Fractured Rocks, Springer.

Smith, F. E., 1962, Tertiary and uppermost Cretaceous of the Brazos River valley. Southeastern Texas, Field excursion no. 2, in Geology of the Gulf Coast and Central Texas and guidebook of excursions, Geol. Soc. America, Ann. Mt.: Houston, Texas., Houston Geol. Soc., p. 132-174.

Stella, M. P., 1986, Paleocommunities of the Weches Formation (Middle Eocene), East Texas. Thesis. Stephen F. Austin State University.

Stenzel, H. B., 1938, The Geology of Leon County, Texas: Texas University Pub. 3818, p. 295.

Stephen E. Laubach, 1988 Subsurface fractures and their relationship to stress history in East Texas basin sandstone, Tectonophysics, Volume 156, Issues 1–2, 10, p. 37-49,

Stone, D. S., 1995, Structure and kinematic genesis of the Quealy wrench duplex: transpressional reactivation of the Precambrian Cheyenne belt in the Laramie basin, Wyoming: AAPG Bulletin, v. 79, p. 1349-1376.

Strubhar, M. K., Fitch, J. L., and Glen E. E. 1975, Multiple, vertical fractures from an inclined well bore-field experiment: Journal of Petroleum Technology, 27, p. 641-647

Thomas, w. A., 1976, Evolution of Ouachita-Appalachian continental margin: Journal of Geology, v. 84, p. 323-342.

Thomas, W.A., 1991, The Appalachian-Ouachita rifted margin of southeastern North America: Geological Society of America Bulletin, v. 103, p. 415–431.

Tullis, T. E., 1981, Stress measurements via shallow overcoring near the San Andreas fault. Mechanical behavior of crustal rocks: American Geophysical Union, Geophysical Monograph 24, the Handin volume, p. 199-213.

Twiss, R.J., and Moores, E.M., 1992, Structural Geology: Chapter 3 Brittle Deformation. W.H. Freeman and Co., New York, 532 pp.

Viele, G.W., Thomas,W.A., 1989. Tectonic synthesis of the Ouachita orogenic belt. In: Hatcher, R.D., Thomas, W.A., Viele, G.W. (Eds.), The Appalachian-Ouachita Orogen in the United States. The Geology of North America, v. F-2. Geological Society of America, Boulder, CO, pp. 695–728.

Weeks, A. W., 1945, Balcones, Luling, and Mexia Fault Zones in Texas: American Association of Petroleum Geologists Bulletin, v. 29, p. 1733-1737.

Wendlandt, E. A., and Knebel, G. M., 1929, Lower Claiborne of East Texas, with special reference to Mount Sylvan dome and salt movements: Am. Assoc. Petroleum Geologists Bull., v. 13, no. 12, p. 1347-1375.

Wickham, J., Roeder, D., Briggs, G., 1976. Plate tectonic models for the Ouachita foldbelt. Geology 4, 173–176.

Wood, D. H. and Giles, A. B., 1982, Hydrocarbon Accumulation Patterns in the East Texas Salt Dome Province, Bureau of Economic Geology, Geological Circular, 82-6.

Wood, M. L., and Walper J. L., 1974, The evolution of the interior Mesozoic basin and the Gulf of Mexico: Gulf Coast Association of Geological Societies Transactions, v. 24.

Woodruff, C. M., Jr., and Caran, S. C., 1984, Lineaments of Texas- Possible surface expressions of deep-seated phenomena: Texas Bureau of Economic Geology, Prepared for the U. S. Department of Energy, Division of Geothermal Energy, Contract No. DE-AS07, 79ID12057, p. 68.

Young, Kieth, 1962, Mesozoic history, Llano region, in Geology of the Gulf coast and central Texas: Houston Geol. Soc. Guidebook, Geol. Soc. America Ann. Mtg. p. 98-106.

Zemanek, J., Caldwell, R. L., Glen, E. E., Jr., Holcomb, S. V., Norton, L. J., and Straus, A. J. D., 1969, The borehole televiewer-a new logging concept for fracture location and other types of borehole inspection: Journal of Petroleum Technology, 21, p. 762-764.

Zoback, M. D., Tsukahara, Hiroaki, and Hickman, Stephen, 1980, Stress measurements at depth in the vicinity of the San Andreas Fault: implications for the magnitude of shear stress at depth: Journal of Geophysical Research, v. 85, no. B11, p. 6157-6173.

Zoback, M.L., and Zoback, Mark, 1980, State of stress in the conterminous United States: Journal of Geophysical Research v. 85, no. B11, p. 6113-6156.

Zoback, Mary Lou. 1992 First- and Second-Order Patterns of Stress in the Lithosphere: The World Stress Map Project. Journal of Geophysical Research v. 97, no. B8, p. 11703-12013.

VITA

After completing his work at the American School of Dubai in 2009, Cory Ellison entered Texas Tech University at Lubbock, Texas. During the summers of 2010 and 2011 he attended the Lonestar Community College in the Woodlands, Texas. He received his Bachelor of Science from Texas Tech University in May 2013. In August 2013, he entered the Graduate School of Stephen F. Austin State University. He was employed as a Teaching Assistant from August 2016 to May 2017. He received the Degree of Master of Science in May 2018.

Permanent Address: 11904 Simmons Drive
Cleveland, TX 77328

Style: Geological Society of America

This thesis was typed by Cory D. Ellison